1-1-2013

Coordinated Control of Power Electronic Converters in an Autonomous Microgrid

Gholamreza Dehnavi
University of South Carolina

COORDINATED CONTROL OF POWER ELECTRONIC CONVERTERS IN AN

AUTONOMOUS MICROGRID

by

Gholamreza Dehnavi

Bachelor of Science
University of Tehran, 1997

Master of Science
Iran University of Science and Technology, 2000

_____

Submitted in Partial Fulfillment of the Requirements

For the Degree of Doctor of Philosophy in

Electrical Engineering

College of Engineering and Computing

University of South Carolina

2013

Accepted by:

Herbert L. Ginn III, Major Professor

Roger A. Dougal, Committee Member

Charles W. Brice, Committee Member

Edward P. Gatzke, Committee Member

Lacy Ford, Vice Provost and Dean of Graduate Studies

To Laleh, my dear wife, for her patience and support during this work

AND

To Alborz, my lovely son, for the happiness he brought us.

ACKNOWLEDGEMENTS

First and foremost, I wish to acknowledge the assistance and guidance of my advisor, Dr. Herbert Ginn, for his mentoring efforts during this research. His positive reinforcement along with belief and patience led me to come up with this work. I will always remember his support and friendliness.

I also wish to thank my advisory committee members, Dr. Roger Dougal, Dr. Charles Brice, and Dr. Edward Gatzke, for their time, interest, helpful comments, and insightful questions.

I would like to acknowledge the funding source that made my Ph.D. work possible. My work was supported by the U.S. Office of Naval Research.

Last but not least, I thank my lovely wife and sweet son who made this work possible by their support and encouragement. My parents receive my deepest gratitude and love for their dedication, support and patience during my life.

ABSTRACT

Advances in power electronics and generation technologies have increased the viability of distributed generation systems. A microgrid is a special category of distributed generation systems that is distinguished by its size and the ability to operate independently as an islanded system. As long as a microgrid is connected to a large grid, quality of the voltage is supported by the main grid and each power source connected to the microgrid generates independently. In contrast, in the islanded operation of microgrids and in electrical islands such as shipboard distribution systems, dynamics are strongly dependent on the connected sources and on the power regulation control of the grid interfacing converters. In this mode, power sources in a microgrid should be controlled in coordination with each other so that a stable balanced three-phase sinusoidal voltage is provided.

In many cases, energy sources in a microgrid are interfaced through power electronic converters. A higher degree of controllability of converters as compared to electrical machines allows for the possibility of ancillary functions for power quality improvement when converters have unused capacity. The present work proposes a cooperative control approach for converters in a microgrid in which, by efficiently utilizing power converters in response to load demand and required ancillary functions, the operation of the microgrid is optimized. Efficient utilization of power converters is determined by a management system according to an optimization function.

A higher level control is also proposed in this work which exchanges set-point values with local controls through low bandwidth communication links in order to eliminate voltage magnitude deviation, frequency error, imbalance and harmonic distortion at a load bus.

Each of a converter's tasks can be expressed in terms of current components measured at a converter's point of connection to the system. Thus, current-based coordination of a microgrid is performed through a decomposition of current into orthogonal components. Different components of a converter's output current are controlled independently in order to enable optimization of various parameters of a microgrid. All converters in the system are considered including converters that are not actively interfacing an electrical energy source to the grid.

Some power units in microgrids are controlled to generate active current according to a reference made by an internal control system such as *MPPT*[1] system or *SOC*[2] controller. The presented cooperative control approach is expanded to allow these units to supply active current in accordance with the local reference while they also contribute to generation of non-active currents in coordination with other units.

Simulation results verify the benefits of the control approach developed here in both coordination and voltage quality improvement. Thus, the method allows operation of the microgrid to be improved by utilizing the available converters to the fullest extent possible. This reduces the need to connect additional resources to the microgrid.

---

[1] Maximum Power Point Tracking
[2] State Of Charge

TABLE OF CONTENTS

LIST OF TABLES

LIST OF FIGURES

CHAPTER I

INTRODUCTION TO COORDINATED CONTROL OF CONVERTERS IN AUTONOMOUS

MICROGRIDS

The world is at the edge of a major shift in the paradigm of electrical energy generation, transmission, distribution and storage, by moving from existing, centralized generation towards DER[3]. The new paradigm has the potential to result in higher stability margins and better reliability, reduction of transmission lines power loss, power quality increase, ability to shift peak loads, etc. Smart grid technologies help utilities to operate, control, and maintain DER as well as interconnect them to the main grid. In the new paradigm of the grid, the complexity of technical tasks have changed from dealing with local $SCADA$[4] data into a variety of massive field data collection, that allows a more comprehensive view of the power system status, energy flows, hierarchical control, asset management, equipment conditions etc. A Microgrid is a localized grouping of DER and loads that has the capability of islanding and operating independently from the grid as well as grid-connected mode of operation. Smart technologies bring about the possibility of a smart microgrid. A smart microgrid typically integrates the following components [1].

a)   Power plants capable of meeting local demand as well as feeding the unused energy back to the electricity grid. Such power plants are often renewable

---

[3] Distributed Energy Resources
[4] Supervisory Control And Data Acquisition

1

sources of energy, such as wind, sun, and biomass.

b)   It services a variety of loads, including residential, office and industrial loads.

c)   It makes use of local and distributed power-storage capability to smooth out the intermittent performance of renewable energy sources.

d)   It incorporates smart meters and sensors capable of measuring a multitude of consumption parameters (e.g., active power, reactive power, voltage, current, harmonics, unbalanced current and so on) with acceptable precision and accuracy.

e)   It incorporates a communication infrastructure that enables system components to exchange information and commands securely and reliably.

f)   It incorporates smart terminations, loads, and appliances capable of communicating their status and accepting commands to adjust and control their performance and service level based on user and/or utility requirements.

g)   It incorporates an intelligent core, composed of integrated networking, computing, and communication infrastructure elements, that appears to users in the form of an Energy Management System that allows command and control on all nodes of the network.

In many cases the energy sources in a microgrid are interfaced through power electronic converters. The controllability of instantaneous output current/voltage of power converters has caused these converters to be used in different applications. Output current of the sources that include interface converters can be controlled with more degrees of freedom. In order to avoid instability in the system and to increase the efficiency of the microgrid operation, all of the converters in a microgrid should be controlled in coordination with each other.

1.1 PROBLEM DESCRIPTION

In the grid-connected mode of operation, a microgrid is supported by the main grid's voltage and frequency. The task of interface converters in this mode is to control current into the established voltage, whereas in islanded mode of operation the task is to establish that voltage. A general architecture of a microgrid is represented in Figure 1.1. In the islanded mode of a microgrid, dynamics are strongly dependent on the connected sources and on the power regulation control of the converter interfaces [2]. This may affect control accuracy and stability of the system. Furthermore, operation of a microgrid should be optimized in terms of fuel cost, power loss, reliability, etc. Therefore, distributed power sources in a microgrid must be controlled in coordination with each other in order to meet the operating criteria of the microgrid as a whole as well as to follow an operation optimization function for the system. A cooperative control approach of converters is required so that every action to respond to load demands or to improve grid operation is coordinated among all power converters in the microgrid including the converters that are not actively interfacing an electrical energy source to the grid.
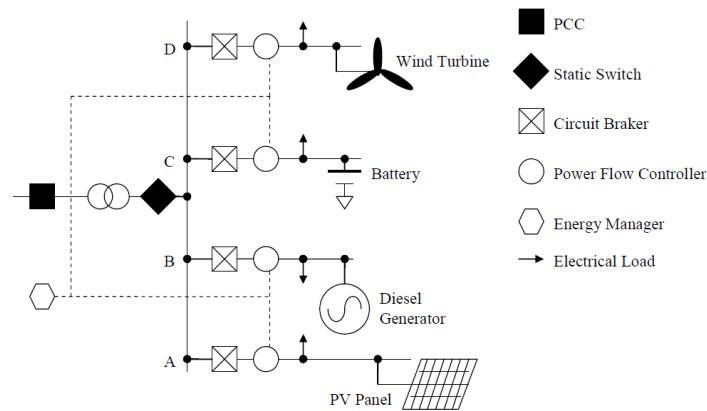
Figure 1.1. General architecture of a microgrid [3]

Also, in the islanded mode of operation, a microgrid can suffer from voltage magnitude deviation, voltage distortion, asymmetry and frequency variation which may affect sensitive loads operation. A control method is required to control power quality indices at sensitive load buses while it does not disturb the desired coordination among power sources. Figure 1.2 shows the two problems that are targeted to be solved in this research.

The term microgrid is not strictly defined and covers a wide range of possible systems. Islanded microgrids have been used in applications of avionics, automotive, marine and rural areas [4]. Electrical islands such as shipboard distribution systems, aircraft distribution systems, and offshore oil/gas platforms differ from microgrids only in that connection and disconnection from a larger scale grid is not a regular event [2]. Therefore, all control applications which are used in islanded mode of a microgrid would be applicable to an electrical island power system. The functionalities expected in these small local grids are active and reactive power flow control, frequency and voltage
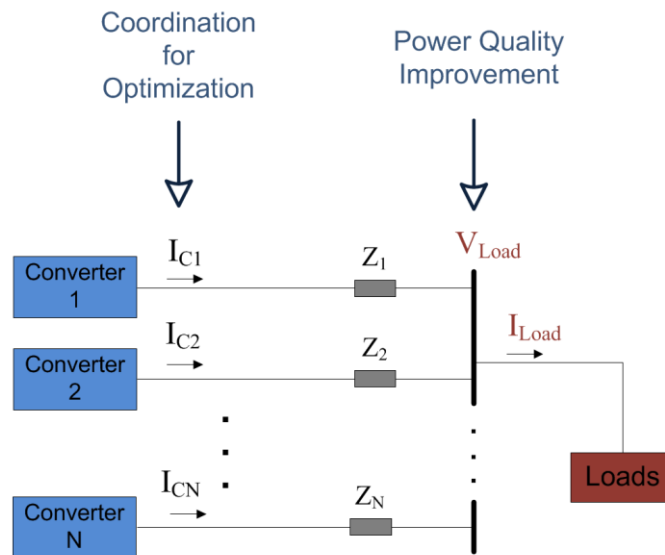
Figure 1.2. Microgrid problems that are solved in this dissertation

stability, black start operation, active power flow capabilities and storage energy management among others [5]. Optimization of microgrid operation requires the functionality of control over harmonics and unbalanced power flow as well.

In *AC* microgrids, there are four major power components, i.e. active, reactive, harmonic, and unbalance components that need to be coordinated. The focus of this dissertation will be on this type of microgrid. For *DC* microgrids, there is only one power component to control i.e. active component which results in simplicity of the control system compared with the *AC* microgrid case. Also power quality indices of *AC* voltage are more numerous as compared to *DC*. Thus, *AC* microgrids are the focus of this dissertation with the expectation that the results are directly extendable to *DC* microgrids.

1.2 LITERATURE REVIEW

Several methods for control of converters in a microgrid have been proposed in the literature. Some of the authors' contribution to converters control in microgrids is distributed compensation, some aim at increase of power quality indices, while others' attention is on power sharing among converters. In general, cooperative control of converters in a microgrid can either be central or decentralized, disregarding master-slave control of converters in microgrids for which only a few papers can be found. For each control method, expansion of the control system has been investigated in the literature and some improvements have been proposed.

1.2.1 Control of converters in a microgrid – central control of distributed compensators

In large scale grids compensators connected to the grid are designed to suit local needs assuming no interactions with the rest of the network, however, in a microgrid

distributed compensators interact with each other and with the rest of the network. In such a context a cooperative control approach of interface power converters and any other Electronic Power Processor acting in the grid is required. Every action to improve grid operation (power flow control, voltage support, unbalance compensation, harmonic mitigation) must be coordinated among all electronic power processors acting in a microgrid including interface power converters, Active Power Filters, Static Var Compensators and *STATCOM*s. References [6-10] introduce a central control method for cooperative control of distributed compensators and interface converters. This includes compensation of reactive power, harmonics and unbalance loading. The architecture of this cooperative control generally includes a Central Control Unit and a set of Local Control Units one per each Electronic Power Processor. In Figure 1.3 the architecture of this control is shown along with the connections to power circuit. Power circuit consists of distributed compensators and the network. All of the loads are considered in network model.
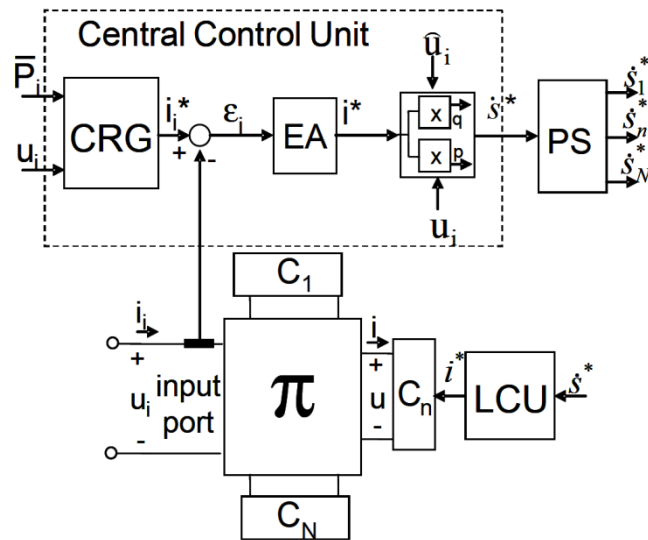
Figure 1.3. Architecture of the control system [10]

The measurement point of central control is PCC^1 which provides reference values for all local control units. The aim of the control is to make it possible the exploitation of both quasi-stationary and dynamic compensators. In this sense, based on the characteristics of different components of current to be compensated, and also considering the speed of each type of compensator the compensation is shared between units. Other factors such as compensator's power rating, distance between the compensator and *PCC*, and workload of each compensator is also considered in sharing of the duties. Quasi stationary compensators are used to take care of parts of the workload of the dynamic compensators and free their capacity to be used when required. Notice that with this strategy, a high bandwidth communication is required especially when harmonics and transient compensation is part of the work. Also, since the configuration of the system is not generally known, an identification process is essential to evaluate the voltage and angle difference between *PCC* and the installation point of each compensator.

1.2.2 Control of converters in a microgrid – decentralized control of converters

Central control and master-slave control of power sources rely on communication for reliable operation. Control commands solely based on local measurements exhibit superior redundancy and reliability, where they can only be achieved at the price of permitting a small error. These controls have only proportional controller for frequency and amplitude of voltage lacking any form of integral control. Due to the small error, these techniques are generally denoted as droop control methods.

---

[1] Point of Common Coupling

One of the applications for droop control of inverters is coordinated control of multiple *APF*s[1] in the grid without real time communication. *APF*s might be installed at a substation [11] to suppress harmonic resonance or along a radial distribution line [12-15]. Multiple *APF*s are installed along the distribution line to damp voltage harmonics produced by series resonance between line inductance and power factor correction capacitors. Each *APF* operates as a harmonic conductance to reduce the voltage harmonic. The *APF*s can share the harmonic filtering workload by using droop control method. The droop relation is between the harmonic conductance command and the volt ampere of each *APF*. A block diagram of the system is shown in Figure 1.4.

With the constant droop line, voltage distortion may not be reduced enough in some cases and may be reduced more than enough in other cases. To utilize the filtering capacity more efficiently, voltage *THD*[2] at the installation point of each *APF* is used in [14] to dynamically adjust the *VA* capacity and the slope of droop characteristics so that
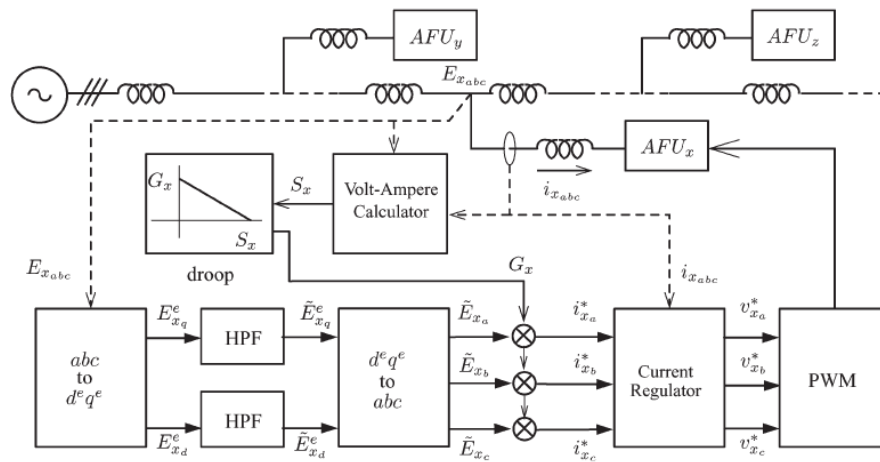
Figure 1.4. Application of droop control for voltage harmonic filtering by parallel APFs [12]

[1] Active Power Filter
[2] Total Harmonic Distortion

the voltage *THD* of the installation point can always be maintained at an allowable level. Also, in this scheme, there is one conductance for all of voltage harmonics and different harmonics are not separated. Therefore, current harmonics can be different based on the value of voltage harmonics. An extension of this control has been proposed in [16] and [17] that enables control of harmonic loads separately for different orders of harmonics.

Authors in [18] introduce a cooperative imbalance compensation method using droop control method. A droop control method based on the reactive power produced by the negative sequence current and positive sequence line voltage is proposed. Authors have proposed that the idea can be merged with the voltage and frequency droop controls and be used for interface converters in the grid. Droop control of interface converters in a microgrid is discussed in [2&4][13][19-27]. This control technique, which is emulating the behavior of large synchronous generators in conventional grids for sharing active and reactive power, consists of dropping frequency when delivered active power increases and dropping voltage amplitude when delivered reactive power increases. *P–f* and *Q–V* droop controls can be implemented as in (1-1) and (1-2). In these equations f_0 and V_0 are the nominal values of frequency and voltage magnitude while S_f and S_v are droop slopes which are determined based on ratio of active and reactive power sharing and with consideration of frequency and voltage limits.

$$f = f_0 - s_f.P \tag{1-1}$$

$$V = V_0 - s_V.Q \tag{1-2}$$

1.2.3 Improvement of droop control method

Authors in [22] have proposed the *P-V* and *Q-ω* boost functions to improve the dynamic of the parallel droop controlled system as in (2-14) and (2-15).

9

$$E = E_0 - n.P - n_d.\frac{dP}{dt} \qquad\qquad\qquad\qquad (1\text{-}3)$$

$$w = w_0 - m.Q - m_d.\frac{dQ}{dt} \qquad\qquad\qquad\qquad (1\text{-}4)$$

Where m and m_d are the proportional and derivative coefficients of reactive power Q, respectively, and n and n_d are those of active power P, respectively.

In [28] authors have proposed an adaptive droop control by using proportional, integral and derivative term in the droop relation. Line impedance is usually an issue in independently control of active and reactive power. This system is able to control active and reactive power flows independently for a large range of grid impedance value. There is a loop for grid parameters estimation in this controller. This estimation is also useful in islanding detection.

Authors of [29] also use derivative and integrative term in droop control to enhance the system dynamic performance both in grid-connected and islanded mode. The method is called mode adaptive droop control. Derivative term is used when grid is islanded while integrative term is used to control output powers of converters when it is connected to the main grid.

1.2.4 Higher level controllers – Hierarchical control Scheme for droop controlled microgrids

Droop control methods alone have several drawbacks that limit their application. One drawback is the increase of voltage magnitude deviation at load bus with load variation. In some papers, an external control loop has been proposed to restore the nominal values of the voltage inside the microgrid. Another disadvantage of traditional droop control is the load dependent frequency deviation. The inverter tradeoff between

frequency/amplitude of voltage and active/reactive power control in islanded microgrid cannot be avoided. Therefore the use of a low bandwidth noncritical communication system seems inevitable. An additional control level can be used to bi-directionally control the power flow in grid-connected microgrids and to tune voltage amplitude and frequency. A hierarchical control structure is proposed in [4] as a general approach toward standardization both for *AC* and *DC* microgrids. Some other authors have already proposed secondary and tertiary controllers in which the main problem to solve is frequency control. In this hierarchical control structure voltage stability and synchronization issues are also considered. It is necessary to ensure that the command and reference signals from one level to the lower levels will have low impact on the stability and robustness performance. Thus the bandwidth must decrease with an increase in the control level. The structure consists of three control levels beside the inner control loop.

Level 0, inner control loops: They consist of current and voltage control loops for a converter.

Level 1, primary control loop: This level is used to implement droop controls, balancing energy between *DG*s and storage systems by improving droop relations. Virtual output impedance, which can also be set independently for different harmonics, are implemented in this level.

Level 2, Secondary control loop: This level is used to compensate for frequency and amplitude deviation and also for synchronization process.

Level 3, Tertiary control loop: When microgrid is connected to the main grid, this level is used for controlling power flow by adjusting frequency and amplitude

11

through *PI* controller. It can also be used to improve power quality. This level allows multiple *DG*s to form a cluster and performs like a primary control for the cluster controlling its power exchange with the rest of the network. Figure 1.5 shows a block diagram of this hierarchical control structure.

1.2.5 Energy Management System

Real time optimization in a microgrid through frequent adjustment of power sources output to minimize cost or meet other targets has been proposed in literatures. Optimization may include using storage capacity to buy energy when price is low and make use of that energy when grid connection is unavailable or price is high [30]. An important consideration when optimizing power generation is system stability especially when the microgrid is operated in islanded mode. In [30] authors have proposed an *EMS*[1] as in Figure 1.6 which adjusts output power of generators in a microgrid to minimize fuel consumption and ensures stability. It's observed that the microgrid is less damped when all inverters have the same droop gain than if one or more have gains below this value. While high droop gains reduce the stability margin, low gains increase the response time which results in poor transient behavior in terms of higher energy storage requirements to deal with increased transient energy exchange [30].

---

[1] Energy Management System
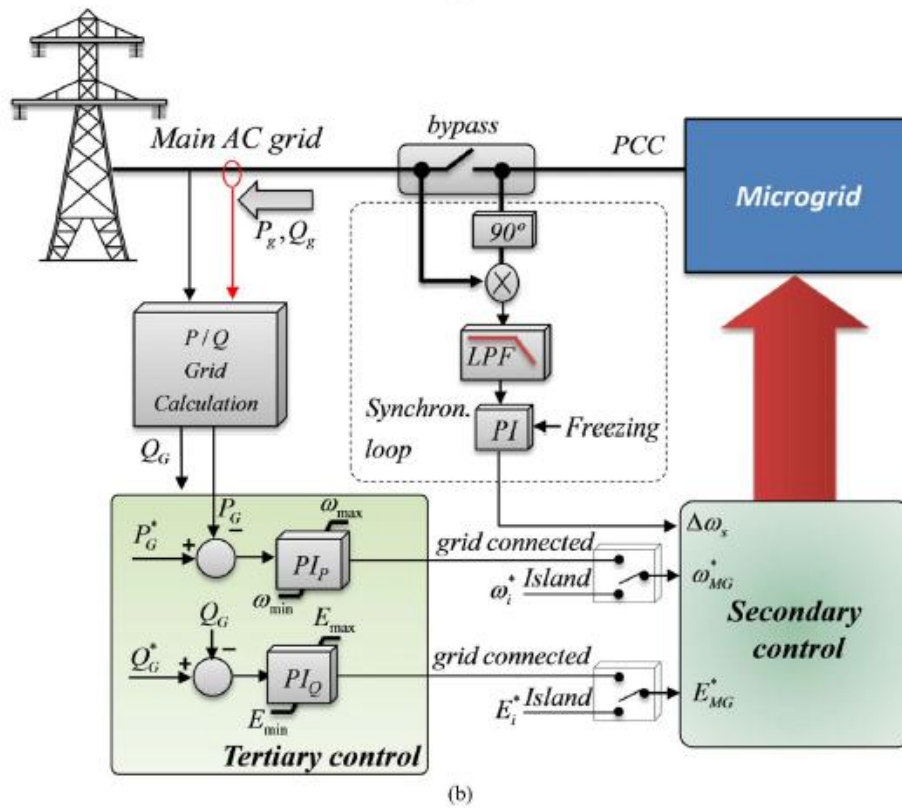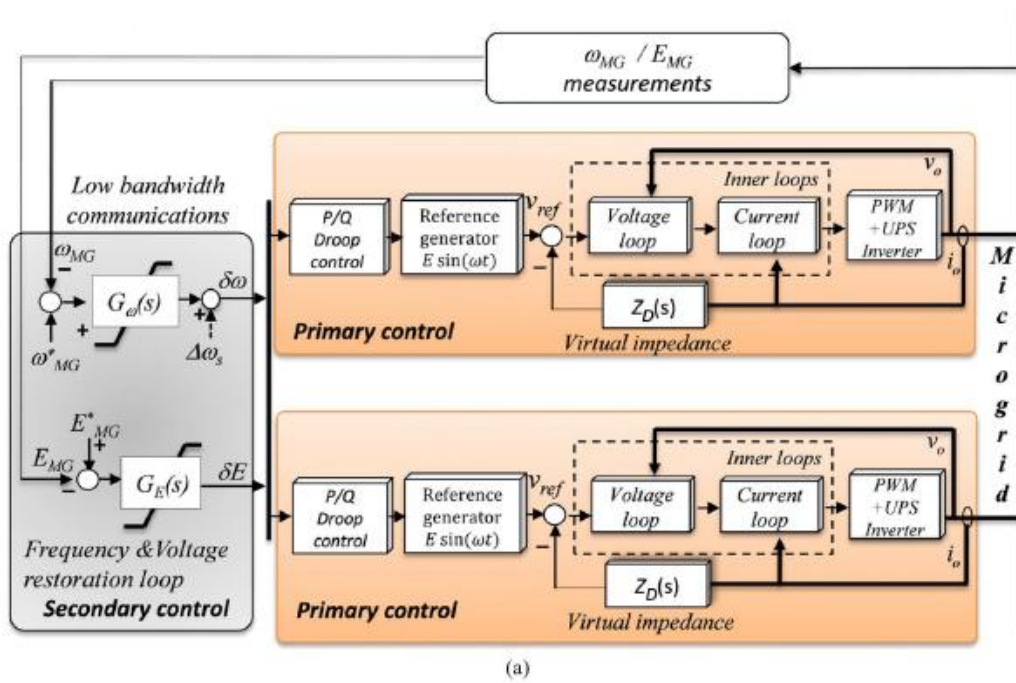
Figure 1.5. Block diagram of the hierarchical control of *AC* microgrid. (a) primary and secondary control (b) tertiary control and synchronization loop [4]
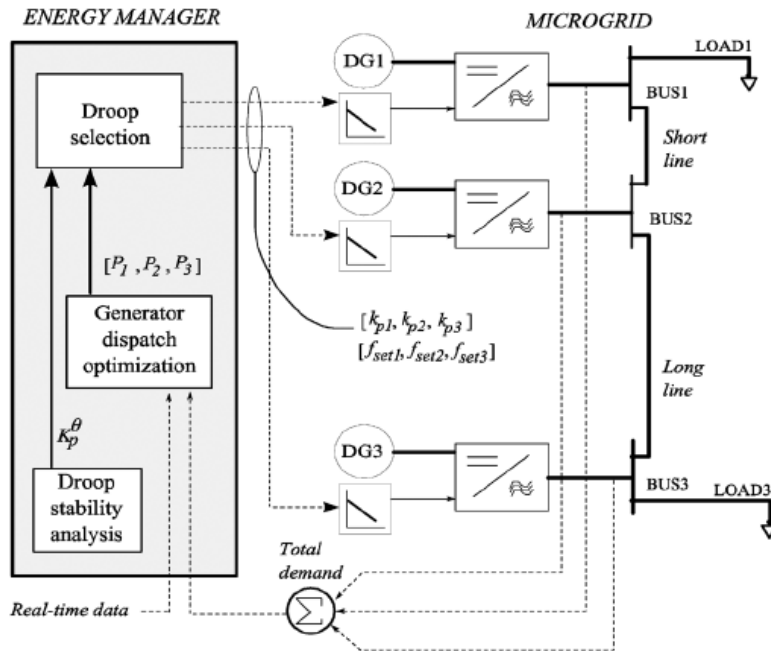
Figure 1.6. Energy management system for microgrid [31]

1.2.6   Low level controllers for harmonics and unbalance voltage control

In order to use droop controllers for the sharing of harmonic currents or negative sequence currents or both between converters in a microgrid, the bandwidth of lower level controllers i.e. current and voltage controllers should be high enough to respond to the high frequency portion of the reference voltage accurately. They also need to be properly designed for both positive and negative sequence component performance. There are a couple of different methods presented in the literature for design of current and voltage controllers in situations where distortion is present. In general, they can be divided into synchronous frame and stationary frame controllers. Authors in [31], [32-35] have utilized stationary frame Proportional + Resonant controllers for the control of converters. Figure 1.7 shows the block diagram of voltage and current controllers by using P+ Resonant controllers. For every harmonic component a P + Resonant controller

14
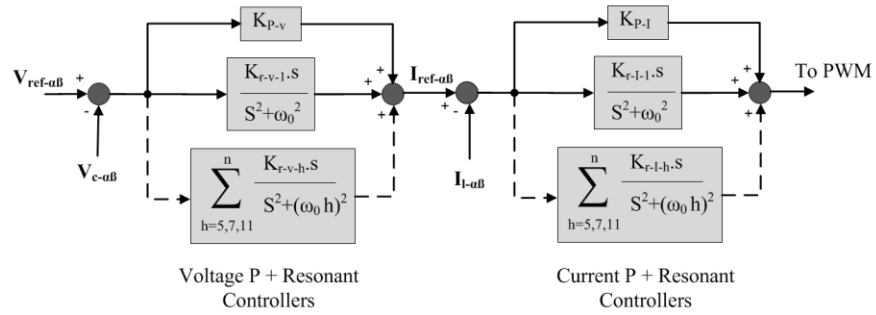
Figure 1.7. Voltage and current P + Resonant controller of a voltage source inverter
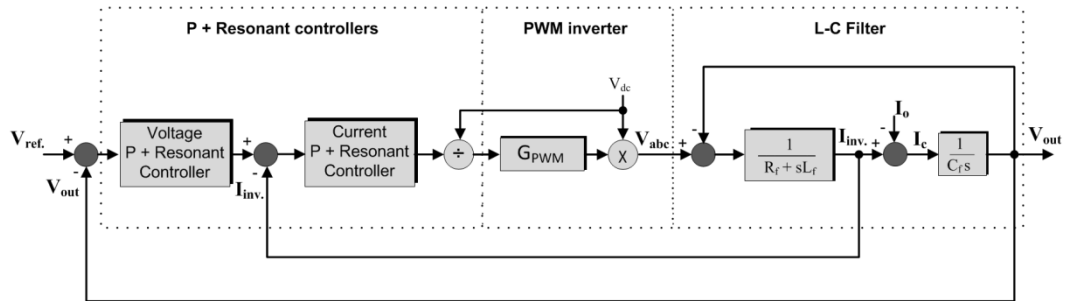
Figure 1.8. Block diagram of the closed loop voltage source inverter

is designed. Figure 1.8 shows the block diagram of the whole closed-loop system.

Authors in [36-39] have proposed different schemes for synchronous frame current and voltage controllers. Three different structures of current controller design under unbalance voltage condition have been proposed in [36]. Synchronous frame voltage controller is presented in [38] for control of a positive and negative components of voltage at selected frequencies. Other control methods may also be used for this purpose. A deadbeat current control is presented in [40] for both positive and negative sequence control. A negative sequence controller in stationary frame is proposed in [41]

15

and authors of [42] present a space vector based control for control of output voltage of *UPS* in the presence of nonlinear and unbalance load.

1.3 OBJECTIVES

Power converters in an *AC* microgrid have unequal capabilities in generation of different components of electrical power. Active and reactive power are generally shared among converters with respect to their ratings but the capability of the converters may vary based on the availability of primary power sources such as wind for wind turbines and sunshine for photocells. Converters with no primary source can be used for generation of reactive power and for harmonic cancellation. They can also be used for unbalanced power generation and the converters with more energy storage capacity on the *DC* bus would be able to generate more unbalanced power with smaller ripple imposed on the *DC* bus. Harmonic sharing mostly depends on the structure of converter as well as the switching frequency. Higher switching frequencies enable converters to control higher order harmonics.

In order to be able to control all of the power components of the load among converters in an autonomous microgrid, so that the flow of power components is optimized within the microgrid, a comprehensive and coordinated control system is required which enables control of each power component of the load independently from other components. In such a system, considering the constraints for converters along with a function for optimization of the system, sharing factors of each converter for any of the power components can be set by a higher level control layer. The optimization function can include target functions such as reducing fuel cost, power loss minimization, equal loading utilization, stability and reliability increase. A control algorithm is required such

that by means of coordinated control of output voltage of each converter, it optimizes the operation of the microgrid toward a targeted objective function.

Also, since in the islanded mode of operation, voltage in a microgrid may suffer from magnitude and frequency deviation, distortion, and imbalance, the control system should include a method to control power quality indices at the load bus.

The objective of this dissertation is to extend distributed control of active and reactive current to ancillary functions of harmonic filtering and unbalance compensation for comprehensive duty sharing among all converters in the microgrid according to an optimization function. Sharing factors for each power source may need to be reset by the management system following any change in the configuration or operation condition of the microgrid depending on the optimization function. Low speed communication links are required for data transfer between the management system in system-level control and local control units. Also, due to an extra degree of freedom in the setting of output voltage of converters for sharing of active and reactive power and ancillary functions, power quality indices at a sensitive bus can be improved. Low speed communication links are required for transmission of power quality indices information at load bus to system-level control. Information from other systems is also required in Management System in order for real-time optimization. A low speed communication link is also needed for data transfer between other systems and the system-level control. A schematic that shows the required structure for the objective of this research is shown in Figure 1.9. In this figure output current/power of each converter includes active, reactive, harmonic and unbalanced components. Each of these components is coordinated among all converters.

17
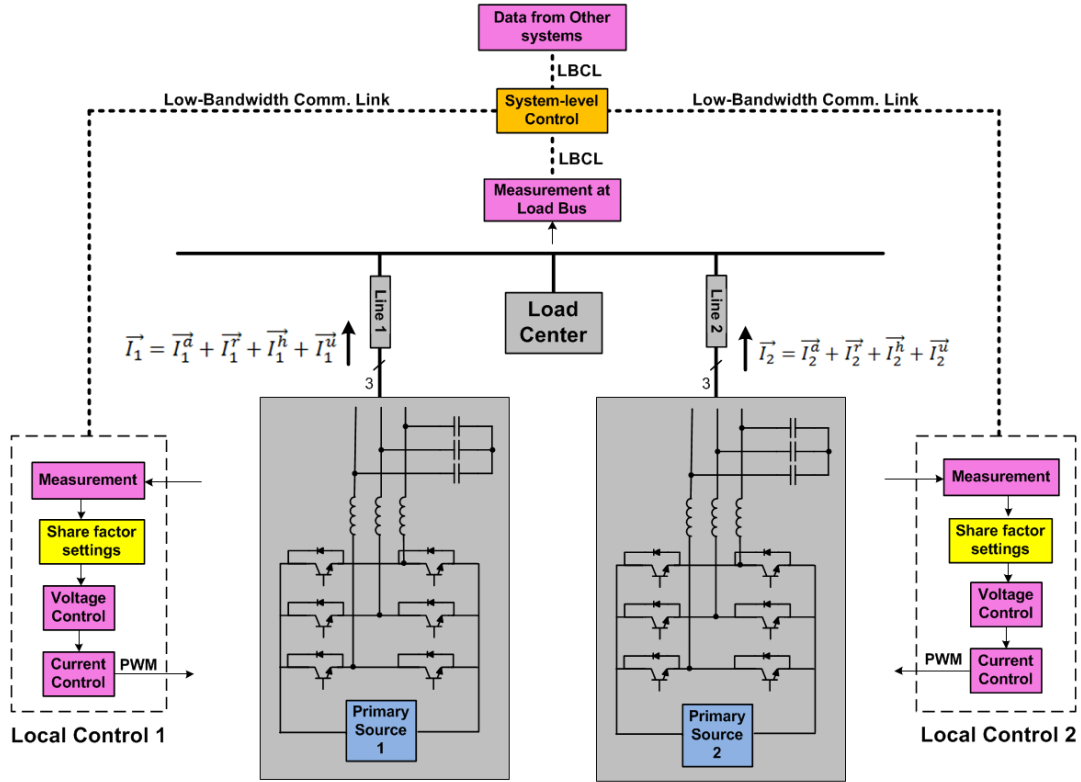
Figure 1.9. Objective plan for optimization of microgrid operation and power quality increase

The Management System sets the output voltage of converters in a way that along with sharing each of the load current/power components among converters according to the optimization function, power quality indices are increased at the load bus.

1.4 ORGANIZATION OF THE DISSERTATION

Control of converters in a microgrid will be reviewed in Chapter II and distributed control of converters in an autonomous microgrid by means of a droop control method will be presented. Droop control which is already available for active and reactive power control, will be extended to harmonic and unbalance power. A sample microgrid will be simulated for verification of the presented approach. Chapter III will introduce current based droop control of all major current components and the sample microgrid will be

18

simulated for verification of the current sharing method. *CPC*[1] theory will be used for decomposition of current into orthogonal components. A Management System and the secondary loop control will be introduced in Chapter IV and simulations will prove that power quality indices at load bus are well improved. The steps for controller parameters design including low-level controllers as well as other layers of control system will be presented in Chapter V. Chapter VI explores the optimization of a microgrid including power units with *MPPT*[2] system such as *PV* units and wind power sources and in Chapter VII a mathematical approach for the optimization of the microgrid operation in presence of *PV* and wind power units will be presented. Chapter VIII outlines key conclusions and contributions of this work along with some ideas for continuation of the research.

---

[1] Current Physical Components
[2] Maximum Power Point Tracking

CHAPTER II

POWER SHARING AMONG CONVERTERS IN AN AUTONOMOUS MICROGRID

A microgrid operates in either grid-connected or autonomous mode depending on the main grid condition/existence. In grid-connected mode, the objective is to export a controlled amount of active and reactive power into an established voltage which is done through the control of active and reactive components of current. The power demands themselves come from the Management System of the microgrid with the exception of Photo Voltaic and heat-led *CHP*[1] sources which generate autonomously [2]. These sources as well as wind power sources follow the value of active power reference generated by an internal control system such as a *MPPT*[2] system. The overall control structure of interface converters in the grid- connected mode is similar to Figure 2.1.
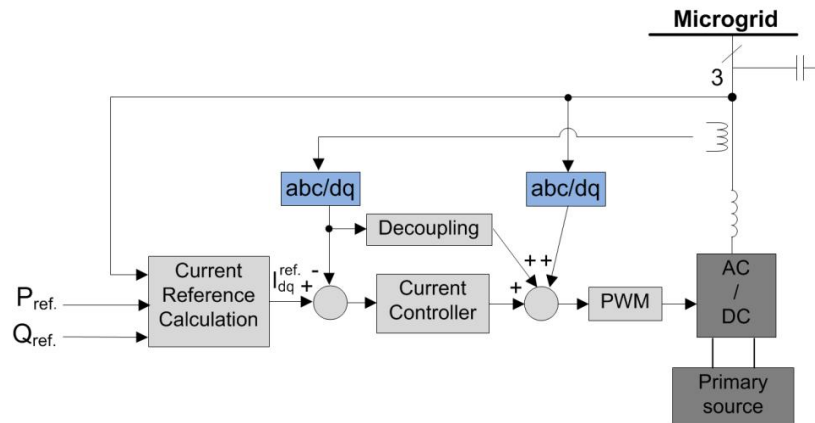
Figure 2. 1. Current control of converters for grid-connected mode of operation

---

[1] Combined Heat and Power
[2] Maximum Power Point Tracking

Whereas the task in grid-connected mode is to control current into an established voltage, the task in autonomous mode is to establish that voltage. Nested control loops have been proposed and used in autonomous mode of microgrids to control output *AC* voltage of an interface converter as shown in Figure 2.2.

Coordinated control of converters in an autonomous microgrid can be performed either using centralized or distributed approaches. Decentralized controls based on the droop approach have the advantage of avoiding the need for high speed communication links as well as removing the single point of failure as opposed to central control method. Droop controls have been introduced for distributed and coordinated control of active and reactive power of sources in an autonomous microgrid. Active and reactive power of the load are shared among converters with sharing coefficients that are determined from the solution of an optimization function. In this chapter, droop controls have been extended to all of the components of power. Reference value for output voltage of the converter is generated by sharing control system which consists of four sharing units, one for each
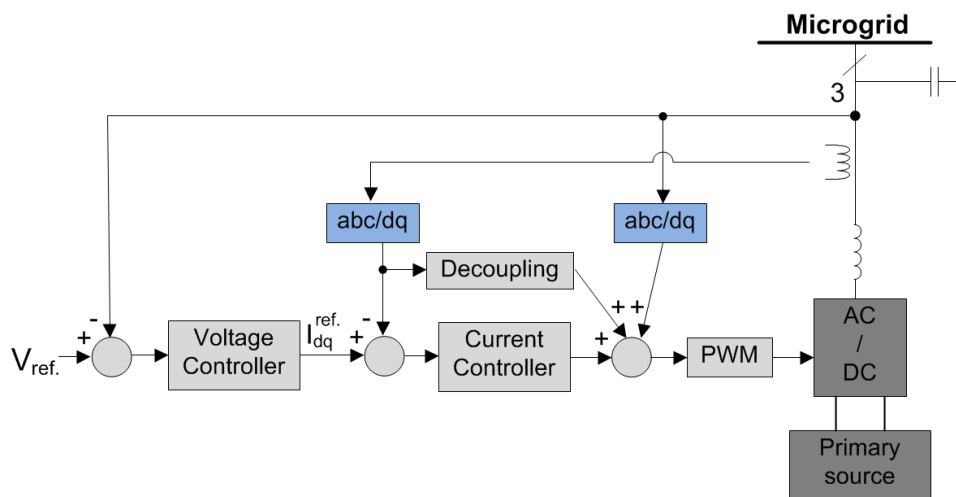
Figure 2. 2. Nested control loops for converters in an autonomous microgrid
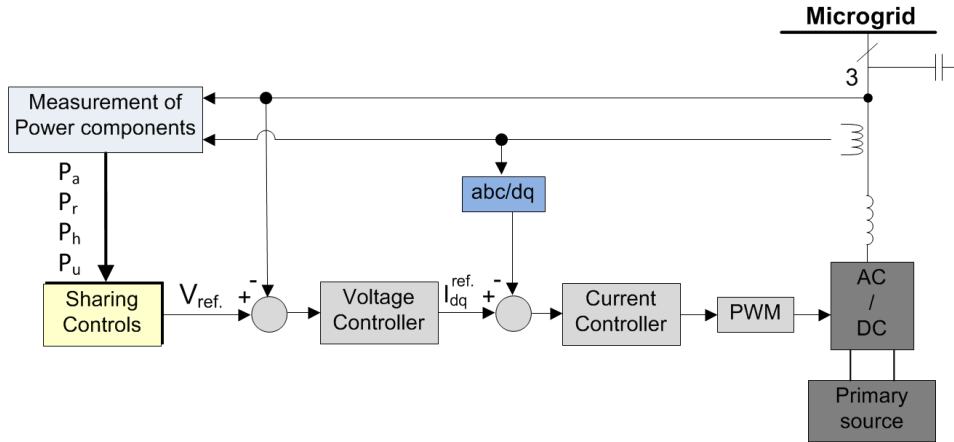
Figure 2. 3. Distributed control of power components in coordination with other converters

power component. Figure 2.3 shows the overall control system for distributed control of converters in a microgrid by means of droop controls.

2.1 DROOP CONTROL FOR ACTIVE AND REACTIVE POWER SHARING

The droop control technique for active and reactive power sharing among converters in an autonomous microgrid is emulated from the behavior of large synchronous generators in conventional grids. It consists of reducing the frequency when delivered active power increases and reducing the voltage amplitude when delivered reactive power increases. Equations (2-1) and (2-2) are the active and reactive power expression from the supply to the grid as shown in Figure 2.4.
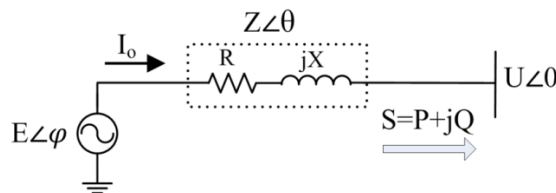
Figure 2. 4. Equivalent circuit of a *DG* unit connected to the common ac bus

$$P = \frac{U}{Z} [(E\cos\varphi - U).\cos\theta + E\sin\varphi.\sin\theta] \tag{2-1}$$

$$Q = \frac{U}{Z} [(E\cos\varphi - U).\sin\theta - E\sin\varphi.\cos\theta] \tag{2-2}$$

Where z and θ are the magnitude and phase of line impedance and E and U are inverter output voltage and common bus voltage with the phase angle difference of φ between them. Assuming that φ is very small we obtain:

$$P \cong \frac{U}{Z} [(E - U).\cos\theta + E.\varphi.\sin\theta] \tag{2-3}$$

$$Q \cong \frac{U}{Z} [(E - U).\sin\theta - E.\varphi.\cos\theta] \tag{2-4}$$

If the line impedance phase θ is close to *90°*, which is the case for conventional power systems, (2-3) and (2-4) will be simplified to:

$$P \cong \frac{U}{Z}.E.\varphi \tag{2-5}$$

$$Q \cong \frac{U}{Z}.(E - U) \tag{2-6}$$

These show that the power angle φ affects predominantly active power P and voltage difference affects predominantly reactive power Q. Control of frequency dynamically controls the power angle φ and thus according to (2-5) power flow. In other words P and Q can be adjusted independently by controlling frequency and magnitude of inverter output voltage. Therefore (*P–f*) and (*Q–V*) droop controls can be implemented with good precision and performance as in (2-7) and (2-8). In these equations f_0 and V_0 are the nominal values of frequency and voltage magnitude while S_f and S_v are slopes of droop characteristic lines. Figure 2.5 shows droop characteristic lines of a source for active and reactive power sharing and Figure 2.6 demonstrates how active and reactive powers are being shared between two sources with respect to their droop settings.
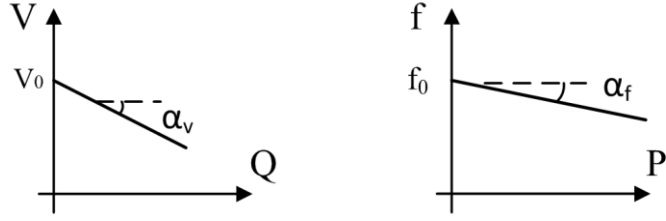
Figure 2. 5. frequency and voltage droop for active and reactive power control

(a)

(b)
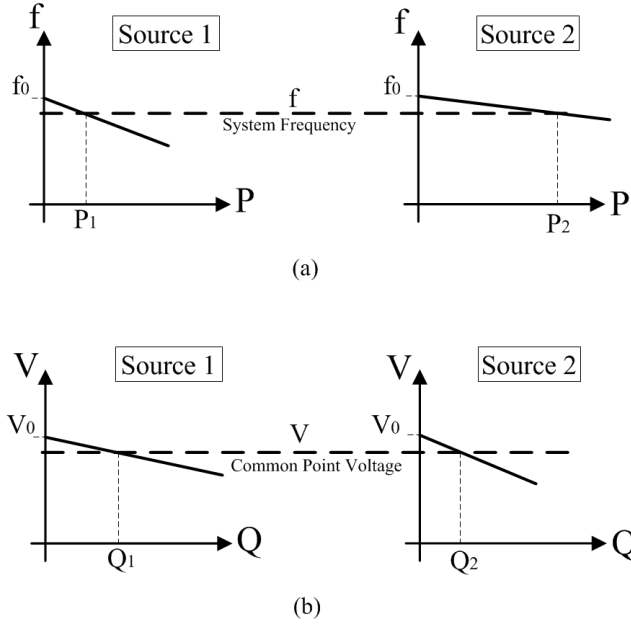
Figure 2. 6. Sharing load power by means of droop controls. a) Active Power b) Reactive power

$$f = f_0 - s_f.P \tag{2-7}$$

$$V = V_0 - s_V.Q \tag{2-8}$$

2.2 EFFECT OF LINE RESISTANCE

The droop method for active and reactive power control is developed based on having a predominantly inductive line impedance. In the case of a low voltage microgrid where θ in Figure 2-4 is not close enough to $90°$, P and Q will be coupled and using the conventional droop control method will lead to poor performance of the system.

2.2.1 Modified active and reactive powers

In order to cope with the problem of coupled active and reactive powers, modified active and reactive powers are introduced as in (2-9) to be used in droop control instead of P and Q.

$$\begin{pmatrix} P' \\ Q' \end{pmatrix} = \begin{pmatrix} sin\theta & -cos\theta \\ cos\theta & sin\theta \end{pmatrix} \begin{pmatrix} P \\ Q \end{pmatrix} \tag{2-9}$$

Applying this transformation on (2-3) and (2-4) results in:

$$P' \cong \frac{U}{Z} . E . \varphi \tag{2-10}$$

$$Q' \cong \frac{U}{Z} (E - U) \tag{2-11}$$

Therefore $(P'-f)$ and $(Q'-V)$ droop controls can be utilized and P' and Q' can be controlled independently.

2.2.2 Virtual output impedance

Another method to avoid coupling of active and reactive powers is to introduce a virtual output inductor. While effective in preventing the coupling between active and reactive power, this approach may increase the reactive power control error due to an increased voltage drop. A couple of methods have been introduced to improve this at the price of more control complexity [23]. A concern with the virtual inductor implementation is voltage drop calculation which involves differentiation of inductor current and can cause high frequency noise amplification and in return may destabilize the *DG* voltage control especially while in a transient state. Therefore, other methods have been proposed for calculation of voltage drop, such as calculation in the $\alpha\beta$ reference frame. Also, in some cases where a microgrid is spatially very small, such as in a shipboard power system, feeder impedance may be too small which decreases the stability of droop control. Therefore, a virtual impedance is implemented in the control
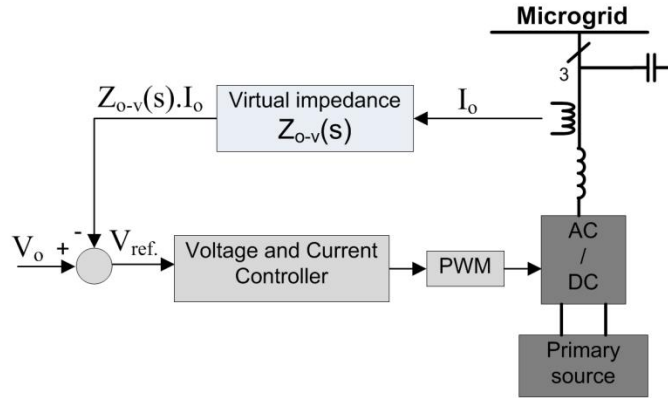
Figure 2. 7. Block diagram of the virtual impedance loop

system to emulate the desired output impedance [21-24]. Figure 2.7 shows a block diagram of the virtual impedance loop.

Authors in [21-24] have proposed that the virtual impedance can have different values than a pure inductive value. While pure inductive and pure resistive output impedances cause decoupling of active and reactive powers, with complex output impedance modified active and reactive powers have to be used. Pure resistive output causes active power to depend upon voltage magnitude and reactive power depend upon frequency. Authors in [22] have proposed using virtual resistive output impedance to decouple active and reactive power. The advantages of such an approach are:

a) The overall system is more damped

b) It provides automatic harmonic current sharing

c) Phase errors barely affect active power sharing

d) Low sensitivity to the line impedance unbalance which has always been a problem for droop control

Purely inductive and purely resistive assumption may not be applicable in the case where the inverter output impedance depends on the adopted control strategy and on the power

26

stage parameters as well as line impedance. Therefore, virtual complex impedance is proposed in [24] and [21] which offers the following advantages over virtual inductive and resistive impedance methods [24]:

a) It can reduce the circulating current

b) Its implementation can reduce the drop of output voltage, which is caused by virtual resistor impedance.

c) High frequency harmonic circulating current of the loads can be automatically shared by the inverters.

d) Less sensitivity to line impedance unbalance

e) It can also be adopted to properly change the impedance angle θ to decouple active and reactive power.

Capacitive virtual impedance is used in [43] to compensate for voltage distortion and voltage imbalance across grid-side inductor of the *LCL* output filter of converter when output current of the converter includes harmonic and unbalanced current. Negative resistive impedance is also introduced in this dissertation and used in some of the simulations. The magnitude of this resistance is equal to that of the resistive impedance of the line which together cause the line impedance to appear to the converter as a purely inductive impedance. Figure 2.8 shows the implementation of negative resistive impedance. In the other simulations of this dissertation, a complex value of output impedance has been implemented and modified powers have been used.

Virtual output impedance can also be used for soft start of the system when connecting the converter to the grid or for hot swap.
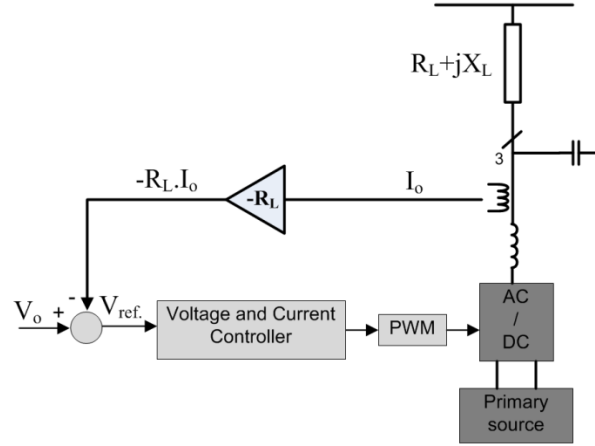
Figure 2. 8. Negative resistive impedance implementation

2.3 INACCURACY OF REACTIVE POWER CONTROL

Another issue with droop control in microgrids is inaccuracy of reactive power control due to line impedance. Unlike frequency which is the same in steady state over the grid, voltage magnitude is different at load bus and supply bus. In a traditional large-scale grid where the line is mainly inductive, inaccuracy in reactive power droop control is caused due to the voltage drop across the line inductance because of reactive load. One method to improve the accuracy is to exaggerate the *V-Q* droop effect and make the line voltage drop negligible. However, this may cause the output voltage to be too small. Therefore, in order for *V-Q* droop to control reactive power accurately, voltage drop across the line inductance should be considered as an additional slope in the droop characteristics of reactive power control to increase the accuracy of reactive power control with droop as in (2-12) [23].

$$K_{Qi} = \frac{X_i}{E_i} \qquad (2\text{-}12)$$

where K_{Qi} is the additional slope of converter i, X_i is the line inductance, and E_i is

28

converter output voltage. In the case of low voltage microgrids where the line resistance is not negligible compared with the line inductance, voltage drop across the resistance is also important and the additional slope should be considered as in (2-13).

$$K_{Qi} = \frac{X_i + \frac{R_i}{tan\alpha_i}}{E_i}$$ (2-13)

where R_i is the line resistance to converter i and α is output current phase angle. This slope compensates the effect of voltage drop due to flow of active power through resistance and flow of reactive power through inductance. More precise performance of reactive droop control can be achieved by compensation of the effect of voltage drop due to flow of active power through inductance and reactive power through resistance.

2.4 EXTENSION OF DROOP CONTROL TO ALL POWER COMPONENTS

While most of the literature on droop control of converters in microgrids such as [44] and [31] have focused only on the control of active and reactive part of the output power, recently authors in [45] have applied droop control along with the virtual impedance to a system comprising two power supplies to control not only active and reactive power but also unbalance and harmonic power. The control method of this reference does not allow independent control over power components and all power components are shared among converters with the same share factors while power electronic converters in a microgrid generally have unequal capabilities for generation of different components of electrical power. Active and reactive power are generally shared between converters with respect to their ratings but the capability of the converters for active power generation may vary based on availability of primary power sources such as wind for wind turbines and sunshine for photocells. Converters with no primary source

29

can be used for generation of reactive power and for harmonic cancellation. They can also be used for unbalanced power generation and the converters with larger amounts of energy storage on the *DC* bus would be able to generate more unbalanced power with smaller ripple imposed on the *DC* bus. Harmonic sharing mostly depends on the structure of the converter as well as the switching frequency.

2.4.1 Extension of droop control to harmonics

An important issue in coordinated control of power supplies in a microgrid is to supply harmonic current required by non-linear loads with proper sharing between sources. In some islanded grids, highly nonlinear loads incorporating rectifiers may even present the major part of the load. Supplying nonlinear loads can be incorporated either in the frequency domain, such as by partitioning the frequency spectrum and applying different controllers to different partitions using only a low bandwidth communication link [2] or in the time domain such as by emulating a virtual impedance. In this dissertation virtual impedance is used for sharing harmonic loads. Different configurations of virtual impedance are shown in [35] which consists of pure resistive, pure inductive, series inductive plus resistive and parallel inductive plus resistive. In this dissertation a parallel and series configuration for output impedance is chosen so that the fundamental component of the current passes virtually through a series complex impedance, and each harmonic components of the current pass virtually through a resistive impedances. Only 5th and 7th harmonics are considered here. The resistors may have different values for different harmonics which help sharing of harmonics with unequal ratios, but in this dissertation they have been considered to have equal values and different orders of harmonic currents are shared among converters with same share

factors. In order for sharing of harmonic currents to be accurate, impedance of line from each converter to load center should be considered in determination of virtual harmonic resistances. Figure 2.9 shows this configuration of the virtual output impedance and the realization of this impedance is shown in Figure 2.10.
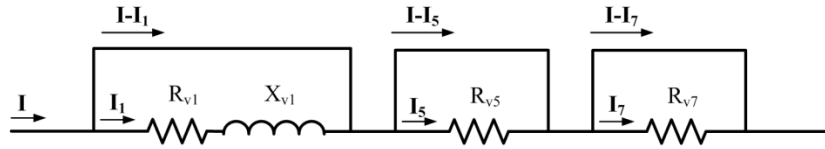
Figure 2. 9. Implemented virtual impedance
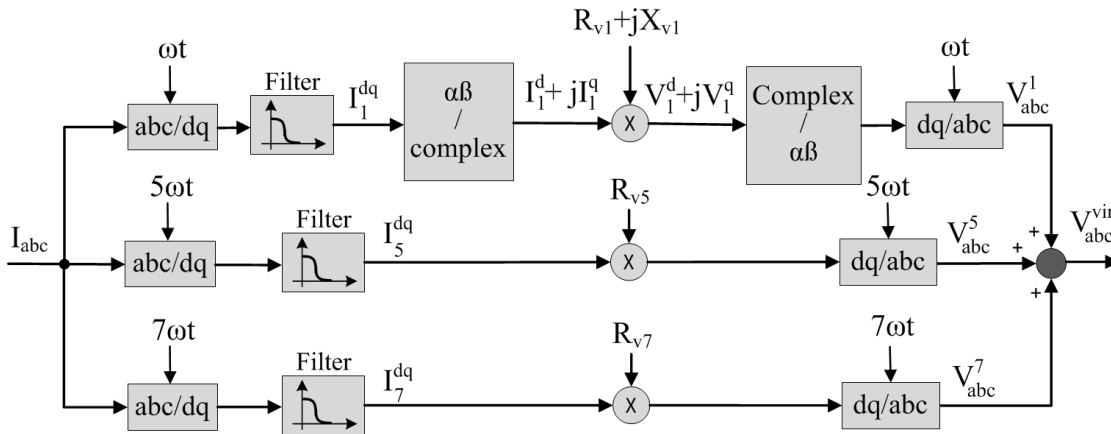
Figure 2. 10. Realization of the virtual impedance

2.4.2   Extension of droop control to unbalanced power sharing

In order to share unbalance load between power sources, a method is developed for negative sequence current sharing which is based on measurement of voltage and current at converter output. A separate control loop is also used for sharing of the increased amount of unbalanced current which is due to the increase of negative sequence voltage by secondary control. Sharing of the latter part of unbalance current will be discussed in chapter IV when secondary control performance is explained. Inner loop controllers of the converters should be properly designed for both positive and negative sequence component performance [40, 42]. In this dissertation, synchronous frame PI controllers are used for both positive and negative sequence components of voltage and current.

Negative sequence current is dependent on both positive and negative sequence voltages, V^+ and V, when load is unbalanced. As V^+ is controlled separately through positive sequence droop controls, the right value of V to control negative sequence current, I^-, is dependent on V^+. Figure 2.11 shows a single line diagram of a microgrid model, where V is power supply voltage, $R+jX$ is the line impedance and R_n+jX_n and V_n are equivalent impedance and equivalent voltage of the grid. Figure 2.12 shows an equivalent circuit of the circuit in Figure 2.11.

Figure 2. 11. Singe line diagram of a microgrid model

32

$$Y_n' = \frac{1}{Z+Z_n}$$
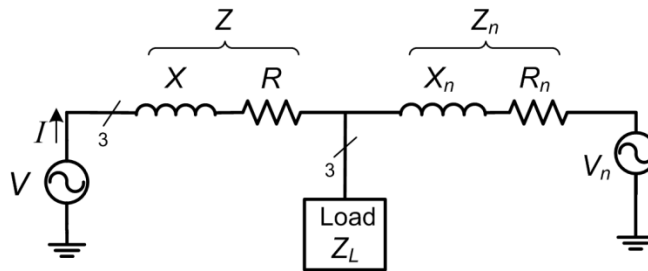
$$Y_L' = \frac{1}{Z+Z_L}$$
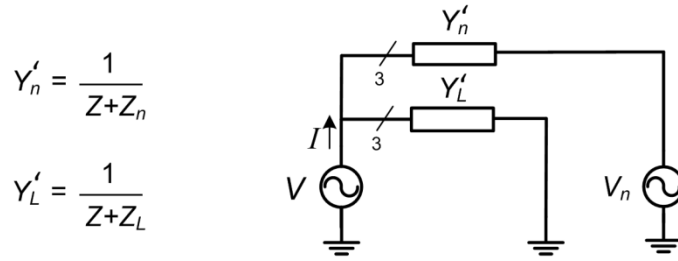
Figure 2. 12. Equivalent circuit of the circuit in Figure 2.11

Three phase equations for this circuit can be written as:

$$\bar{I} = \overline{Y_L'}.\bar{V} + \overline{Y_n'}.(\bar{V} - \bar{V_n}) \tag{2-14}$$

where $\overline{Y_L'}$ and $\overline{Y_n'}$ are vectors of three phase admittances as shown in Figure 2.11 and in matrix form the relations for three phases would be as follows:

$$\begin{pmatrix} I_a \\ I_b \\ I_c \end{pmatrix} = \begin{pmatrix} Y_{L\,a}' & 0 & 0 \\ 0 & Y_{L\,b}' & 0 \\ 0 & 0 & Y_{L\,c}' \end{pmatrix} \begin{pmatrix} V_a \\ V_b \\ V_c \end{pmatrix} + \begin{pmatrix} Y_n' & 0 & 0 \\ 0 & Y_n' & 0 \\ 0 & 0 & Y_n' \end{pmatrix} \begin{pmatrix} V_a - V_{na} \\ V_b - V_{nb} \\ V_c - V_{nc} \end{pmatrix} \tag{2-15}$$

Substituting three phase values with sequential components of voltages and currents results in:

$$A.\overline{I_s} = \overline{Y_L'}.A.\overline{V_s} + \overline{Y_n'}.A.(\bar{V} - \bar{V_n})_s \tag{2-16}$$

Where V_s and I_s are symmetrical components matrix of voltages and currents and A is the Fortescue conversion matrix from symmetrical to *abc* values. Multiplying each side of (2-16) by A^{-1} we have:

$$\overline{I_s} = A^{-1}.\overline{Y_L'}.A.\overline{V_s} + A^{-1}.\overline{Y_n'}.A.(\bar{V} - \bar{V_n})_s \tag{2-17}$$

By defining

$$\overline{Y_s} = A^{-1}.\overline{Y_L'}.A \tag{2-18}$$

$$\overline{Y_{ns}} = A^{-1}.\overline{Y_n'}.A \tag{2-19}$$

33

and multiplying matrices we will have:

$$\bar{Y}_s = \begin{pmatrix} Y_{11} & Y_{12} & Y_{13} \\ Y_{21} & Y_{22} & Y_{23} \\ Y_{31} & Y_{32} & Y_{33} \end{pmatrix}$$

$$= \frac{1}{3} \begin{pmatrix} Y'_{La} + Y'_{Lb} + Y'_{Lc} & Y'_{La} + a^2 Y'_{Lb} + a Y'_{Lc} & Y'_{La} + a Y'_{Lb} + a^2 Y'_{Lc} \\ Y'_{La} + a Y'_{Lb} + a^2 Y'_{Lc} & Y'_{La} + Y'_{Lb} + Y'_{Lc} & Y'_{La} + a^2 Y'_{Lb} + a Y'_{Lc} \\ Y'_{La} + a^2 Y'_{Lb} + a Y'_{Lc} & Y'_{La} + a Y'_{Lb} + a^2 Y'_{Lc} & Y'_{La} + Y'_{Lb} + Y'_{Lc} \end{pmatrix} \qquad (2\text{-}20)$$

and for Y_{ns},

$$\bar{Y}_{ns} = \begin{pmatrix} Y'_n & 0 & 0 \\ 0 & Y'_n & 0 \\ 0 & 0 & Y'_n \end{pmatrix} \qquad (2\text{-}21)$$

Considering (2-18), (2-19), (2-20) and (2-21), (2-17) can be written in in matrix form as (2-22):

$$\begin{pmatrix} I^0 \\ I^+ \\ I^- \end{pmatrix} = \begin{pmatrix} Y_{11} & Y_{12} & Y_{13} \\ Y_{21} & Y_{22} & Y_{23} \\ Y_{31} & Y_{32} & Y_{33} \end{pmatrix} \begin{pmatrix} V^0 \\ V^+ \\ V^- \end{pmatrix} + \begin{pmatrix} Y'_n & 0 & 0 \\ 0 & Y'_n & 0 \\ 0 & 0 & Y'_n \end{pmatrix} \begin{pmatrix} V^0 - V_n^0 \\ V^+ - V_n^+ \\ V^- - V_n^- \end{pmatrix} \qquad (2\text{-}22)$$

Since there is no zero sequence voltage, negative sequence current can be calculated as:

$$I^- = Y_{32}.V^+ + Y_{33}.V^- + Y'_n.(V^- - V_n^-) \qquad (2\text{-}23)$$

V^- should increase or decrease the value of I^- produced by positive sequence voltage in such a way that the required sharing condition for unbalance load is provided. If the factor of increase or decrease is K, then V^- can be calculated as:

$$(Y_{33} + Y'_n).V^- = K.Y_{32}.V^+ \qquad (2\text{-}24)$$

So:

$$V^- = \frac{Y_{32}}{Y_{33}+Y'_n}.V^+.K \qquad (2\text{-}25)$$

V^+ is calculated by measurement of three phase voltages. Y_{32} and Y_{33} can be calculated according to (2-20) by measuring impedance of each phase at the converter output. Y'_n can be measured at no load condition and it is constant with load variations. Now, the

question is how to choose the *K* factor. For simplicity of calculations it is assumed that line impedances are close enough thereby load impedance from the point of different converters is almost identical. If line impedances are extremely different, it should be considered in calculation of *K* factor at each local control system. Equivalent line impedances results in almost equal sharing of unbalanced load before applying negative sequence voltage, *V,* as positive sequence voltages are closely equal for all sources (within a margin from the rated voltage). Before *V* is applied each converter generates *1/n* of the unbalance load with n being the number of connected converters in the microgrid. *K* which is a factor for relative increase or decrease of unbalanced current can be calculated for each source as follows:

$$K_i = \frac{SF_i - \frac{1}{n}}{\frac{1}{n}} = n.SF_i - 1 \qquad (2\text{-}26)$$

where *i* is the number of the converter and *SF* shows the desired sharing factor for each converter. If the summation of *K* factors for converters in the grid equals zero, that means unbalance load transfers between converters thereby sharing factors change accordingly. If in a microgid that is comprised of two sources, it is desired that unbalance power is shared between two converters with the ratio of ½ sharing factor for one converter would be *SF₁*=1/3 and for the other one *SF₂*=2/3. Therefore according to 2-26, *K₁*= -1/3 and *K₂*=1/3 should be chosen. This will cause the unbalance load at converter 1 to be 2/3 of the original value and at converter 2 to be 4/3 of the original value, which shows the sharing ratio of ½ for converter 1 with respect to converter 2.

As mentioned earlier, there is another term for unbalanced current which appears when a secondary control is implemented for power quality improvement at a load bus. That will be discussed in Chapter IV.

2.5 SIMULATIONS

In order to verify the analysis and the presented method for sharing of load among converters a simple microgrid comprised of two converter-interfaced power sources along with constant load, switched unbalance load, as well as switched harmonic loads, has been considered as in Figure 2.13.
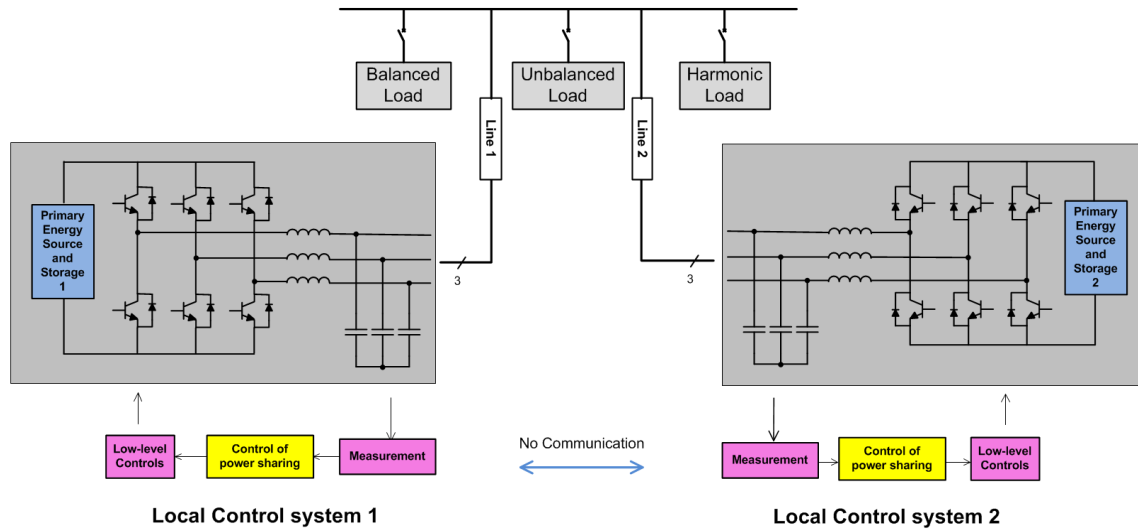
Figure 2. 13. A simple microgrid considered for power sharing simulations

Each local control system operates autonomously with no communication with the rest of the grid. A more detailed diagram of the control system is shown in Figure 2.14.

Due to the complex values of the line impedance which leads to coupling of active and reactive power in droop controls, modified active and reactive powers are used which enables decoupled control of those powers. In order to increase the precision of droop controls, voltage drop across line impedance is added to droop characteristics as an additional slope as in (2-13). Also, virtual output impedance is implemented at converters' outputs, due to the small values of line impedance, which results in better stability of the droop control. Instantaneous P-Q power theory [46][47] has been used as

36
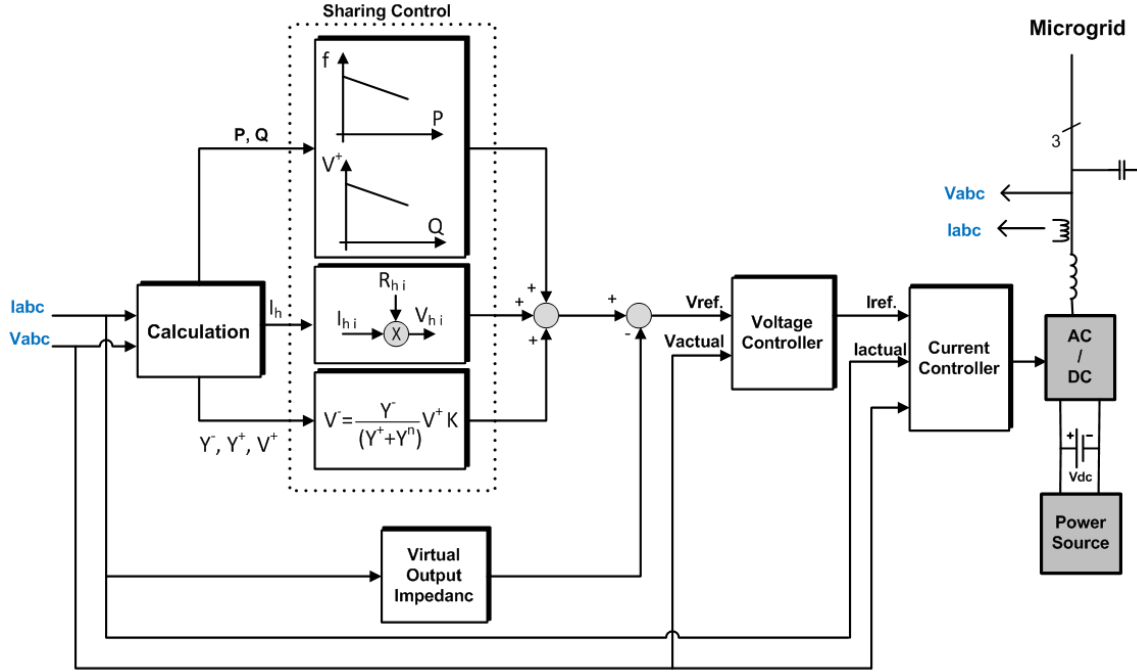
Figure 2. 14. Local control system of each converter

in (2-27) and (2- 28) for the calculation of output active and reactive power of each converter. Negative sequence current which represents unbalanced current in 3-wire systems has been calculated using Clarke transformation matrix.

$$P = v_\alpha i_\alpha + v_\text{ß} i_\text{ß} \tag{2-27}$$

$$Q = -v_\text{ß} i_\alpha + v_\alpha i_\text{ß} \tag{2-28}$$

Table 2-1 shows the parameters of the microgrid which is used in the simulation along with control strategies. It is assumed that due to different converter structures as well as switching frequencies of power supplies converter 1 is able to generate twice as much harmonic as converter 2 does. But due to smaller capacity of supply and converters half as much active and reactive power as converter 2 generates. Unbalanced current is also always shared between two converters with the ratio of ½ for converter 1 with respect to converter 2. All of the power components are controlled independently from

each other. Sharing factors in local controls can be re-tuned by the system operator in order to comply with new requirements of the system or to follow another goal for system optimization.

Table 2.1. Parameters of the simulated system

DC bus voltage:	*700V*	Line impedance:	*0.754+0.377j*
AC bus rated *RMS* voltage (phase):	*120V*	Virtual impedance:	*0.754+0.377j*
AC bus rated frequency:	*60Hz*	Constant loads:	*25kW + 25kVar*
Switching frequency:	*12kHz*	Switched Load:	Unbalanced load of *45kW + 30kVar* and a Thyristor rectifier with firing angle of 30 degrees
LC filter inductance:	*1mH*	Load Switching times	*t=1* s (switching on) and *t=2* s (switching off)
LC filter capacitance:	*123uF*	Strategy of the sharing control:	share harmonics with the ratio of *2/1* and active, reactive and unbalanced powers with the ratio of *1/2* between the two sources

Figure 2.15, 2.16, 2.17., and 2.18 show active, reactive, harmonic and unbalance load sharing respectively between the two sources both with and without the switched load. There is a balanced linear load constantly connected and a load which includes distorted current as well as unbalanced current switches *ON* and *OFF* at times *1s* and *2s* respectively. It can be seen that power components are shared between the two sources closely with the predefined share factors and with a relatively fast response time.
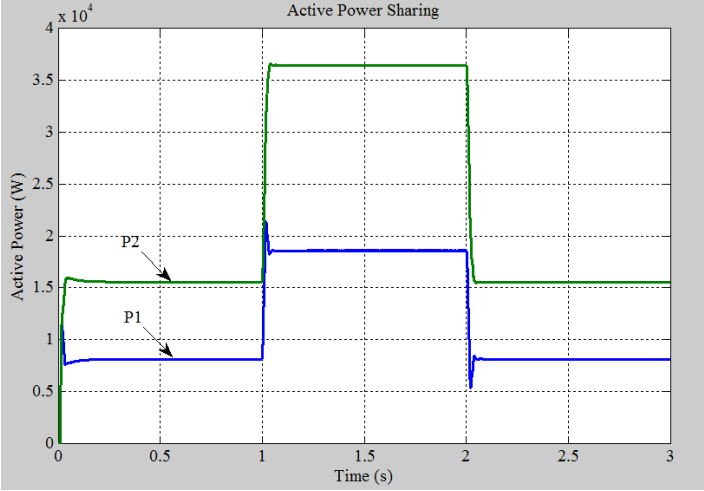
Figure 2. 15. Sharing of active current between two converters with the ratio of ½
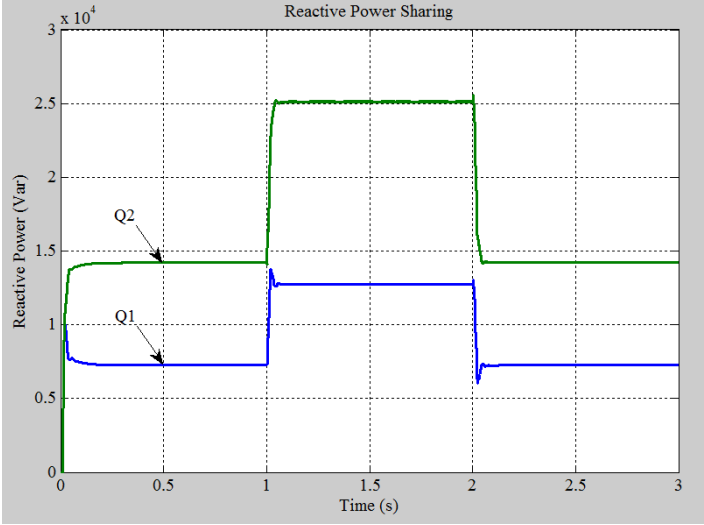
Figure 2. 16. Sharing of reactive current between two converters with the ratio of ½
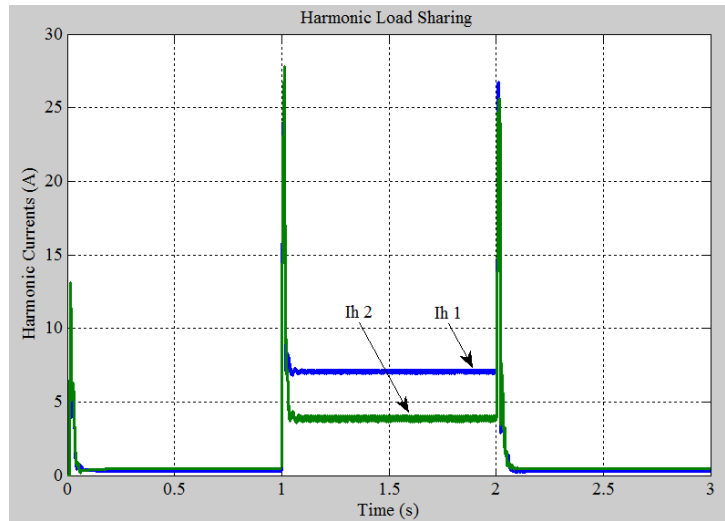
Figure 2. 17. Sharing of harmonic current between two converters with the ratio of 2/1
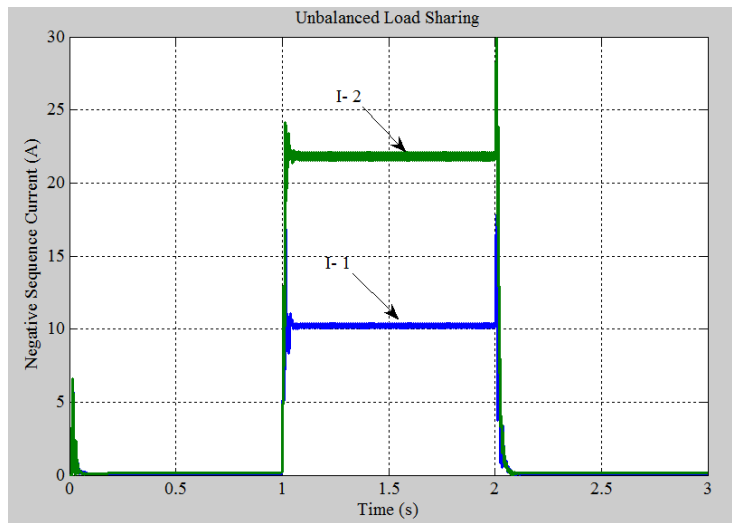
Figure 2. 18. Sharing of Unbalance current between two converters with the ratio of ½

2.6 SUMMARY

Microgrid optimization requires full control over all of the components of demanded power. Capabilities of interface power converters in providing different components of power will vary due to the availability of primary sources such as photovoltaic or wind, converter rating, converter structure and switching frequency of the converter. In this chapter, droop control for reactive power control was improved by considering the voltage drop across line inductance as well as line resistance. Negative virtual resistance was introduced in order to decouple active and reactive power. Also, decentralized control of active and reactive power was extended to harmonic and unbalanced power sharing. Four components of power are concurrently shared among power converters in the microgrid according to the sharing factors that can be different for each component. Sharing factors can be reset by the system operator after any change in the operating condition of the microgrid toward an optimization function such as cost minimization, power loss minimization, stability increase, and/or reliability increase. Simulation results show that the presented approach is able to share all power components between converters independently from each other according to the predefined settings.

CHAPTER III

CURRENT-BASED DROOP CONTROL AND *CPC* POWER THEORY

Control of output current components of a converter in a microgrid has advantages over control of power components. Current-based coordinated control of converters in a microgrid has the property of short-circuit current limiting while power-based control has an adverse impact in the presence of a short-circuit fault. Furthermore, power components may be dependent on each other under certain conditions while according to some power theories, current components are always orthogonal. In this chapter, distributed control of orthogonal current components will be presented along with simulation results for verification of the approach.

3.1 *CPC*[1] POWER THEORY

In order for distributed control of converters in a mirogrid such that all of the major power/current components are controlled independently, a comprehensive power theory must be utilized. Especially in the case of autonomous microgrids where system voltages might be asymmetrical and/or distorted, power definitions should be accurate with independent components, to prevent degrading of the coordinated control. Several power theories have been proposed and used in different applications, such as Conservative Power Theory, *p-q* theory, and Current Physical Components theory. Among those *CPC* power theory has definitions for all current components which are

---

[1] Current Physical Components

independent from each other [47-49]. The *CPC* theory provides a physical interpretation of power phenomena in three-phase systems under unbalanced and non-sinusoidal conditions and the applications of this theory under non-ideal supply voltage have been shown in [50-53].

For sinusoidal conditions, a subset of the theory decomposes the current into active, reactive, and unbalanced components. Consider a sinusoidal and symmetrical voltage source which is supplying a load zone as in Figure 3.1.
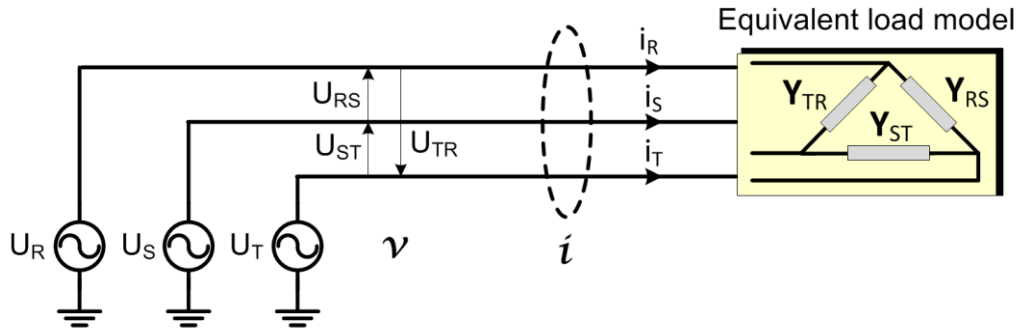
Figure 3. 1. Equivalent model of a load supplied by a three-phase voltage source

Voltage and current vectors are $\boldsymbol{u}$ and $\boldsymbol{i}$ as in (3-1) and (3-2).

$$\boldsymbol{u} = \boldsymbol{u}(t) = [u_R \quad u_S \quad u_T]^T$$

$$= \sqrt{2}\,Re\{[U_R \quad U_S \quad U_T]e^{j\omega t}\} = \sqrt{2}\,Re\{\boldsymbol{U}e^{j\omega t}\} \tag{3-1}$$

$$\boldsymbol{i} = \boldsymbol{i}(t) = [i_R \quad i_S \quad i_T]^T$$

$$= \sqrt{2}\,Re\{[I_R \quad I_S \quad I_T]e^{j\omega t}\} = \sqrt{2}\,Re\{\boldsymbol{I}e^{j\omega t}\} \tag{3-2}$$

Three-phase *RMS* voltage and current are defined as:

$$\|\boldsymbol{i}\| = \sqrt{\|i_R\|^2 + \|i_S\|^2 + \|i_T\|^2} \tag{3-3}$$

$$\|\boldsymbol{u}\| = \sqrt{\|u_R\|^2 + \|u_S\|^2 + \|u_T\|^2} \tag{3-4}$$

In order to perform the decomposition the load is expressed in terms of two admittances, the equivalent admittance and unbalanced admittance. The equivalent admittance is expressed as:

$$Y_e = G_e + jB_e = Y_{RS} + Y_{ST} + Y_{TR} \tag{3-5}$$

and the unbalance admittance is:

$$A = |A|e^{j\varphi} = -(Y_{ST} + \alpha Y_{TR} + \alpha^* Y_{RS}) \tag{3-6}$$

where $\alpha = 1e^{j120}$ and $\alpha^* = 1e^{-j120}$. Having these admittances the three-phase current vectors can be decomposed into mutually orthogonal components as (3-7).

$$i = [i_R \quad i_S \quad i_T]^T = i_a + i_r + i_u \tag{3-7}$$

where i_a, i_r, and i_u are active, reactive and unbalanced components of the current. Equivalent admittances at the point of measurement, Y_{RS}, Y_{ST}, and Y_{TR} can be calculated by the measurement of currents and voltages at this point. Current components can be calculated by means of equivalent and unbalance admittances as:

$$i_a = \sqrt{2}\, G_e Re\{U e^{j\omega t}\} \tag{3-8}$$

$$i_r = \sqrt{2}\, B_e Re\{U e^{j\omega t}\} \tag{3-9}$$

$$i_u = \sqrt{2}\, A\, R\, Re\{U e^{j\omega t}\} \tag{3-10}$$

where:

$$R = \begin{pmatrix} 1 & 0 & 0 \\ 0 & \alpha & 0 \\ 0 & 0 & \alpha^* \end{pmatrix} \tag{3-11}$$

Active, reactive and unbalanced currents are at the fundamental frequency, therefore harmonic current of the load can be calculated by subtracting them from the total current.

$$i_h = i - i_a - i_r - i_u \tag{3-12}$$

If the voltage source is non-sinusoidal, a new component appears in current which is called scattered current [49]. The amount of this component is very small as compared with major current components and it is neglected in this dissertation.

$$i = i_a + i_r + i_u + i_h + i_s \tag{3-13}$$

When voltage is also asymmetrical, as it might be in the case in an autonomous microgrid, a new term appears in calculation of active and reactive components of the current as in (3-14) and (3-15) compared to symmetrical voltage case in (3-8) and (3-9) [50].

$$i_a = \sqrt{2}\,(G_e + G_d)Re\{U e^{j\omega t}\} \tag{3-14}$$

$$i_r = \sqrt{2}\,(B_e + B_d)Re\{U e^{j\omega t}\} \tag{3-15}$$

where:

$$Y_d = Y_e - \frac{3}{\|u\|^2}\left(Y_{ST}U_R{}^2 + Y_{TR}U_S{}^2 + Y_{RS}U_T{}^2\right) = G_d + jB_d \tag{3-16}$$

As for the unbalance current there are two counter-rotating unbalance currents each of which is with respect to one sequence of source voltage.

$$I_u^n \triangleq A^p U^{p\#} - Y_d U^n \tag{3-17}$$

$$I_u^p \triangleq A^n U^{n\#} - Y_d U^p \tag{3-18}$$

where:

$$A^P = -(Y_{ST} + \alpha Y_{TR} + \alpha^* Y_{RS}) \tag{3-19}$$

$$A^n = -(Y_{ST} + \alpha^* Y_{TR} + \alpha Y_{RS}) \tag{3-20}$$

U^p and U^n are vectors of positive and negative sequence components of source voltage where the second and third element of these vectors are swapped in $U^{p\#}$ and $U^{n\#}$ as defined in [50]. Unbalance component of the current can be calculated by the use of these two parts.

$$i_u = \sqrt{2}\, Re\{(I_u^n + I_u^p)e^{j\omega t}\} \tag{3-21}$$

Harmonic component of the current can be extracted by subtraction of active, reactive, and unbalance current from the total current as in (3-12).

3.2 CONTROL OF ACTIVE AND REACTIVE COMPONENTS

Coordinated control of active and reactive current is performed by the use of current based droop control as in (3-22) and (3-23) which is derived from droop control of active and reactive power in (2-7) and (2-8).

$$f = f_0 - S_f^I . I_a \tag{3-22}$$

$$V = V_0 - S_V^I . I_r \tag{3-23}$$

where f_0 and V_0 are the nominal values of frequency and voltage magnitude and S_f^I and S_v^I are slopes of current–based droop characteristic lines of active and reactive currents as in Figure 3.2.
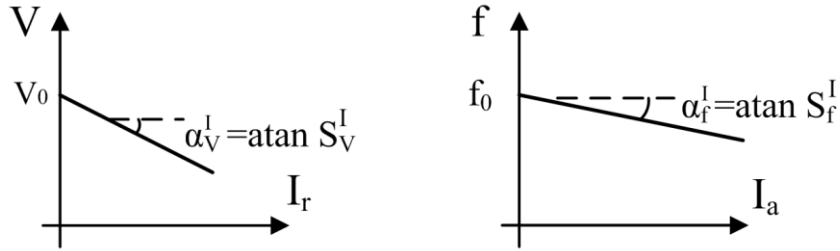
Figure 3. 2. Current-based droop characteristics for active and reactive components

As in the case of droop control for power components, modified active and reactive current can be introduced as in (3-24) to help decouple active and reactive current control when output impedance is not close enough to pure inductive as it is in the case of low voltage microgrids.

$$\begin{pmatrix} I_a{}' \\ I_r{}' \end{pmatrix} = \begin{pmatrix} sin\theta & -cos\theta \\ cos\theta & sin\theta \end{pmatrix} \begin{pmatrix} I_a \\ I_r \end{pmatrix} \tag{3-24}$$

Also, to improve reactive current droop control, voltage drop across line impedance need to be considered as an additional slope (K_i^{Ir}) in droop characteristics.

$$K_i^{Ir} = X_i + \frac{R_i}{tan\alpha_i} \tag{3-25}$$

In this equation, X_i and R_i are reactance and resistance of the line connecting the ith converter to the load center and α_i is the current phase angel with respect to voltage.

Computation of *CPC* signals is performed according to section 3-1. Fundamental components of voltages and currents have been calculated based on an efficient recursive discrete Fourier transform (*RDFT*) algorithm [54-55] as in Figure 3.3.

Ns : Number of samples per power period
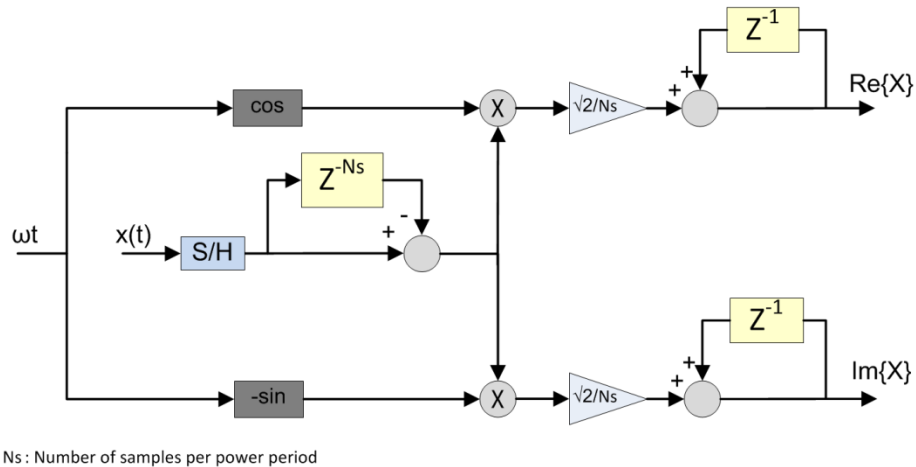
Figure 3. 3. Computation of voltage and current fundamental phasor based on *RDFT*

3.3 COORDINATED CONTROL OF HARMONIC COMPONENT OF THE LOAD CURERNT

Control of the harmonic component of the load current is performed similar to what was presented for coordinated control of each harmonic order in Chapter II. In order to share harmonic component of the load current among converters, a negative harmonic

voltage proportional to harmonic component of the current at each converter terminal, which is extracted based on *CPC* power theory, is added to the source voltage of that interface converter to implement harmonic virtual resistance. This can be seen as a droop characteristic line for harmonic sharing. The slope of this characteristic which is inversely proportional to the amount of harmonic current generated by that converter, is determined by the operator or a secondary control. In harmonic sharing of Chapter II a virtual resistance is required for each harmonic order whereas with *CPC* based current decomposition there is only one harmonic component and all of the harmonic orders of the current will be considered for sharing by a single harmonic virtual resistance, though sharing coefficients would be identical for all of the harmonic orders. Figure 3-4 shows the implementation of harmonic virtual impedance along with fundamental virtual impedance.
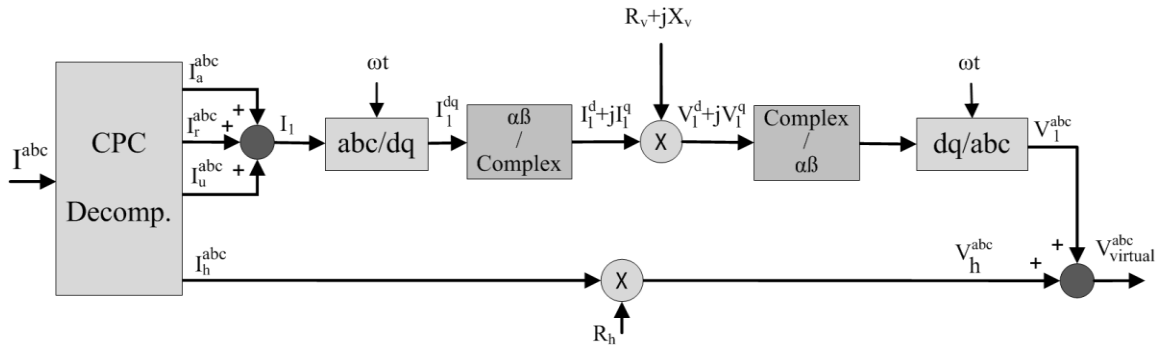
Figure 3. 4. Implementation of harmonic and fundamental virtual impedances

3.4 COORDINATED CONTROL OF UNBALANCED COMPONENT OF THE LOAD CURERNT

Based on *CPC* theory for asymmetrical voltage situations, unbalanced current consists of two parts, one with respect to positive and the other with respect to negative sequence voltage as in (3-17) and (3-18). Within the constraints of the converters

48

parameters, it is necessary to determine which part of unbalanced current is important to control. The goal might even be a minimization of both with specific weighting coefficients. Since in a microgrid the main component of the voltage is the positive sequence, unbalance current with respect to positive sequence voltage is considered to be shared among converters in this dissertation. A method is developed which is based on setting the negative sequence voltage to compensate a part of the negative sequence current produced by positive sequence voltage due to unbalance loading. The amount of this part depends on the share of converter for unbalanced current generation. If a secondary control exists, as will be explained in Chapter IV, there would be an extra part in unbalanced current. In Chapter IV it will be shown that another controller is also used in such a case for sharing of the increased amount of unbalanced current due to the increase of negative sequence voltage by the secondary control.

As mentioned above, unbalanced current of an asymmetrically supplied load in terms of *CPC* power theory has two counter-rotating parts. One is with respect to positive sequence voltage and the other with respect to negative sequence voltage. The former current is negative sequence and the later one is positive sequence current.

$$I_u^n = \begin{pmatrix} I_{u-R}^n \\ I_{u-S}^n \\ I_{u-T}^n \end{pmatrix} = (A^P U^P - Y_d U^n) . \begin{pmatrix} 1 \\ \alpha \\ \alpha^* \end{pmatrix} \tag{3-26}$$

$$I_u^P = \begin{pmatrix} I_{u-R}^P \\ I_{u-S}^P \\ I_{u-T}^P \end{pmatrix} = (A^n U^n - Y_d U^P) . \begin{pmatrix} 1 \\ \alpha^* \\ \alpha \end{pmatrix} \tag{3-27}$$

where I_u^n is the vector of three-phase negative sequence unbalance current and I_u^p is the vector of three-phase positive sequence unbalance current. U^p and U^n are phasors of phase R for positive and negative sequence of the supply voltage. Here, the calculation is

formed to share the negative sequence part of the unbalance current as in (3-26), but it can be extended to a combination of the two parts. Equation (3-26) for the phase R of the current yields

$$I_{u-R}^n = \mathbf{A}^P U^P - \mathbf{Y}_d U^n \tag{3-28}$$

The first term of unbalance current in (3-28) is due to load imbalance and exists even with balanced voltage. The second term appears in the presence of negative sequence voltage on the unbalance load.

In the following, U^n is the part of negative sequence voltage which is applied in the local control and does not include the part that may be added by the secondary control. In order for U^n to be able to control I_{u-R}^n it is easier if the two parts in (3-28) be kept in the same phase. Therefore:

$$-\mathbf{Y}_d U^n = K\mathbf{A}^P U^P \tag{3-29}$$

where K is a real value that controls the negative sequence current. Substituting the values of $\mathbf{Y}_d$ and $\mathbf{A}^P$ in (3-29) and converting the phase voltages to symmetrical components yields a vector equation as in (3-30) for the calculation of the magnitude and phase of U^n.

$$-|U^n|^2 (A \cos\varphi + \sqrt{3}B \sin\varphi)(\cos\varphi + j \sin\varphi) = C \left(|U^n|^2 + |U^p|^2 \right) \tag{3-30}$$

$|U^n|$ and $|U^p|$ are the magnitude of negative and positive sequence voltage and φ is the angle of U^n with respect to U^P. Also in this equation:

$$A = \mathbf{Y}_e - 3\mathbf{Y}_{ST} \tag{3-31}$$

$$B = \mathbf{Y}_{TR} - \mathbf{Y}_{RS} \tag{3-32}$$

$$C = K\mathbf{A}^P \tag{3-33}$$

In order for this equation to have a solution there are two conditions as below:

$$(\sqrt{3}\,\text{Im}\{BC^*\} + \text{Re}\{AC^*\})^2 - 4\sqrt{3}\,\text{Re}\{BC^*\}\,\text{Im}\{AC^*\} \geqslant 0 \tag{3-34}$$

$$\frac{d}{a\cos^2\varphi + b\sin^2\varphi + c\sin\varphi\cos\varphi + d} \leqslant 0 \tag{3-35}$$

where:

$$a = Re\{A\} \tag{3-36}$$

$$b = -\sqrt{3}\,Im\{B\} \tag{3-37}$$

$$c = -Im\{A\} + \sqrt{3}\,Re\{B\} \tag{3-38}$$

$$d = Re\{C\} \tag{3-39}$$

The last two conditions may not always be true, but in the calculation of phase impedances i.e. Y_{RS} , Y_{ST} , and Y_{TR} there is an extra degree of freedom which gives infinite set of impedances all of which bring about the same line current. Therefore, the impedance values are checked and a set of impedances which satisfies the above conditions is picked. Change of K in (3-29) leads to change of negative sequence voltage applied which in turn changes the negative sequence unbalance current in (3-28). The amount of the first term in unbalance current, $A^P U^P$, is known for converters with the knowledge of line impedances. K factors can be set to increase or decrease unbalance current to reach to a desired sharing of unbalance current among converters.

3.5 SIMULATIONS

This control method for current-based sharing of load components based on *CPC* power theory was applied in a simulation to a microgrid comprised of two converter interfaced power sources which are connecting to a load center through lines impedances. The load center includes a constant balanced load, a switched balanced and a switched unbalance load, as well as a switched harmonic load. Figure 3.5 shows the block diagram of the simulated microgrid and Figure 3.6 shows the control system implemented on each

interface converter in the microgrid. Table 3.1 shows the circuit parameters of the microgrid which are used in the simulation, along with control strategies.

For the simulations shown in this chapter, no specific optimization function is considered. It is assumed that due to different structures as well as switching frequencies of the power supply interface converters, converter 1 is able to generate twice as much harmonic current as converter 2; but due to smaller capacity of the primary supply as well as smaller converter rating, converter 1 is able to generate half as much active and reactive power as converter 2. Unbalanced current also is considered to be shared between the two converters with proportion to ½ for converter 1 with respect to converter 2 due to larger capacitor on the *DC* bus of converter 2. The sharing ratios are shown in Table 3.1. All of the current components are controlled independently from each other. Sharing factors in local controls can be re-tuned by the operator or a secondary control in order to comply with new requirements of the system or to follow another target for
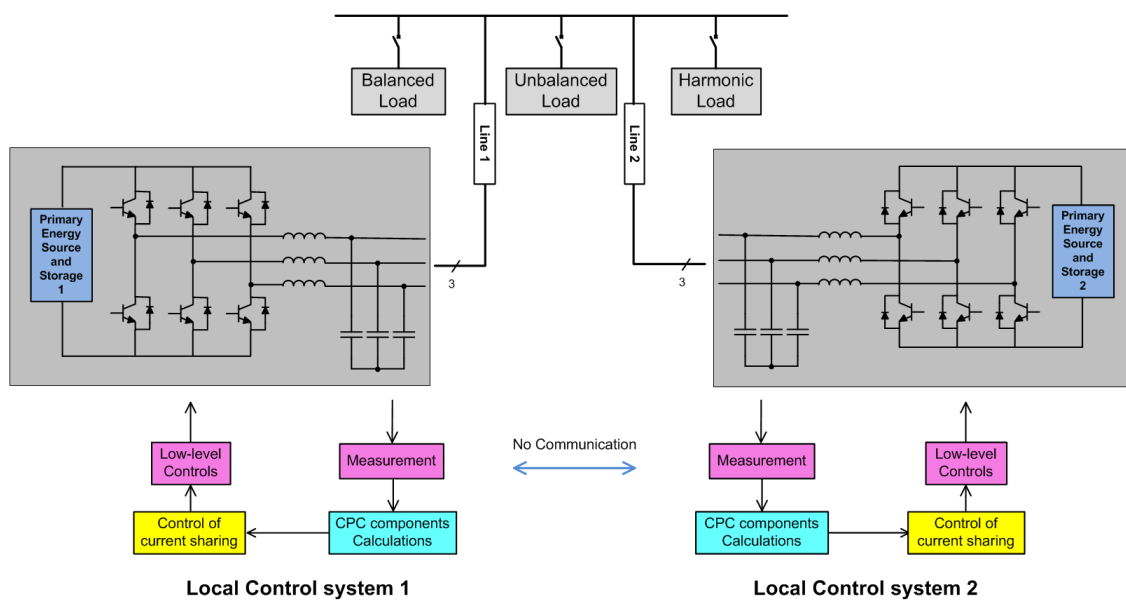
Figure 3. 5. Simulated microgrid for current components sharing

52
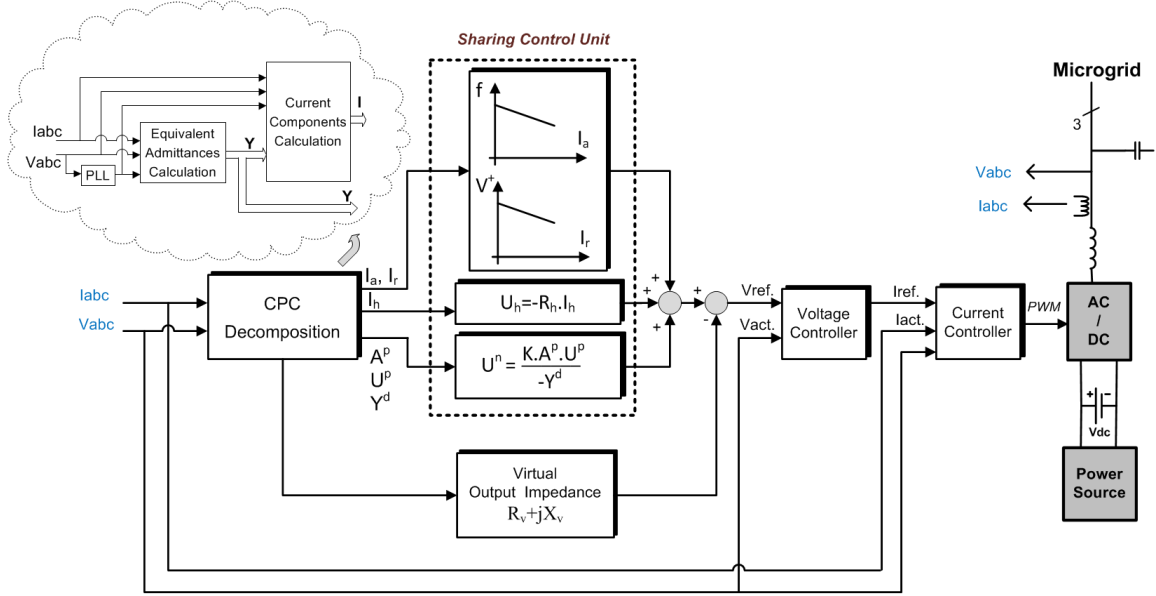
Figure 3. 6. Block diagram of the local control system

Table 3.1. Parameters of the simulated system

DC bus voltage:	*1000V*	Line impedance:	*0.754+0.377j*
AC bus rated *RMS* voltage (phase):	*120V*	Virtual impedance:	*0.754+0.377j*
AC bus rated frequency:	*60Hz*	Constant loads:	*21kW + 15kVar*
Switching frequency:	*12kHz*	Switched Load:	Balanced load of *15kW + 10kVar* . Unbalanced load of *30kW + 20kVar* and a thyristor rectifier with firing angle of 30 degrees
LC filter inductance:	*1mH*	Load Switching times	*t=1 s* (switching on) and *t=2 s* (switching off)
LC filter capacitance:	*123uF*	Strategy of the sharing control:	share harmonics with the ratio of *2/1* and active, reactive and unbalanced powers with the ratio of *1/2* between the two sources

system optimization. Figures 3.7, 3.8, 3.9, and 3.10 show active, reactive, harmonic and unbalance current sharing respectively between the two sources, both with and without the switched load. There is a constant balanced load in the grid and an unbalanced load and a harmonic load are switched on at *t=1s* and switched off at *t=2s*. It can be seen that

53

current components are shared between two sources with the predefined share factors. Figure 3.11 shows load bus three phase voltages during the load switching and the quality of voltage at load bus. When an unbalanced and distorted load switches in, voltage magnitude decreases, frequency drops and voltage is distorted and unbalance. This is due to voltage drop across transmission line as well as drop of voltage magnitude and frequency by droop control and also the effect of harmonic and unbalance sharing control. In the next chapter a higher level control will be introduced and implemented to improve the quality of voltage at load bus.
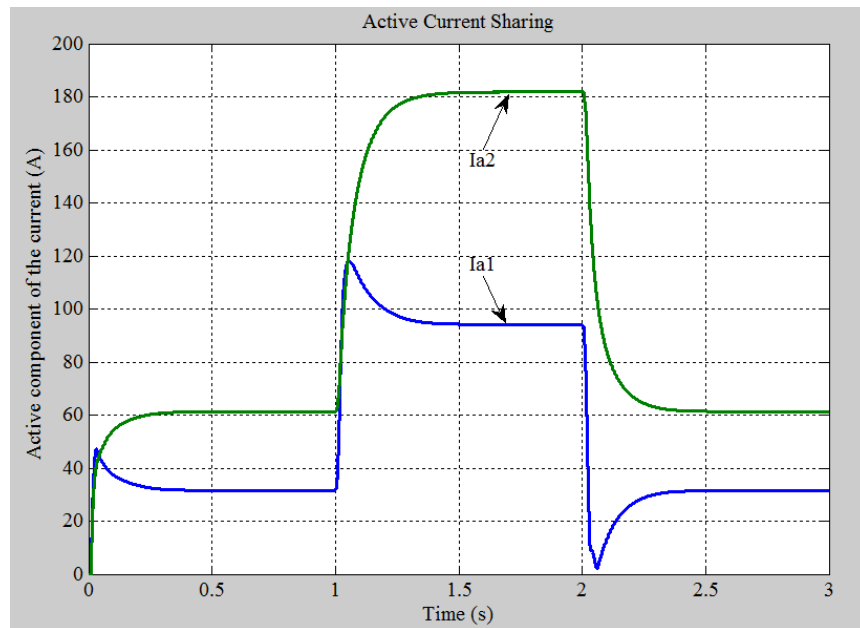
Figure 3. 7. Active current sharing between two converters with the ratio of *1/2*
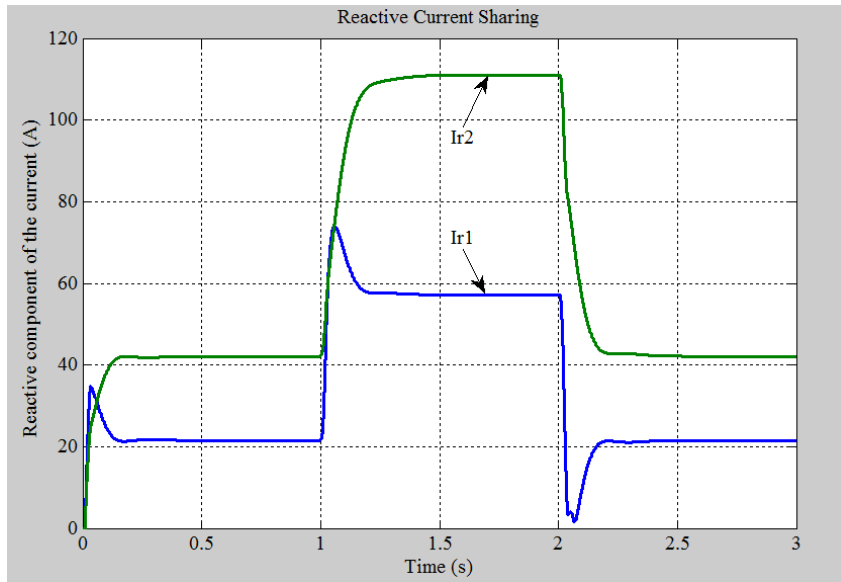
Figure 3. 8. Reactive current sharing between two converters with the ratio of ½
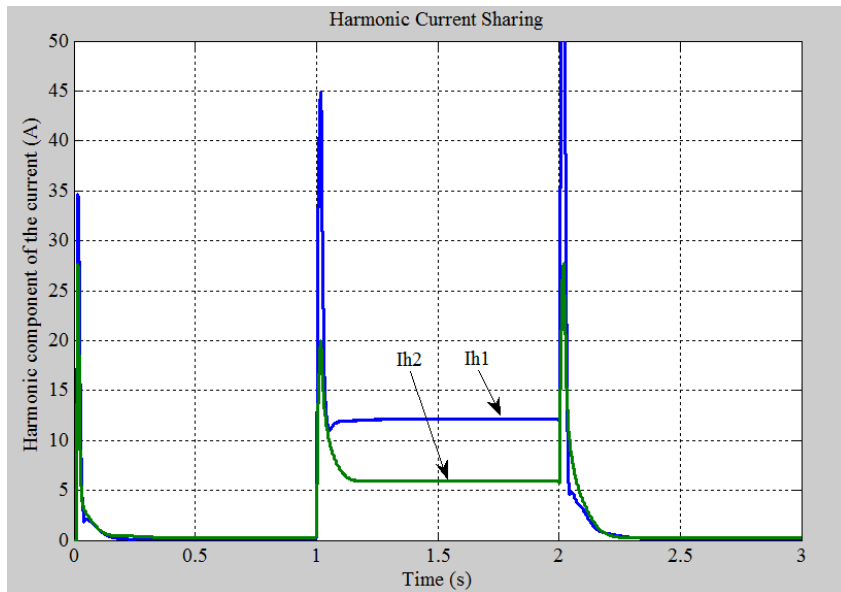
Figure 3. 9. Harmonic current sharing between two converters with the ratio of *2/1*
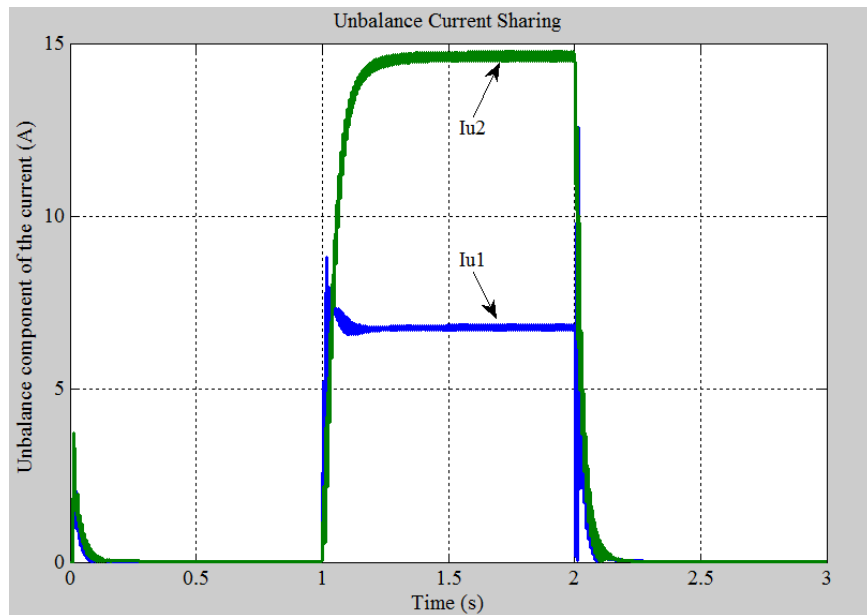
Figure 3. 10. Unbalance current sharing between two converters with the ratio of *1/2*
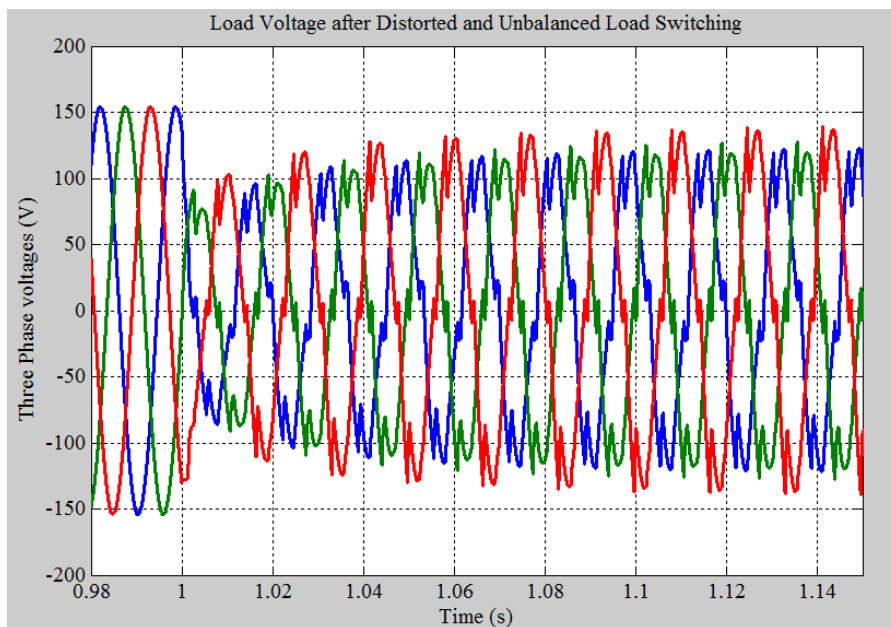
Figure 3. 11. Three phase voltages at load bus at the time of load switching

56

3.6 SUMMARY

Coordinated control of current components among converters in an autonomous microgrid was presented in this chapter. Current-based control of load sharing has advantages over power-based control including fault current limiting as well as independence of current components under *CPC* power theory. This theory has been used for decomposition of current into orthogonal components. *CPC* power theory for systems with distorted and asymmetrical supply was briefly introduced and equations for active and reactive current sharing was presented along with improvement of reactive power control by considering voltage drop across line as an extra slope for droop line characteristics. Based on *CPC* power theory, unbalanced current under asymmetrical voltage has two counter-rotating components each of which is with respect to one sequence of the voltage. As the major part of the voltage is positive sequence voltage, the unbalance current component with respect to positive sequence of voltage was considered for sharing among converters. A simulation verifies this method of coordinated control of current components. Since the load is unbalanced and distorted, due to voltage drop across line as well as the effect of current components sharing on the source voltage, the load bus voltage is unbalance and distorted which shows the requirement for power quality increase at load bus. This is performed through development of a higher level control in the next chapter with simulations for verification.

CHAPTER IV

POWER QUALITY IMPROVEMENT BY SECONDARY CONTROL LOOP

Distributed control of converters in an autonomous microgrid enables sharing of load components among converters with no need for high-bandwidth communication link as well as any single point of failure. In return, it impacts the quality of voltage throughout the microgrid. Droop control methods for active and reactive power control consists of recuding frequency and magnitude of voltage as output active and reactive power of the converter increases which causes the magnitude and frequency of load bus voltage deviate from their rated values. Furthermore, there is a voltage drop across the lines connecting sources to the load bus which increases voltage magnitude deviation on the load bus. Distributed control of harmonics and unbalanced current of the converters, which was explained in Chapters II and III, increases *THD* and unbalance component of the voltage at load buses in a similar way. In order to improve the quality of voltage at sensitive load buses, a secondary control is introduced in this chapter. This control layer has lower bandwidth compared with local controls and utilizes *LBCL*[1] to transmit data between local controls and secondary control. Secondary control collects data of voltage quality at sensitive loads bus and dispatches *DC* signals to local control systems in order to correct the reference value for output voltage in such a way that voltage quality at load bus is improved while sharing coefficients are not influenced. This control layer can also

---

[1] Low Bandwidth Communication Link

be used for management and online optimization of the microgrid as it is explained in chapter VII. For online optimization of the microgrid, management system in the secondary layer receives data of microgrid configuration, emissions, fuel availability and cost, weather conditions, the spot-market price of electricity, etc. and computes the new solution of the objective function. The new sharing factors, which are the solution of the objective function, will be sent to local controls afterwards.

4.1 ALLEVIATION OF VOLTAGE MAGNITUDE AND FREQUENCY DEVIATION AT THE LOAD BUS

Control of active and reactive power sharing by means of droop control method is performed through setting of the slope of droop characteristic line; $|V|$-Q droop for reactive power sharing and f-P droop for active power sharing. Bias of droop characteristic line is supposed to be the rated voltage magnitude for $|V|$-Q droop and rated frequency for f-P droop characteristic as it is shown in Figure 2.5. Bias of droop characteristic line should be equal for sources throughout the grid. In Figure 2.6, it can be seen that, keeping the slope of droop lines constant, increase or decrease of the bias does not affect the sharing status. Control of frequency and voltage magnitude at load bus is performed through setting of droop lines bias. Secondary control receives information about voltage magnitude and frequency at load bus through *LBCL*s and two *PI* controllers, which are properly designed to maintain voltage magnitude and frequency close to their rated values, send Δf and $\Delta|V|$ signals to local controls. Since the changes in the bias of droop lines are equal for all of the sources, sharing condition is not impacted. Figure 4.1 shows voltage magnitude and frequency correction loop in the secondary control.
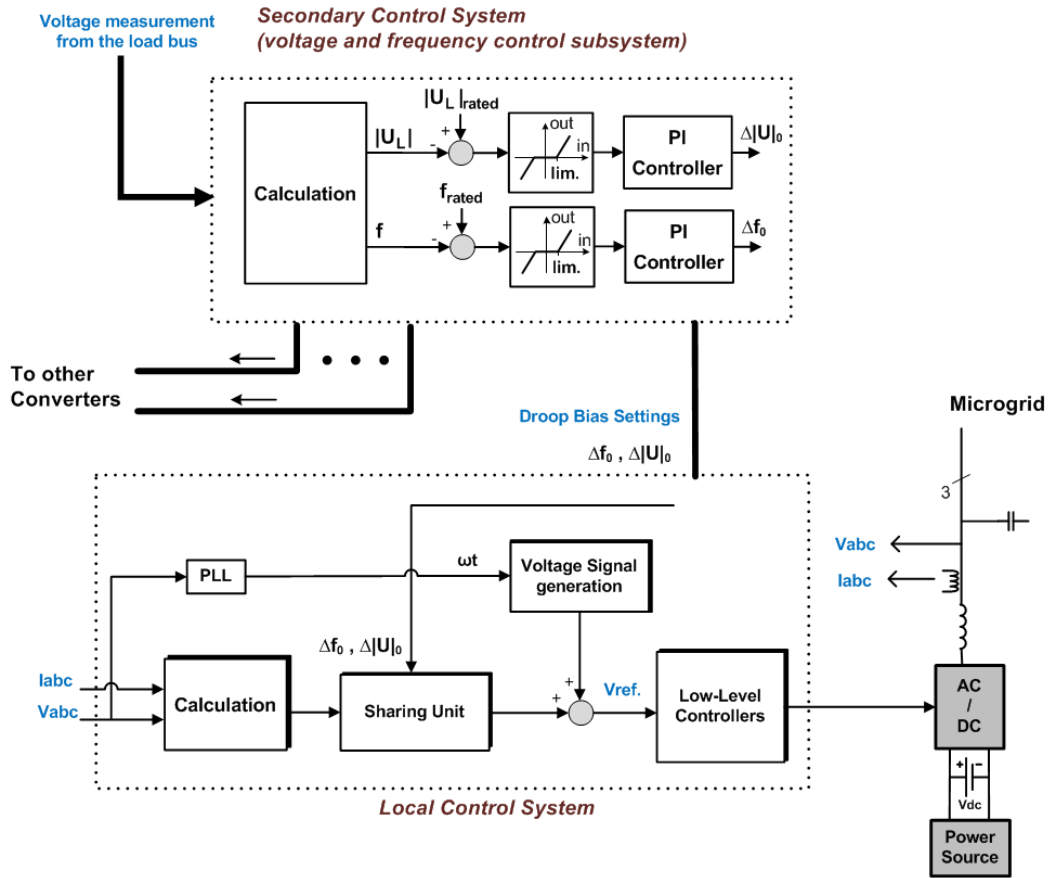
Figure 4. 1. Voltage magnitude and frequency control loop

4.2 VOLTAGE BALANCING AT THE LOAD BUS

Voltage at load bus can be balanced by tuning the negative sequence voltage at generation units. In order to do that, negative sequence voltage at load bus is measured and its magnitude is compared with zero. If the difference is inside a permissible band, no change is required in the voltage of the sources. Otherwise, the difference is inserted to a properly designed *PI* controller where the controller output is transmitted to local controls through *LBCL*s along with the phase of negative sequence voltage to be added to be added to source voltage reference value.

A complication in load voltage balancing is that negative sequence voltage of the source is already tuned in order to share unbalance current of the load among sources

60

with proper sharing ratios. Therefore, change of negative sequence voltage of sources should be in such a way that unbalanced load sharing is not affected. When load balancing in not implemented in the secondary controller, unbalance current has two parts as mentioned earlier in chapters II and III. One is due to the existence of the unbalanced load and positive sequence voltage and the other part is due to negative sequence voltage which is applied locally to control unbalance load sharing. According to general definition of unbalanced current:

$$I^n = \boldsymbol{Y}_{32}.U^P - \boldsymbol{Y}_{33}.U^n \tag{4-1}$$

with the definition of the parameters as in chapter II. With *CPC* decomposition unbalance current is:

$$I_u^n = \boldsymbol{A}^P U^P - \boldsymbol{Y}_d U^n \tag{4-2}$$

with the definition of the parameters as in chapter III. In (4-1) and (4-2) negative sequence voltage is set so that unbalanced current is shared properly among converters. Addition of a new part for U^n in the right hand side of the above equations in order to balance the voltage at load bus, should be in such a way that it does not affect unbalance current sharing. In order to maintain the proper sharing ratios a controller is used in the secondary control layer which receives the magnitude of negative sequence current at converter outputs through *LBCL*s. This controller dispatches control signals to each local control system in order to tune the magnitude of negative sequence voltage which is applied locally so that sharing condition of unbalanced current remains at the desired state while load bus voltage is also being balanced to the permissible limit. Unbalanced current can be written as:

$$I^n = \boldsymbol{Y}_{32}.U^P - \boldsymbol{Y}_{33}.[(U^n + \Delta U^n) + U_b^n] \tag{4-1}$$

61

In the above equation, U^n is the negative sequence voltage which is computed and applied locally to share unbalanced current when load voltage balancing controller does not exist. U_b^n is the output of the voltage balancing controller which is added to source voltage in order to balance voltage at load bus. Phase of this voltage is in accordance with the phase of negative sequence voltage at load bus. ΔU^n is a voltage, in phase with U^n and is added to correct the sharing ratios after addition of U_b^n to source voltage. Load bus voltage balancing control loop of the secondary control layer is shown in Figure 4.2

4.3 REDUCTION OF VOLTAGE DISTORTION AT THE LOAD BUS

When load is nonlinear voltage drop across line impedance leads to distortion on the voltage at load bus. Also harmonic sharing control which adds a distorted voltage to voltage reference value in local control causes the increase of distortion on load bus voltage. Harmonic components of the load bus voltage can be minimized by tuning the output voltage of the generation units. In the secondary control layer, each main harmonic component of the load bus voltage is calculated, compared with zero and inserted to a properly designed *PI* controller which generates the signal for the appropriate voltage of that harmonic order which needs to be added to the source voltage. One controller is required for each harmonic order. The number of considered harmonics depends on *THD* reduction requirements at load bus as well as load current characteristics. The voltage signal which is generated by each controller is transmitted to local control through *LBCL* to be added to voltage reference. It should be noted that change of harmonic currents of the load due to the addition of harmonics to source voltages is very small and negligible. Also, since the harmonic voltages that are added to different sources are identical it does not generate a flow of harmonic currents between

62

power sources. Figure 4.3 shows the control loops in the secondary control layer that are used to minimize voltage *THD* at load bus.
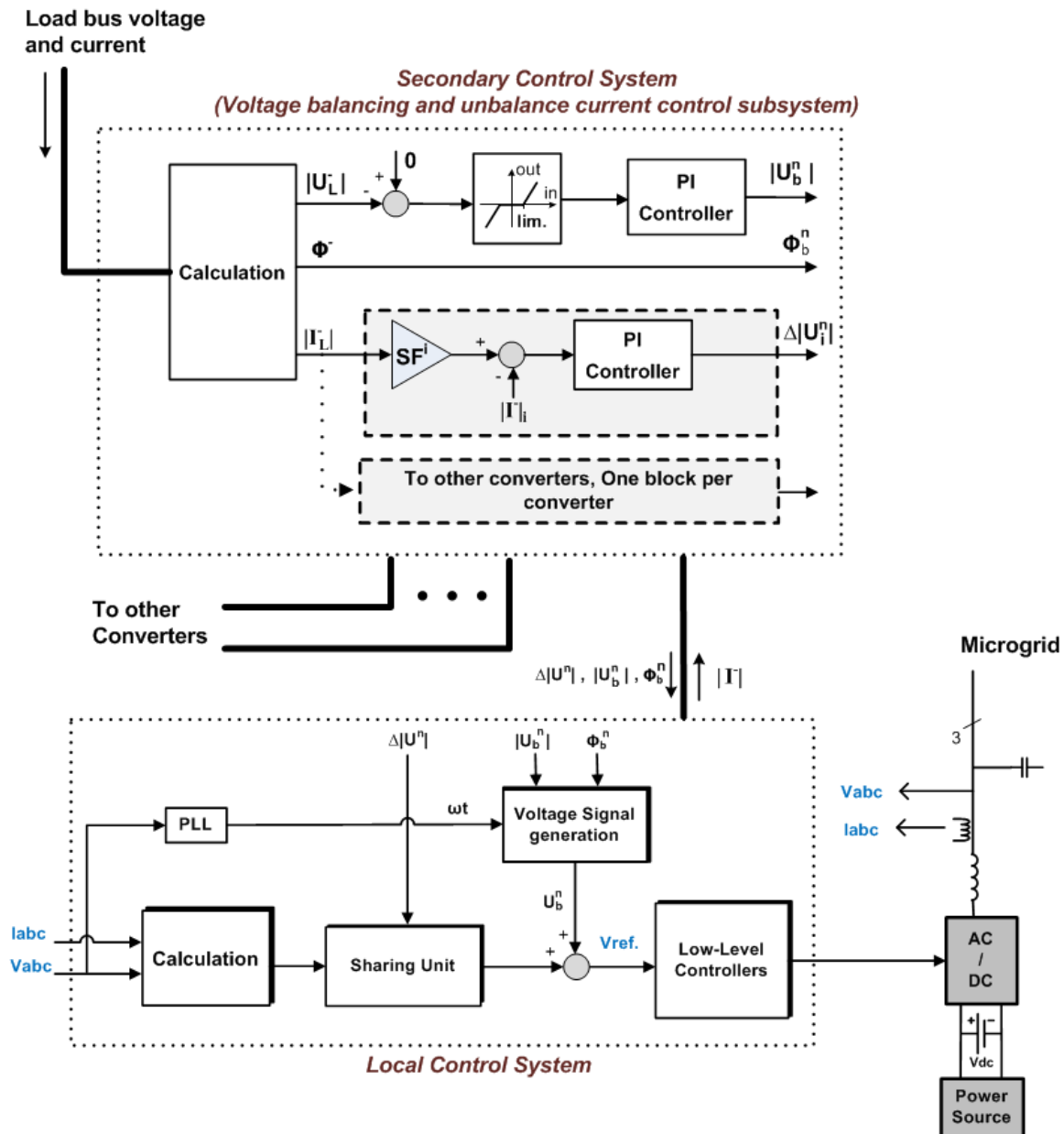
Figure 4. 2. Voltage balancing at load bus along with control of unbalance load sharing

63
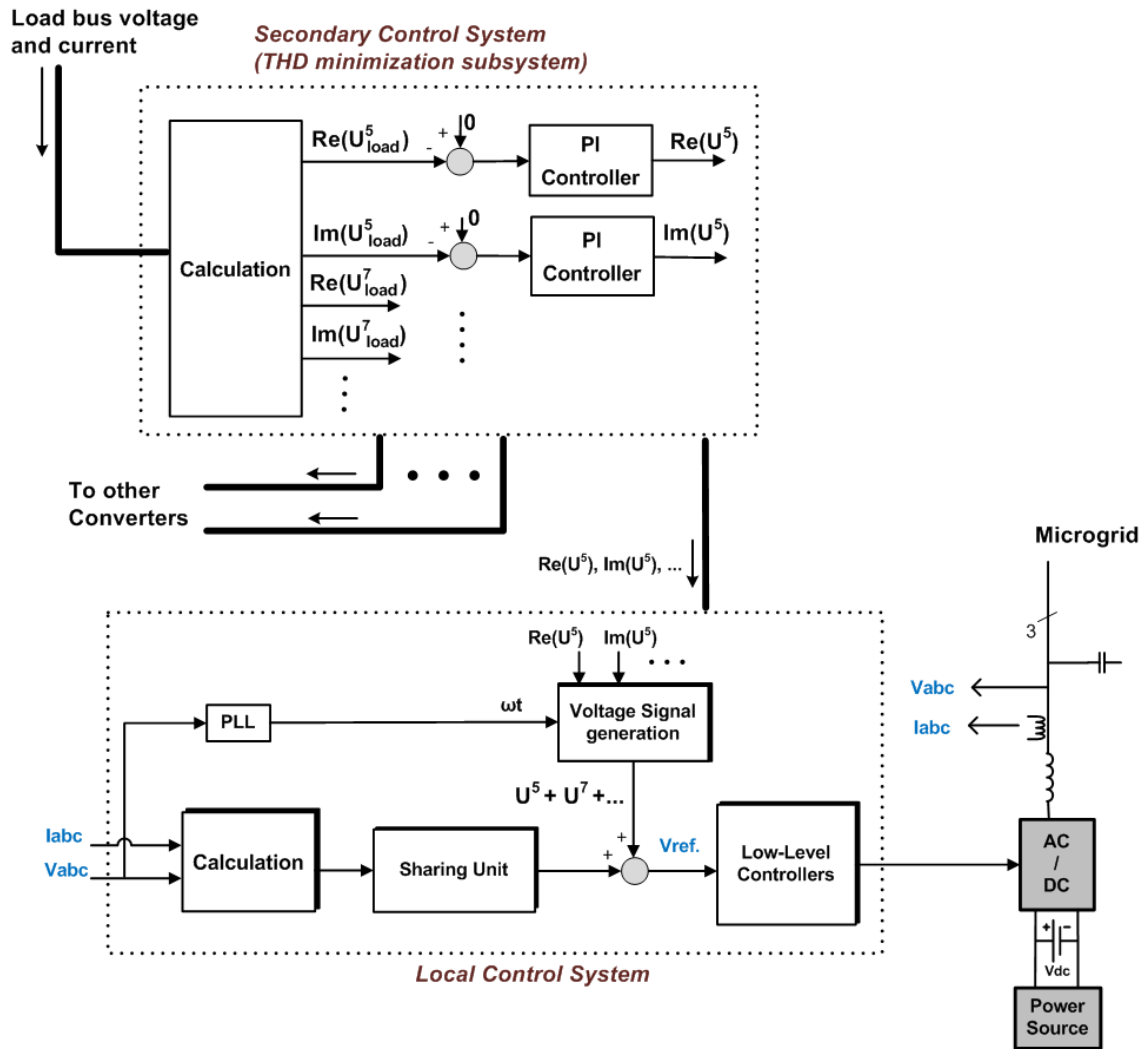
Figure 4. 3. *THD* minimization at load bus by secondary control

4.4 SIMULATIONS

Secondary control layer was added to the simulation files which were used in chapters II and III. The configuration of the system is shown in Figure 4.4. In chapter II, power-based load sharing was simulated. After switching of the load which is nonlinear and unbalanced, the magnitude and frequency of the voltage at load bus deviate from rated values and voltage is distorted as well as unbalance. Secondary control is added here to improve quality of the voltage. Parameters of the system and sharing strategies

64
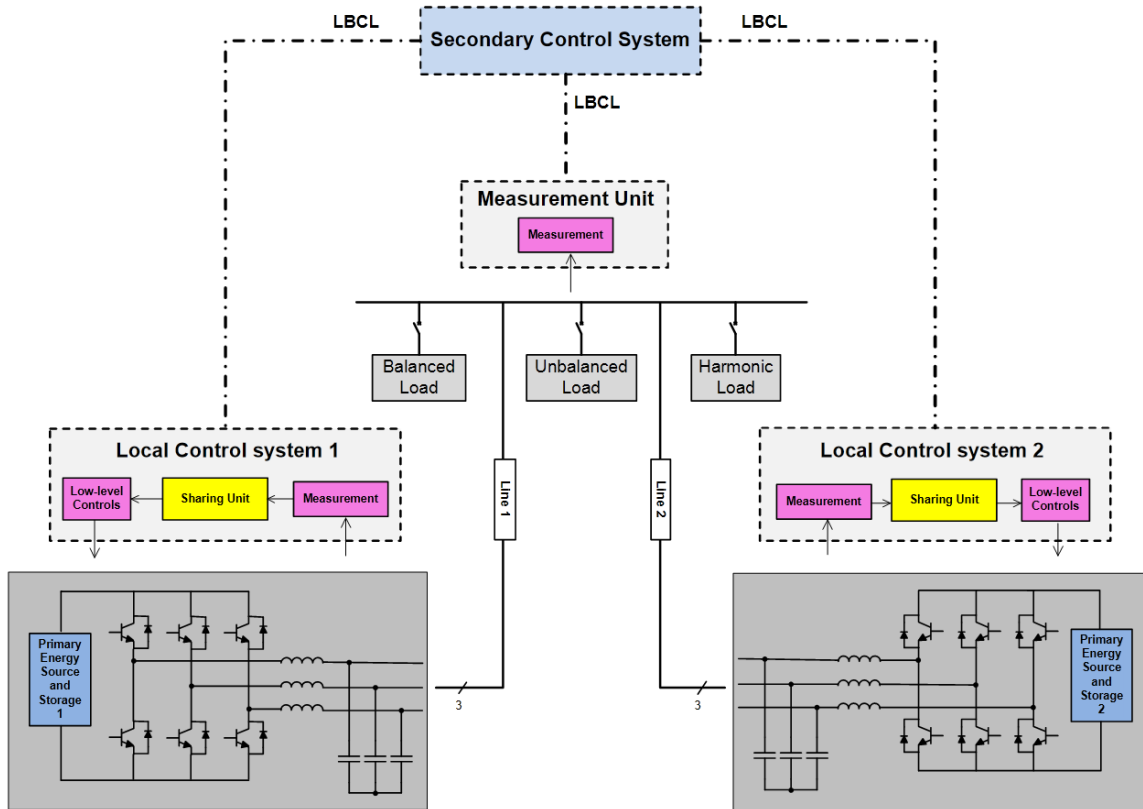
Figure 4. 4. configuration of the simulated system

are the same as shown in table 2.1. Figure 4.5 to 4.8 show that after addition of the secondary control layer sharing condition remains as desired. Compared with the results in chapter II it takes more time for the load components to reach their steady state values which is because of the slow correction of voltage due to low bandwidth of the secondary control. Figure 4.9 and 4.10 show voltage magnitude and frequency during the simulation time. It can be seen that at the time of switching, a deviation appears on frequency and voltage magnitude which is corrected by the secondary control. Figure 4.11 shows the unbalance voltage magnitude at load bus. After unbalanced load switching, a negative

sequence voltage appears at load bus which is removed by the secondary control afterwards. *THD* of the load bus voltage is measured both before and after the secondary control implementation and shown in Figure 4.12 and 4.13 which indicate the improvement of *THD* by the secondary control. Figure 4.14 shows three phase voltages during and right after load switching that confirms power quality increase at load bus.
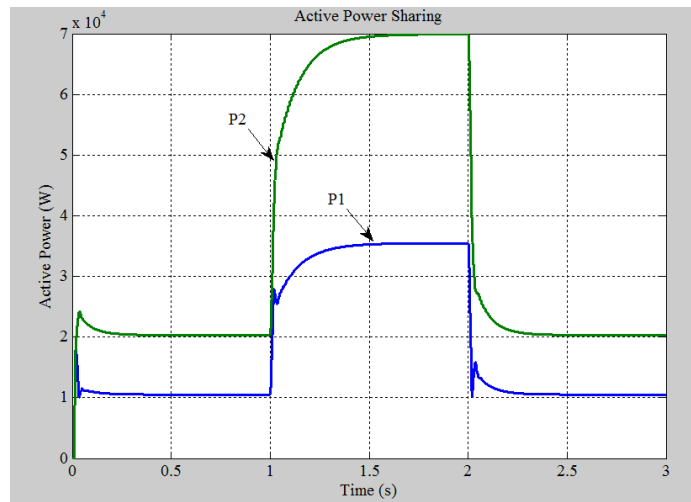
Figure 4. 5. Sharing of active power between the two converters with ratio of *1/2*
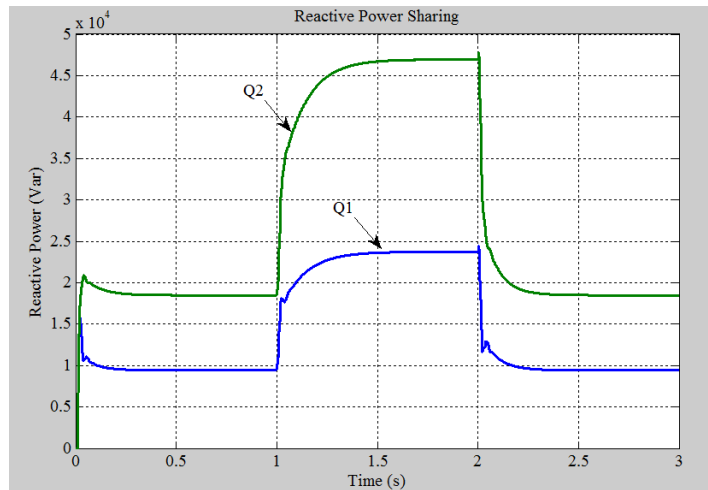
Figure 4. 6. Sharing of reactive power between the two converters with ratio of *1/2*
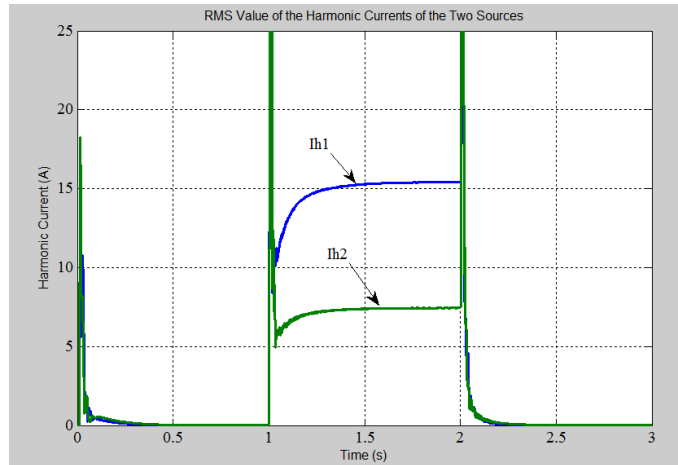
Figure 4. 7. Sharing of harmonic current between the two converters with ratio of *2/1*
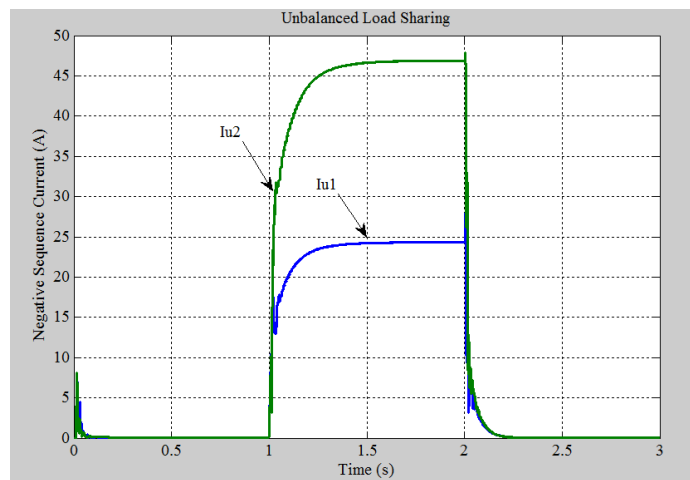
Figure 4. 8. Sharing of unbalanced current between the two converters with ratio of *½*
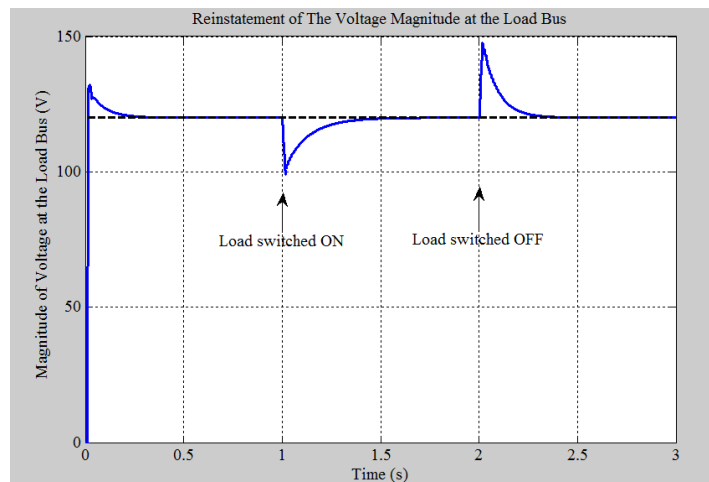
Figure 4. 9. Reinstatement of voltage magnitude at Load bus by the secondary control
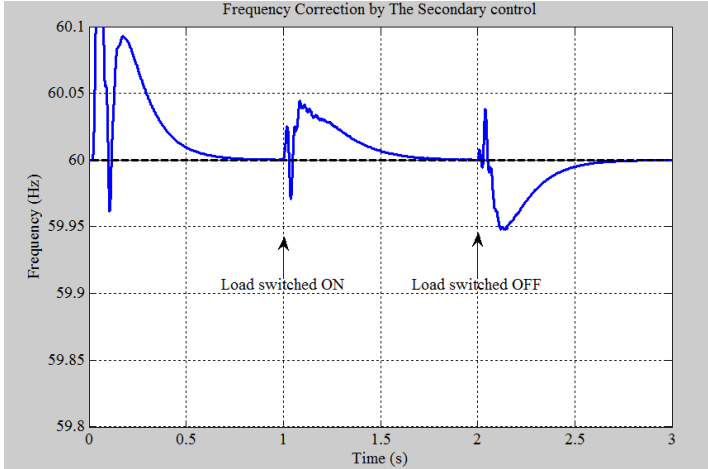
Figure 4. 10. Frequency correction by the secondary control
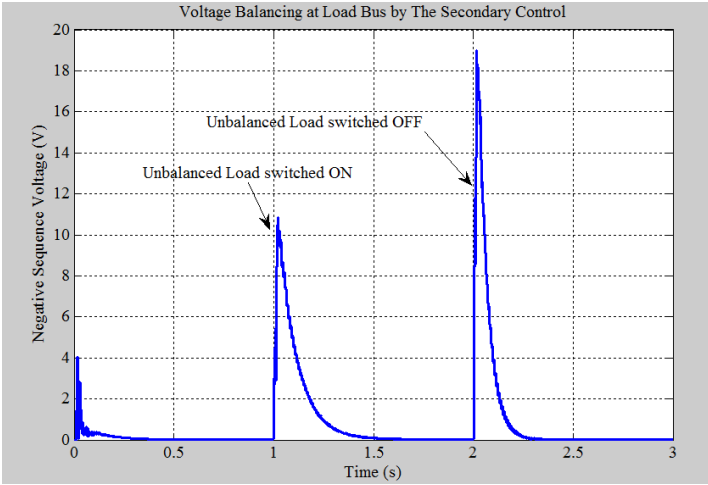
Figure 4. 11. Elimination of negative sequence voltage at load bus by secondary control
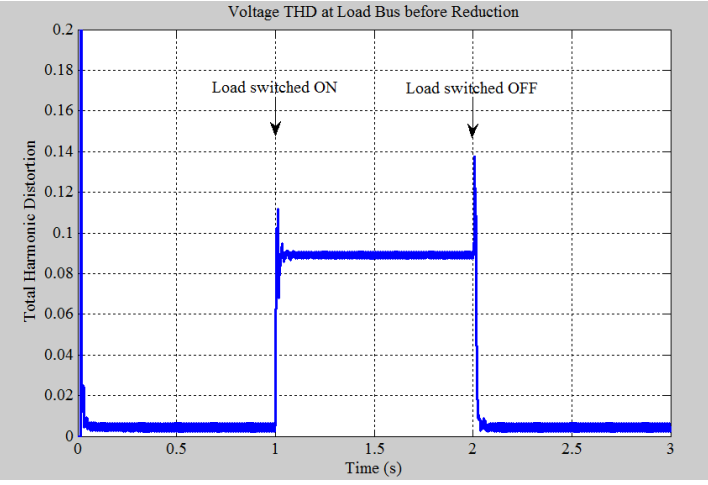
Figure 4. 12. *THD* of the voltage at load bus before implementation of the secondary control

68
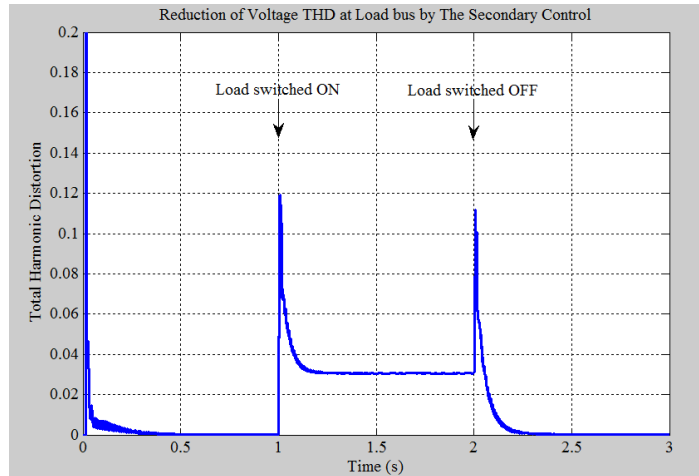
Figure 4. 13. Reduction of Voltage *THD* by the secondary control
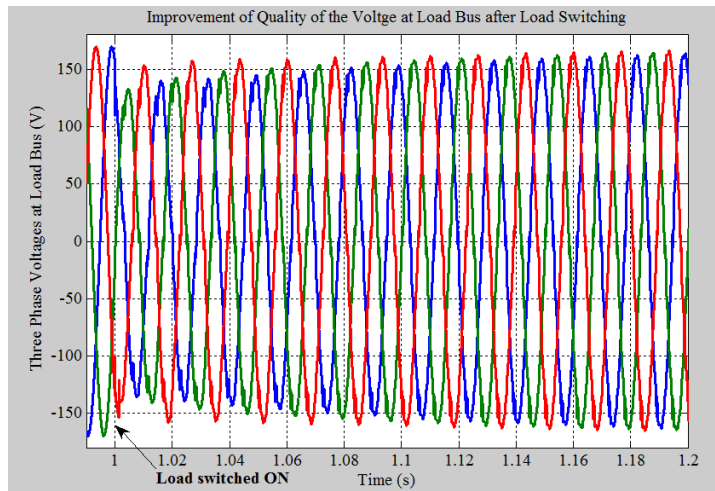
Figure 4. 14. Three phase voltages at load bus during and after load switching

In the simulations of chapter III current-based load sharing according to *CPC* power theory was shown. In this chapter, secondary control is added to that simulation with the same parameters and sharing strategy. Figure 4.15 to 4.18 show that addition of secondary control does not corrupt sharing ratios. Figure 4.19 to 4.23 show the performance of secondary control in improving the power quality indices and Figure 4.24 confirms that by showing the three phase voltages during and after switching of the load. Figure 3.10 shows these voltages before the secondary control is implemented.

69
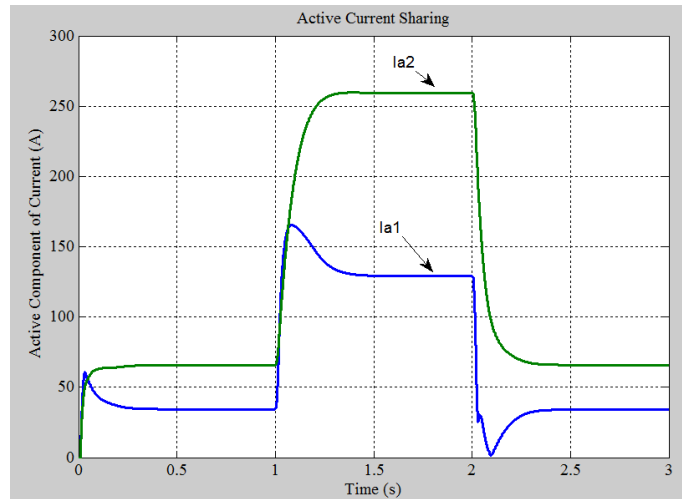
Figure 4. 15. Sharing of active current between the two converters with ratio of *1/2*
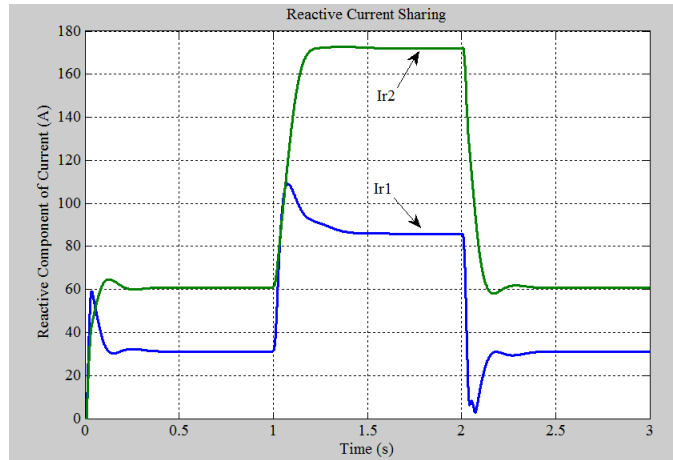
Figure 4. 16. Sharing of reactive current between the two converters with ratio of *1/2*
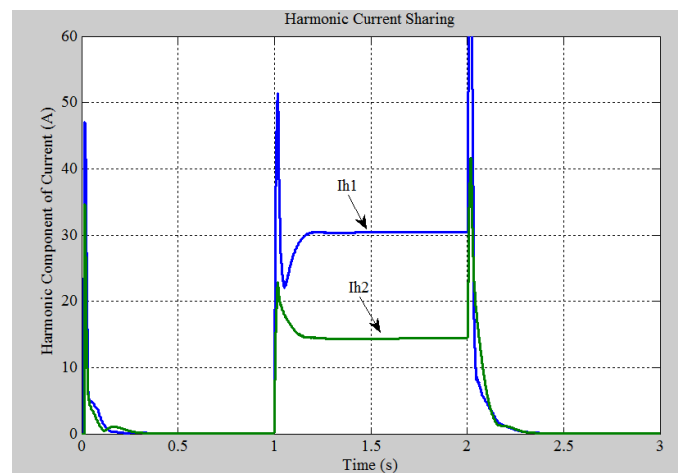
Figure 4. 17. Sharing of harmonic current between the two converters with ratio of *2/1*
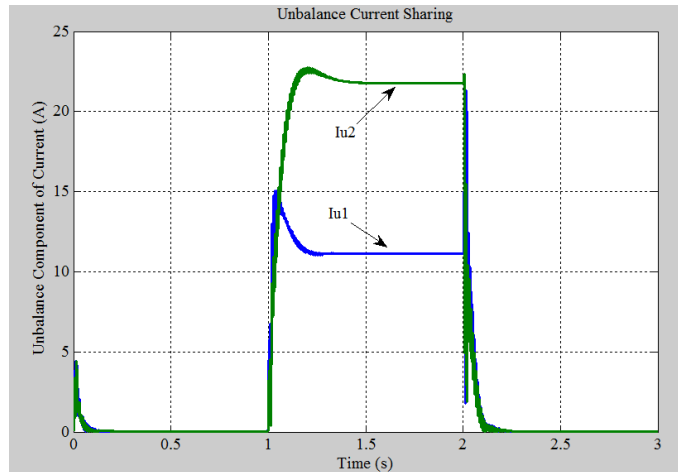
Figure 4. 18. Sharing of unbalanced current between the two converters with ratio of *1/2*
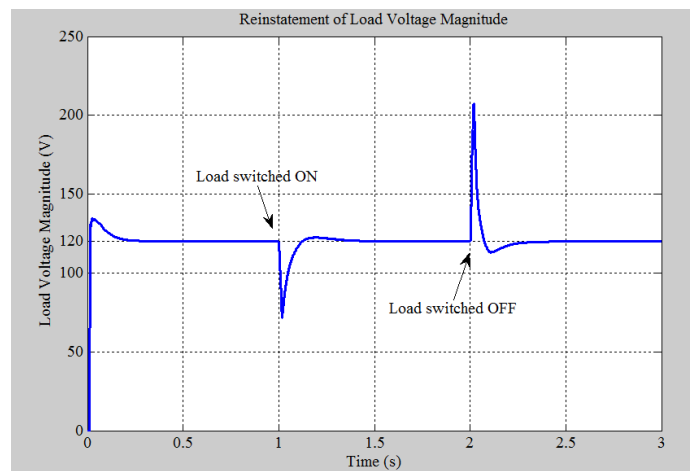
Figure 4. 19. Reinstatement of voltage magnitude at load bus by secondary control
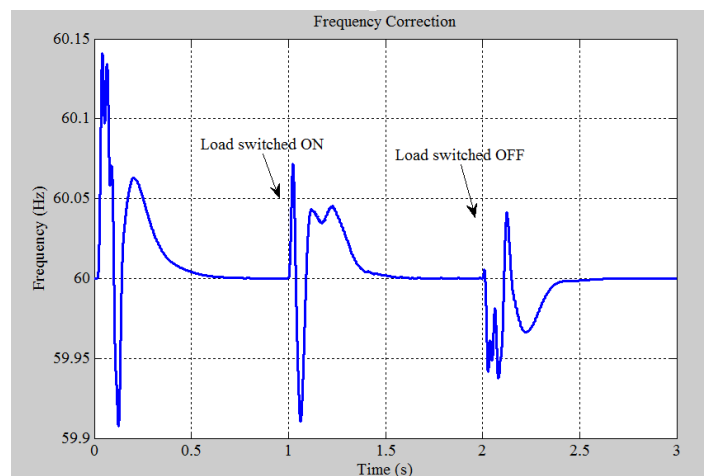
Figure 4. 20. Correction of frequency at load bus by secondary control

71
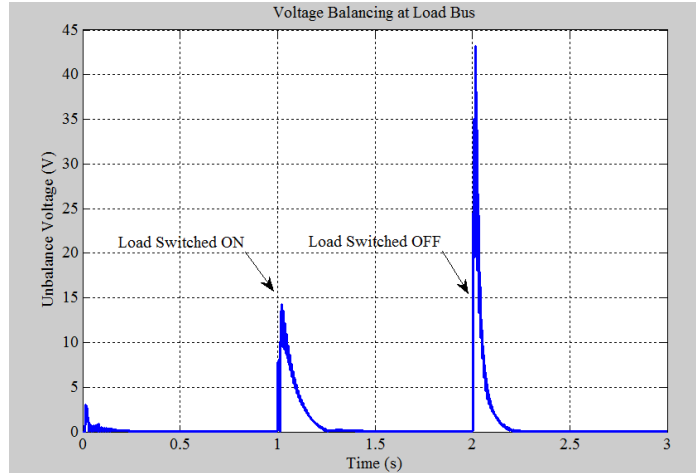
Figure 4. 21. Elimination of negative sequence component of the voltage at load bus
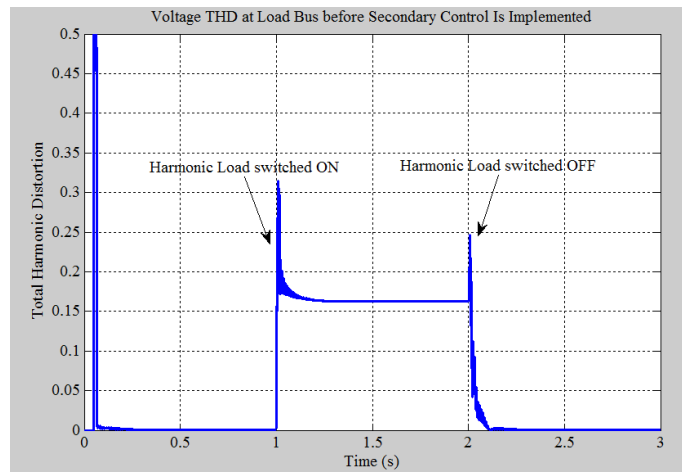
Figure 4. 22. *THD* of the voltage at load bus when secondary control is not implemented
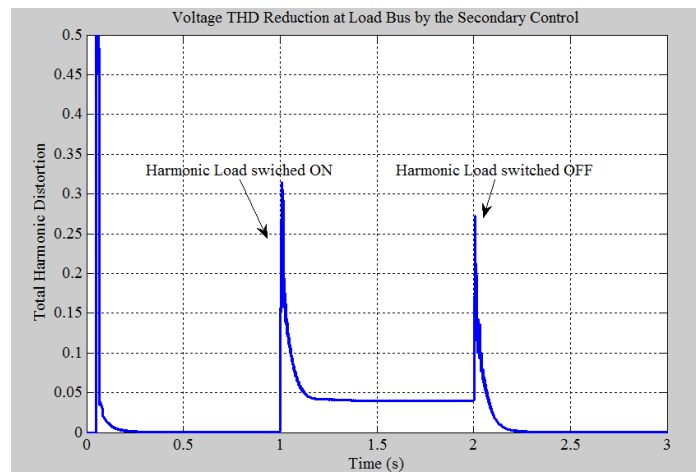
Figure 4. 23. *THD* of the voltage at load bus after secondary control is implemented

72
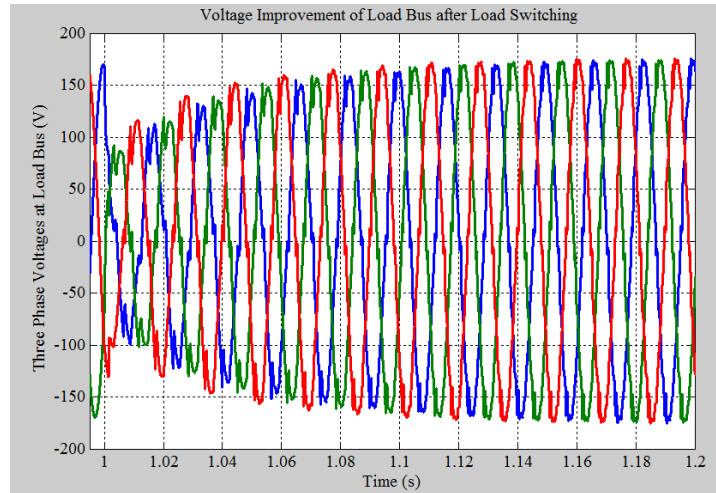
Figure 4. 24. Improvement of quality indices of the voltage at load bus - three phase voltages

4.5 SUMMARY

Switching of loads in an autonomous microgrid has an adverse impact on the quality of voltage. While load switching generally affects the magnitude of voltage at the load bus, nonlinear and unbalanced loads cause distortion and imbalance on the load voltage. The effect is increased by the performance of the load sharing units in local control systems. The load sharing unit also impacts the frequency of the system after each load switching. As local controls are operating in accordance with each other they cannot individually act toward voltage quality increase or the sharing condition will be disrupted. In order to improve the quality of voltage at load bus a secondary control layer was designed in this chapter which receives power quality indices of the load bus and applies correction signals to each local control system so that along with load voltage improvement, sharing conditions remain as desired. Control loops for improvement of each voltage index i.e. voltage magnitude, frequency, imbalance and distortion were presented. Simulation results verify the performance of secondary control in increasing power quality and confirm that desired sharing conditions are maintained.

73

CHAPTER V

Design of The Control parameters and Stability Analysis

In this chapter, the controller structure and parameters of the local control system as well as secondary control will be designed and analyzed from the viewpoint of stability issues for the range of variables. It is shown that control system is stable with reasonable stability margins.

5.1 CURRENT CONTROL LOOP

This loop is the most inner control loop and should have the highest bandwidth among all control loops. This is important considering the high bandwidth of voltage reference when converters are being controlled in coordinated with each other to supply a harmonic and unbalanced load. This controller can be of any type such as *PID* controller, adaptive deadbeat controller, P + Resonance controller, etc. For a converter supplying a load in an autonomous operation such as in Figure 5.1 a deadbeat current controller is designed and compared with a *PI* controller. The parameters of the grid are shown in table 1 considering that output *AC* voltage is not controlled in this step and only output current is being controlled. Figure 5.2 represents the response of these two controllers to a distorted current reference, shown with dots. Although deadbeat current controller causes a delay of two modulation period due to the nonzero computational time of the microprocessor and the conversion time of *A/D* converters, it shows a better dynamic response [56]. Therefore, Current controller is chosen to be a deadbeat controller.
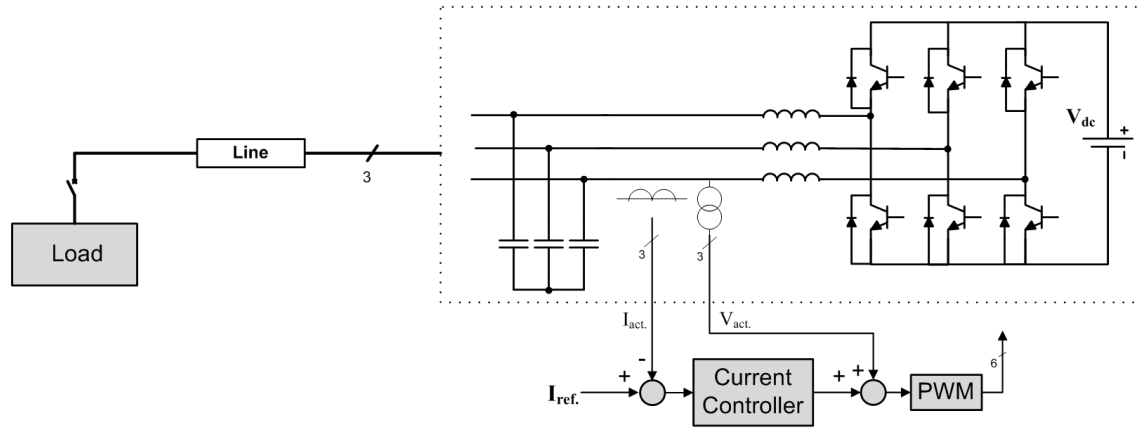
Figure 5. 1. Current controller design for a converter not connected to an active grid
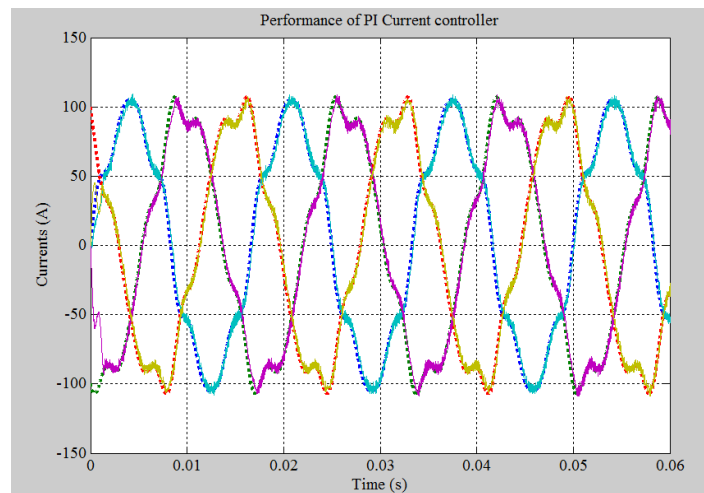
(a)
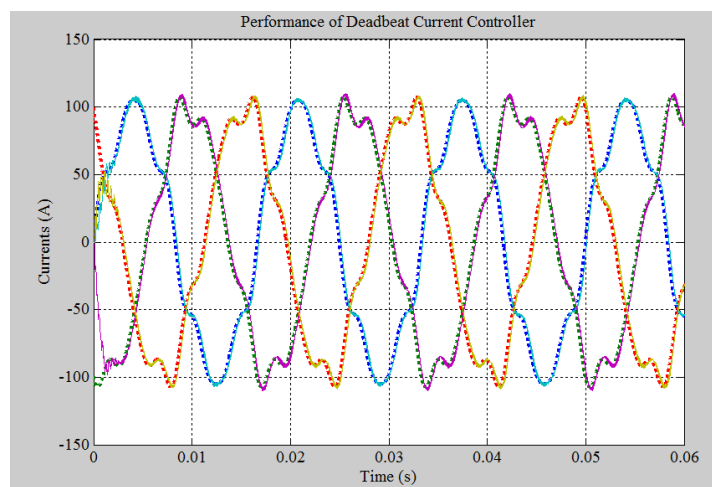
(b)

Figure 5. 2. Comparison of two current controllers, a) *PI* controller b) Deadbeat controller

75

5.2 VOLTAGE CONTROL LOOP

Voltage controller is chosen to be a *PI* controller designed in rotating synchronous frame for both positive and negative sequences of voltage as shown in Figure 5.3. The performance of this controller will be compared with that of a deadbeat voltage controller after it is designed. Figure 5.4 shows the block diagram of the inner loop controllers with the converter model.
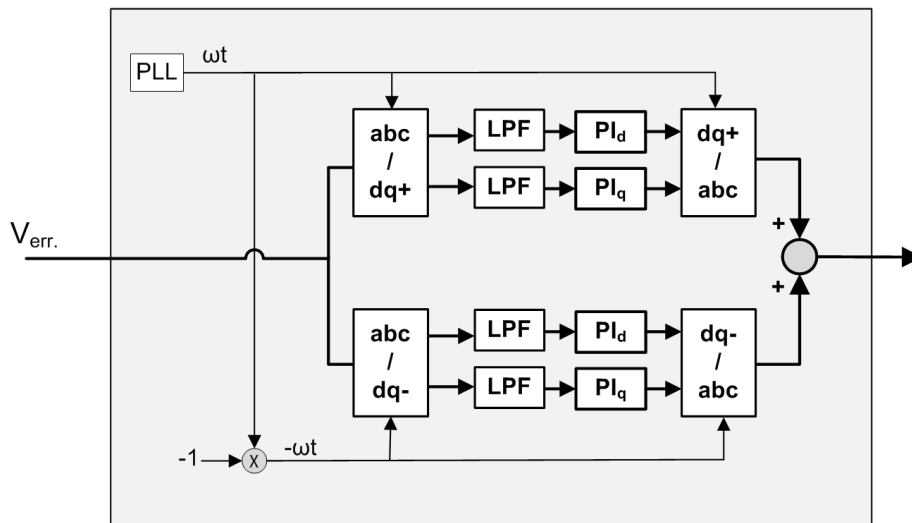
Figure 5. 3. Configuration of the voltage controller
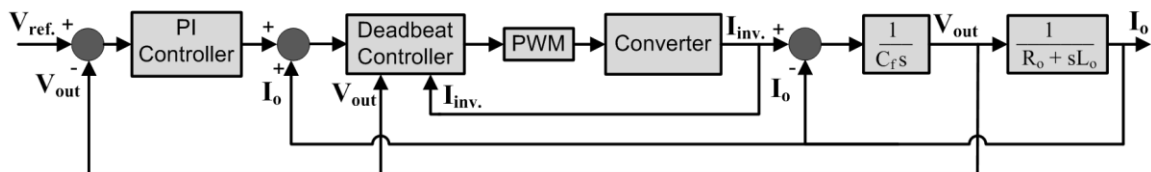
Figure 5. 4. Voltage and current controller loops with converter model

Where:

76

- *PWM* transfer function is $G_{PWM}(s) = \dfrac{1-s\frac{T_S}{4}}{1+s\frac{T_S}{4}}$; which is the first order Padé

approximation of *PWM* delay in continuous time domain.

- Converter transfer function is $G_{conv.}(s) = \dfrac{V_{DC}}{R_f + L_f s}$; with R_f and L_f being

resistance and inductance of the output filter.

- *PI* transfer function is $G_{PI}(s) = K_P + \dfrac{K_I}{s}$

Circuit parameters data are given in table 1.

Table 5.1: circuit parameters of the system

Inverter output *AC* voltage : *120 Vrms*	Output fundamental frequency *(f_0): 60Hz*
Inverter *DC* bus voltage: *700V*	Output filter Inductance *(L_f): 1mH*
Switching frequency *(f_s): 12kHz*	Output filter Resistance *(R_f): 0.02 Ω*
Sampling frequency *(f_c): 12kHz*	Output filter Capacitance *(C_f): 122.623 µF*

Since deadbeat current controller is dynamically equivalent to a two-modulation-
period delay, by using Padé approximation, the current control loop can be approximated
by

$$G_{CL-I}(s) = \frac{1-s\,T_S}{1+s\,T_S} \tag{5-1}$$

Therefore open loop transfer function of voltage controller is:

$$G_{OL-V}(s) = \frac{1-s\,T_S}{1+s\,T_S} \cdot \frac{1}{sC_f} \cdot (K_P + \frac{K_I}{s}) \tag{5-2}$$

Magnitude of G_{OL-V} at cross-over frequency is 0 *dB* and phase of that at this frequency

yields phase margin of the system.

$$|G_{OL-V}|_{w=w_{cl}} = 1$$

Calculation of the magnitude of G_{OL-V} at w_{cl} in (5-2) gives:

$$\frac{\sqrt{w_{cl}{}^2.K_P{}^2+K_I{}^2}}{w_{cl}{}^2.C_f}=1 \tag{5-3}$$

And for phase margin we'll have:

$$-180 + PM = -180 - 2\,tan^{-1}(w_{cl}.T_{s)} + tan^{-1}(\frac{w_{cl}.K_P}{K_I}) \tag{5-4}$$

Voltage controller needs to have at least a cross-over frequency of $w_{cl} = 5000\ rad/s$ for a proper performance of converter in sharing harmonic components of load current. Substituting $K_P = 0.592$ and $K_I = 793$ in (5-3) gives the required cross-over frequency. Also plugging in the values for w_{cl} , K_P and K_I in (5-4) yields $PM \cong 30°$. Gain margin can also be calculated which is $GM \cong 6.7$ for these parameters. From (5-2):

$$G_{OL-V}(s) = \frac{-T_sK_ps^2+(K_P-K_I.T_s).s+K_I}{T_s.C_f.s^3+C_f.s^2} \tag{5-5}$$

Therefore closed loop transfer function of the voltage controller is:

$$G_{CL-V}(s) = \frac{-T_sK_ps^2+(K_P-K_I.T_s).s+K_I}{T_s.C_f.s^3+(C_f-T_s.K_P).s^2+(K_P-K_I.T_s).s+K_I} \tag{5-6}$$

Plugging in the values of parameters and calculating the closed loop system poles gives:

$$s_1 = -2600 + 5800j$$

$$s_2 = -2600 - 5800j$$

$$s_3 = -1870$$

Bode plot of open loop transfer function is shown in Figure 5.5 with stability margins. Figure 5.6 shows zero-pole locations of the closed loop system. Figure 5.7 shows the locations of zero-poles of the discretized system with $T_s=1/f_s=1/12000$ s. In Figure 5.8 performance of the designed voltage controllers to a voltage reference which includes harmonics as well as unbalance component is shown.

Deadbeat voltage controller is also designed for the system and response of the system with deadbeat voltage controller is compared with that of synchronous frame *PI* controller to identical voltage references. For the voltage control application, sampling period of the deadbeat voltage controller should be two times the sapling period of current controller. The delay of the voltage control would be 4 times switching period. In this dissertation switching frequency of the converters is *12 kHz* which means the delay of deadbeat voltage control would be *4/12000* seconds which is equivalent to *7.2* degrees phase delay in voltage waveform which makes the deadbeat control inappropriate for this application especially with regard to the need for harmonic and unbalance voltage control. Deadbeat voltage controller response is shown in Figure 5.9.
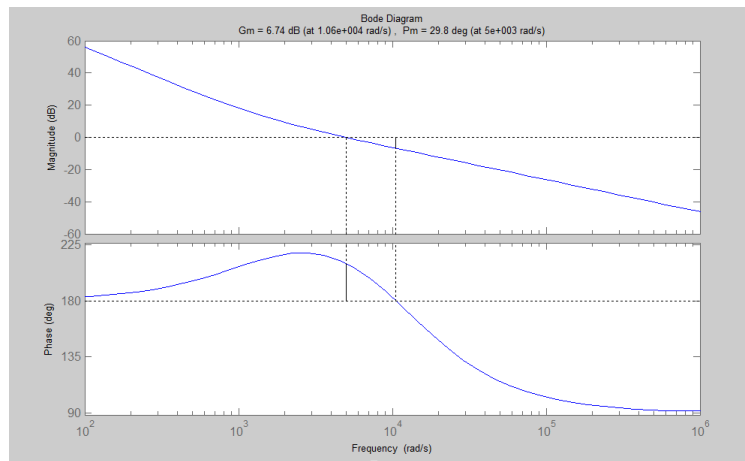
Figure 5. 5. Bode plot of voltage controller
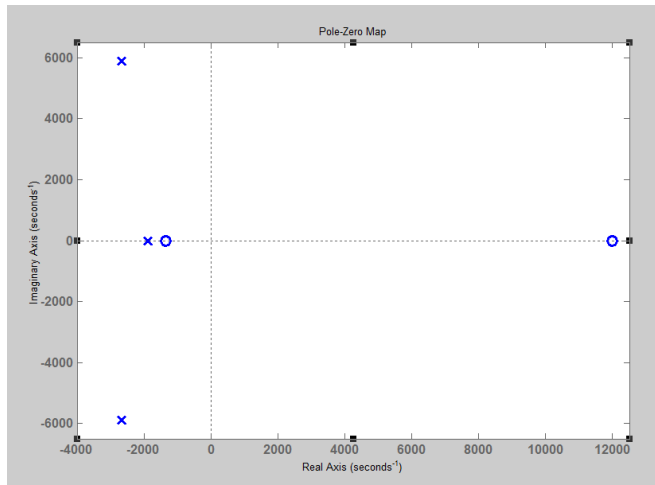
Figure 5. 6. Zero poles of voltage control closed loop system
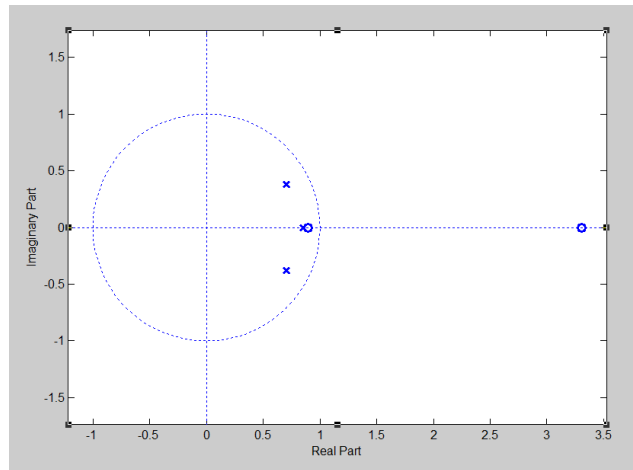
Figure 5. 7. Zero poles of the discretized voltage control closed loop system
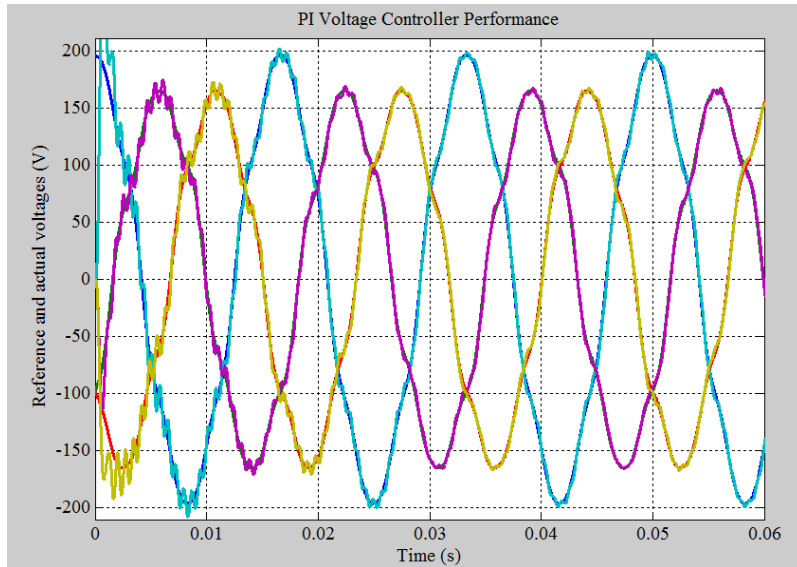
Figure 5. 8. Response of the designed *PI* voltage controller
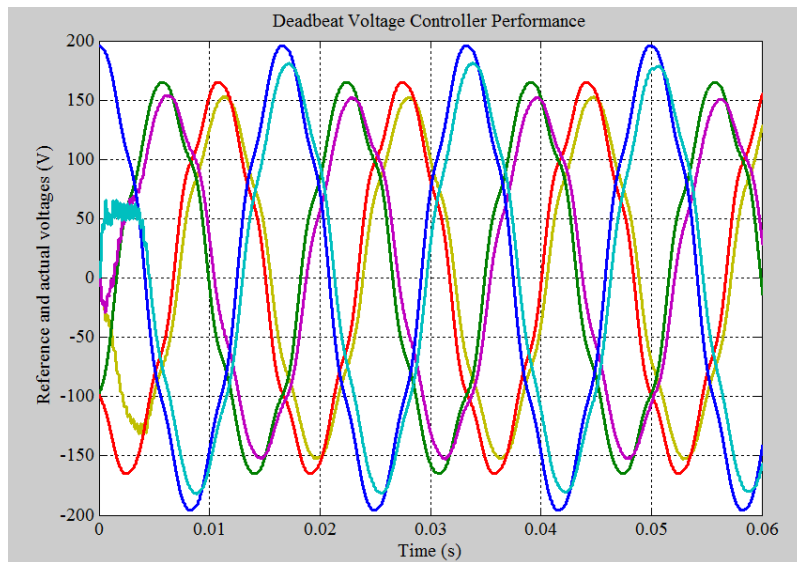
Figure 5. 9. Response of deadbeat voltage controller for this system

5.3 VIRTUAL IMPEDANCE LOOP

Figure 5.10 shows the control loop for virtual impedance implementation. In this loop, $G_{CL-V}(s)$ is closed loop transfer function of voltage controller and converter system. $G_{fil}(s)$ is transfer function of a second order low-pass filter with cut-off

81

frequency $w_c = 2\pi * 10$ and damping factor $\xi = 0.9$, R_o and L_o are output resistance and output inductance of the converter and R_v and L_v are virtual resistance and virtual inductance.
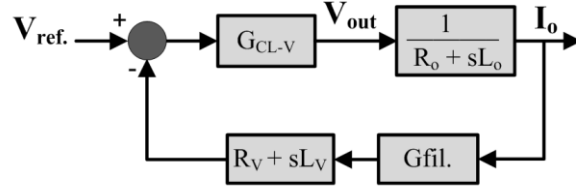
Figure 5. 10. Virtual impedance loop

$$G_{fil}(s) = \frac{w_c{}^2}{s^2 + 2\xi w_c s + w_c{}^2} \tag{5-7}$$

In order to extract certain harmonics of current (fundamental component for virtual impedance implementation in above block diagram and other harmonics for harmonic sharing loop), it is multiplied by $\sin(nwt)$ and $\cos(nwt)$ where n is the order of the harmonic. *DC* values of the two obtained signals which are extracted by a second order low-pass filter are real and imaginary parts of the nth order harmonic of current. Closed loop transfer function of virtual impedance loop is:

$$G_{CL-vir}(s) = \frac{\frac{G_{cl-V}}{R_O + sL_O}}{1 + \frac{G_{cl-V}}{R_O + sL_O} \cdot G_{fil} \cdot (R_v + sL_v)} \tag{5-8}$$

Range of variation for R_o and L_o is calculated with regard to nominal power of the source. Considering $R_o = 1.6 \, \Omega$ and $L_o = 1.7 \, \text{mH}$ poles of closed loop transfer function are calculated as:

$$s_1 = -2600 + 5800j$$

$$s_2 = -2600 - 5800j$$

$$s_3 = -1870$$

$$s_4 = -930$$

$$s_5 = -60 - 40j$$

$$s_6 = -60 - 40j$$

Root locus of the system in MATLAB shows that variation of output impedance magnitude has a very small impact on the location of system poles. Also variation of angle of the output impedance has a negligible effect on the location of the poles. Note that line impedance provides a bias for output resistance and output inductance of the converter.

Following the same method for calculation of closed loop poles of the harmonic sharing system we can see that poles are always in the left half of the s-plane. For each harmonic component to be shared among converters, a pair of poles is added in left half plane.

5.4 DROOP CONTROL LOOP

Figure 5.11 shows the block diagram of droop control loop where $G_{CL-vir}(s)$ is the closed loop transfer function of virtual impedance loop including voltage controller and converter system.
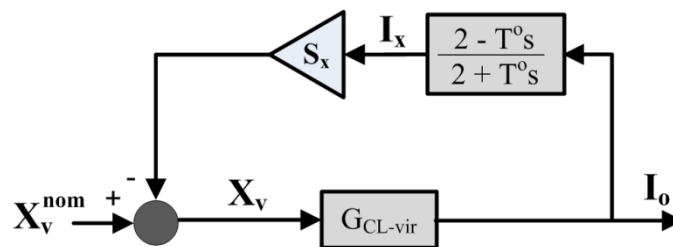
Figure 5. 11. Droop control loop

Dynamic for calculation of power/current components is approximated by a line frequency period delay. In this figure I_x represents any of the components of power/current and X is a characteristic of output voltage which directly impacts I_x. The slope of droop characteristic for this component of current is represented by S_x. Calculation for the locations of poles of closed loop transfer function of this system yields the following poles.

$$s_1 = -3100 + 6200j$$

$$s_2 = -3100 - 6200j$$

$$s_3 = -1500$$

$$s_4 = -230 + 360j$$

$$s_5 = -230 - 360j$$

$$s_6 = -60 + 30j$$

$$s_7 = -60 - 30j$$

5.5 SECONDARY CONTROL LOOP

Figure 5.12 shows the secondary control loop where R_L and L_L represent resistance and inductance of transmission line. A calculation delay of T_0 is considered for extraction of load bus voltage parameters i.e. frequency, magnitude, imbalance component and harmonic component. In this figure, x_v represents any of voltage quality parameters.

A delay is also considered for low speed communication link as of 1 second. In this control diagram calculation delay and communication delay are:

$$G_{cal}(s) = \frac{2-0.017s}{2+0.017s} \tag{5-9}$$

$$G_{comm.}(s) = \frac{2-s}{2+s} \tag{5-10}$$

$$G_{PI}(s) = K_P + \frac{K_I}{s} \tag{5-11}$$
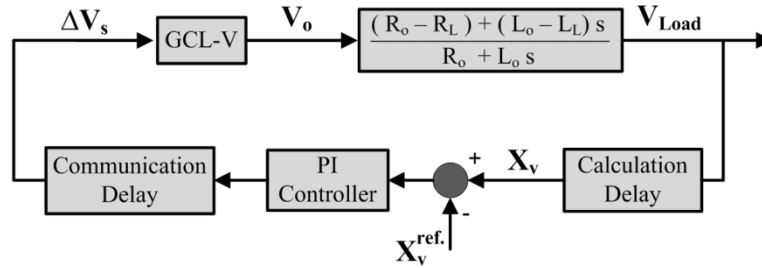
Figure 5. 12. Secondary control loop

Choosing the *PI* controller parameters as $K_P = 0.1$ and $K_I = 0.5$ gives a gain margin of $GM \cong 17$ and phase margin of $PM \cong 72°$. Closed loop transfer function was calculated which by plugging in the parameters of the system and controllers, pole locations of the system are found as follows:

$$s_1 = -2500 + 6300j$$

$$s_2 = -2500 - 6300j$$

$$s_3 = -1800$$

$$s_4 = -940$$

$$s_5 = -100$$

$$s_6 = s_7 = -1$$

Figure 5.13 shows the entire control block diagram of the system.

Figure 5. 13. Entire Control block diagram of the system

5.6 SUMMARY

Stability of the control approach that is presented in this dissertation was analyzed and control parameters were designed in this chapter. Performance of the controllers was compared with other types of controllers when appropriate. For current controller, voltage controller, droop control loop, as well as the secondary control loop, the closed loop transfer function was computed and pole locations were calculated. Analyses showed that the proposed control system is stable for the entire range of operating points.

CHAPTER VI

Microgrid Optimization in the Presence of Storage, *PV* and Wind Power Units

In grid-connected mode of operation, the objective of a microgrid is to export a controlled amount of active and reactive power into an established voltage. This is performed through the control of active and reactive components of current in the current-source mode of converter operation. The power demands themselves come from the Management System of the microgrid with the exception of Photo Voltaic, heat-led *CHP*[1] sources, wind power units and storage systems, which generate autonomously [2]. These types of power sources follow the active power reference generated by an internal control system such as *MPPT*[2] system or *SOC*[3] controller. Whereas the task in grid-connected mode is to control current into an established voltage, the task in autonomous mode is to establish that voltage by operation of the converters in voltage-source mode.

Optimization of an autonomous microgrid by sharing each power/current component was presented in chapter II and III. In order to share power/current components of the load among converters, output voltage of converters, which are operating as voltage sources, are manipulated and set through sharing control loops. Generation of power/current components by converters in the microgrid is proportional to their sharing coefficient. The exact amount of generation of power/current components

---

[1] Combined Heat and Power
[2] Maximum Power Point Tracking
[3] State Of Charge

by each converter depends on the existing load and cannot be set by sharing coefficients, whereas for some types of power sources such as PV^1, wind power units, and storage systems there are local criteria for active power/current generation which have priority over global optimization function. These criteria might be increase of efficiency through *MPPT* system, Maintaining *SOC* of the battery in storage system, etc. These types of units can be operated in current-source mode so they can follow active power generation commanded by local control system; however in this mode they lose the coordination with other converters for sharing other components of power/current. This may lead to either the requirement for installation of parallel converters to provide reactive, harmonic, and unbalance current, or the occupancy of the capacity of the other interface converters which results in less capacity for active power generation by those power sources. In this chapter, a variable droop control scheme is proposed which allows the active current for interface converters of *PV,* wind power sources and storage systems be set to the value which is computed locally according to the information received about weather, battery *SOC*, etc. while those inverters contribute in the generation of the other components of the current with other converters according to the sharing factors that are set by the Management System toward a global optimization function. The rest of demanded active current is shared among other types of power sources.

6.1 POWER UNITS WITH LOCALLY CONTROLLED ACTIVE POWER

6.1.1 PhotoVoltaic

This type of power source consists of converting energy from sunlight to electrical power by means of photo cells which are connected together in modules or arrays. The efficiency of PhotoVoltaic power source is between 10%-15% [57]. Output

---

[1] PhotoVoltaics

voltage of photo cell modules or arrays is a *DC* voltage that is generally required to be boosted to a higher level before being applied to the inverter. Figure 6.1 shows a general configuration of a PhotoVoltaic system.

There is a control system that according to weather condition sets the parameters for output voltage and current of the source in order to optimize the operation by extracting the maximum amount of power from the array at each weather condition. This control is called Maximum Power Point Tracking system. *MPPT* system command may affect either boosting *DC-DC* converter or the interfacing inverter. If *MPPT* output signal is sent to *DC-DC* converter, this converter transmits the requested active power from photo cells to *DC* bus. Interfacing inverter would be in charge of controlling the *DC* bus voltage level and supplying the power from *DC* side to *AC* grid. It is usually operated in current-source mode assuming that the *AC* voltage is strong enough already. In the case when *MPPT* system sends active power reference to *DC-AC* converter, this converter transmits the requested active power from a constant-voltage *DC* bus to *AC* grid where *DC-DC* converter is responsible to provide a constant voltage on the *DC* bus by transmitting the required power, which is equivalent to output power of inverter in steady state, from photo cells and battery to *DC* bus.
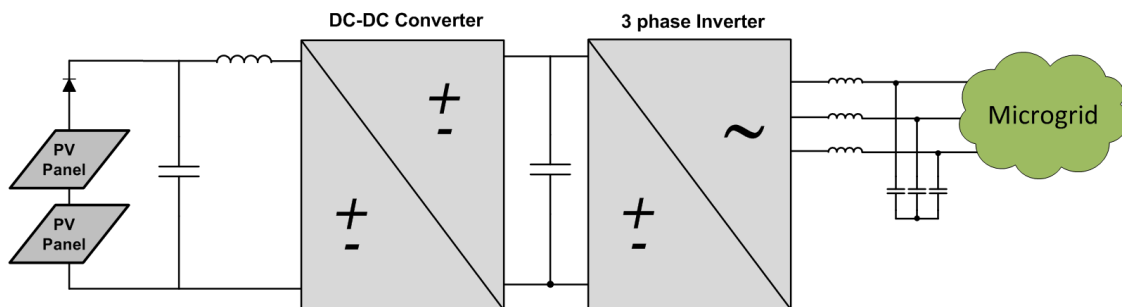
Figure 6. 1. PhotoVoltaic power source

90

6.1.2 Wind Power

Wind turbines convert kinetic energy of the wind to electrical energy. They use synchronous generators or induction generators to generate *AC* voltage. If a synchronous generator is driven by the wind turbine, an interface power electronic converter is required to connect to the grid whereas induction generators can be connected directly to the grid. Connection of a wind turbine-generator to the grid through power electronic converter unit is shown in Figure 6.2. This unit is usually made of a rectifier, a boost *i* converter and an interfacing inverter.

Wind energy although abundant, varies during the day as speed of wind varies. A control system is required to optimize the operation of the wind power unit by maximizing the energy harvest at any given time. Regardless of the control implementation method, Maximum Power Point Tracking system in a wind turbine unit receives wind speed information and generates the reference signal for output power of the unit. It may also control blade angle of the turbine. One option for *MPPT* system is to send reference signal for active power to *DC-DC* boost converter, in that case, interface inverter is controlled to maintain *DC* bus voltage constant. The inverter is usually
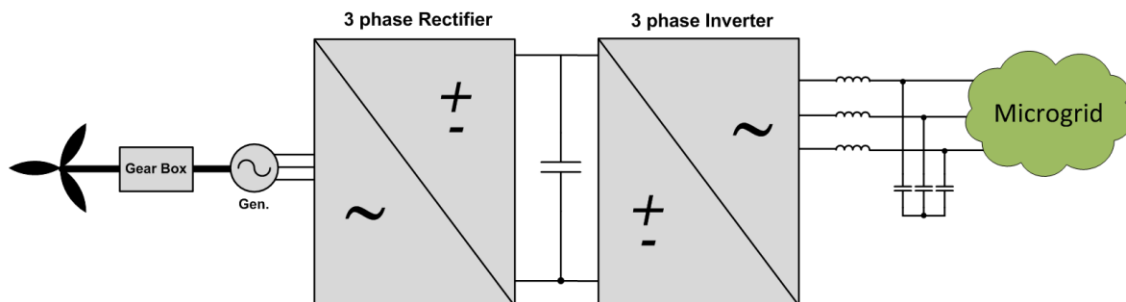
Figure 6. 2. Wind power source

controlled in the current source mode and non-active currents can be controlled to match the grid requirements locally. Another option for *MPPT* is to send active power reference to interface inverter. In that case, the *DC-DC* converter is in charge of controlling *DC* bus voltage by transmitting the appropriate amount of active power, which is in steady state equivalent to the inverter output active power, from wind turbine and battery to *DC* bus.

6.1.3 Storage Systems

Battery storage is generally used in a microgrid to harvest the excess energy during low loading condition and release this energy back to the grid when it is needed, in order to eliminate the need for costly generating units. Figure 6.3 shows a storage system configuration. There is a control system in a battery storage unit that decides whether the battery should operate in charging mode or discharging according to the loading condition. This control has the information of daily loading profile and its output is based on the time of operation. It is also important to maintain State Of Charge of the battery inside the permissible boundary. Therefore it might not be possible for storage to generate active power even if loading condition is high or absorb active power even if loading condition is low. *SOC* controller sends the active power signal to power
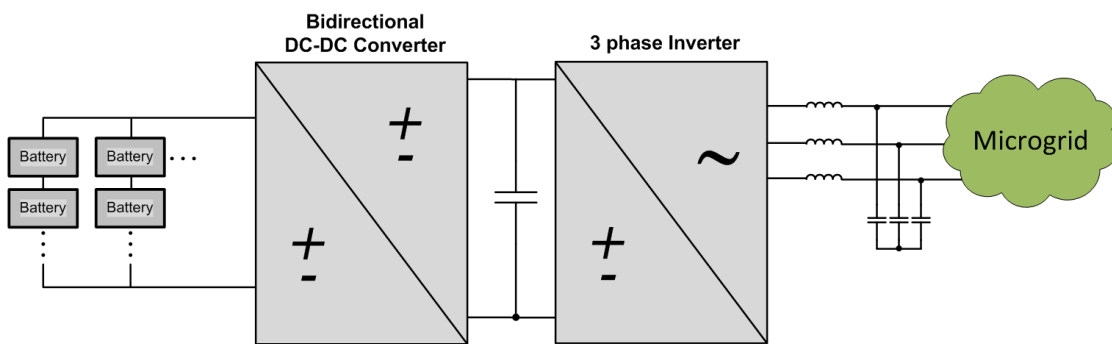
Figure 6. 3. Battery Storage unit

electronic unit. Power electronic unit might have different control systems for charging and discharging modes. If active power reference signal is sent to the front end *DC-DC* converter, the inverter is required to maintain *DC* bus voltage constant but if active power reference signal is sent to inverter, the *DC-DC* converter maintains the *DC* bus voltage.

6.1.4 Required control system

In all of the power sources that were mentioned above, interfacing converter usually operates as a current source to comply with the active power generation requested by *MPPT* or maintain the *DC* bus voltage. It can also generate non-active currents according to the grid requirements as a local compensator. But, it is not able to be operated in coordination with the other units to share the required non-active current components as discussed in chapter II and III. In this chapter a control system is designed that allows the active current to be set to the value that is commanded by *MPPT* system or *SOC* controller while the converter is able to also contribute to generation of other components of the load current in coordination with other converters in the grid. In the proposed approach the interfacing converter operates as a voltage source and the control of the microgrid is distributed.

6.2 PROPOSED CONTROL SCHEME

In principle, Management System of the microgrid defines how any of the power/current components is required to be shared among power converters in the microgrid, according to an objective function. Sharing coefficients for each converter are constrained by the rating of primary source as well as rating and the configuration of the interface converter. As mentioned above, *PV* units, wind power sources, and storage systems are preferred to follow their internal command for active current generation to

achieve maximum efficiency. Distributed and coordinated control methods presented in chapters II and III which enables sharing current components among converters only enables determination of sharing coefficients and the exact output current would depend on the existing load. A control method is presented here in which a control loop as shown in Figure 6.4 is added to the local control system of these types of units. By this method the advantage of sharing current components is maintained while active current component is particularly controllable. This control loop sets the bias of active current droop characteristic to control output active power to the value set by *MPPT*. Dynamic change of the frequency at these units versus the other sources in the microgrid results in a phase shift which causes a change in active current flow. As mentioned in chapter IV, sometimes a secondary control system controls bias of droop characteristics of all interface converters in the microgrid to compensate for the frequency error resulted from droop control method. This control layer does not disturb the control of active current generation at these power units since the relative change in bias frequencies of droop controls made by this layer, with respect to the other converters, is zero. Secondary control can perform other functions as well to further improve quality of the voltage as mentioned in chapter IV. In the simulations of this chapter, control of frequency and the magnitude of voltage at the load bus is considered for secondary control

If active power/current reference from *MPPT* or *SOC* controllers is applied to the inverter, local controller matches the output current /power of the unit with that reference, while if the reference is sent to the front-end converter, the interface inverter would be in charge of *DC* bus voltage control which results in equality of active power reference and the actual value in steady state, regardless of power losses. Figure 6.5 shows the proposed

94

control loop added to inverter control system when active power reference is applied to the front-end converter.
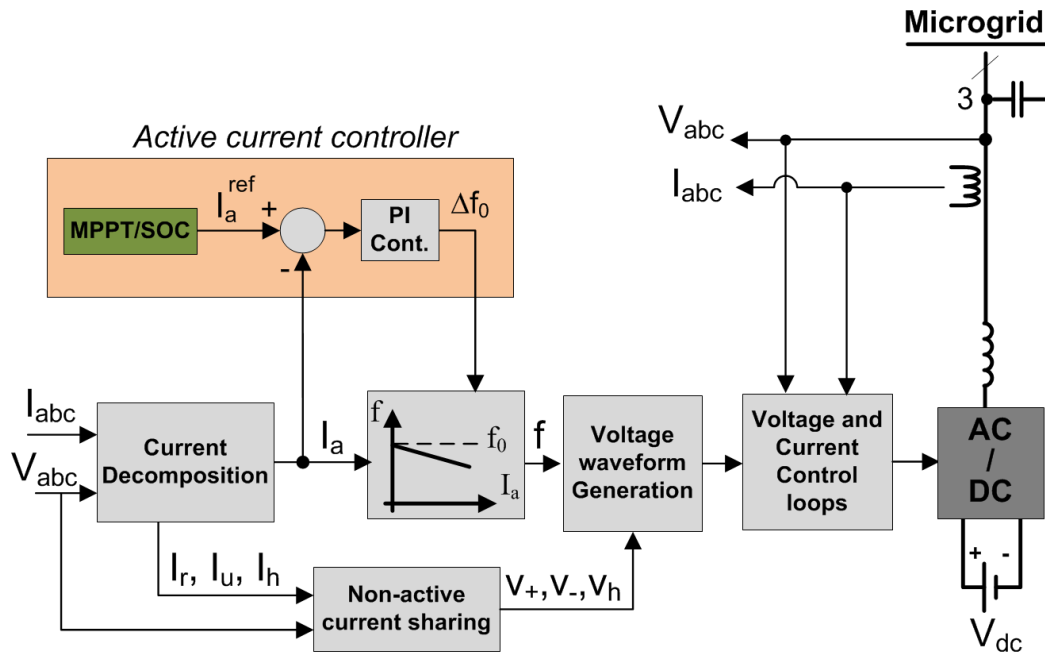
Figure 6. 4. Output active current control loop - Reference directly sent to interface inverter
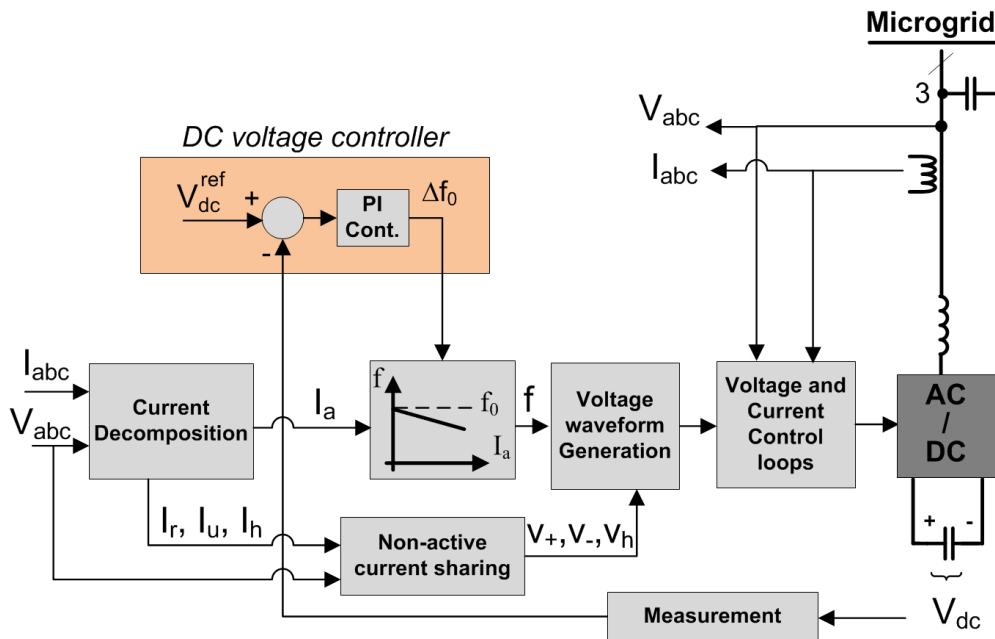
Figure 6. 5. DC voltage control loop - Reference sent to front-end converter

Simulation results for both cases show that by using this control scheme, active currents of *PV* units, wind power units, and storage system follow the reference from *MPPT* system and other components of current are shared with specified sharing coefficients. In the case where active power reference is followed by the front-end converter, the interface inverter is able to maintain *DC* bus voltage at the rated level. Figure 6.6 shows the entire local control system of each converter with active power reference sent to the inverter while Figure 6.7 shows it for the case where active power reference is sent to front-end converter.
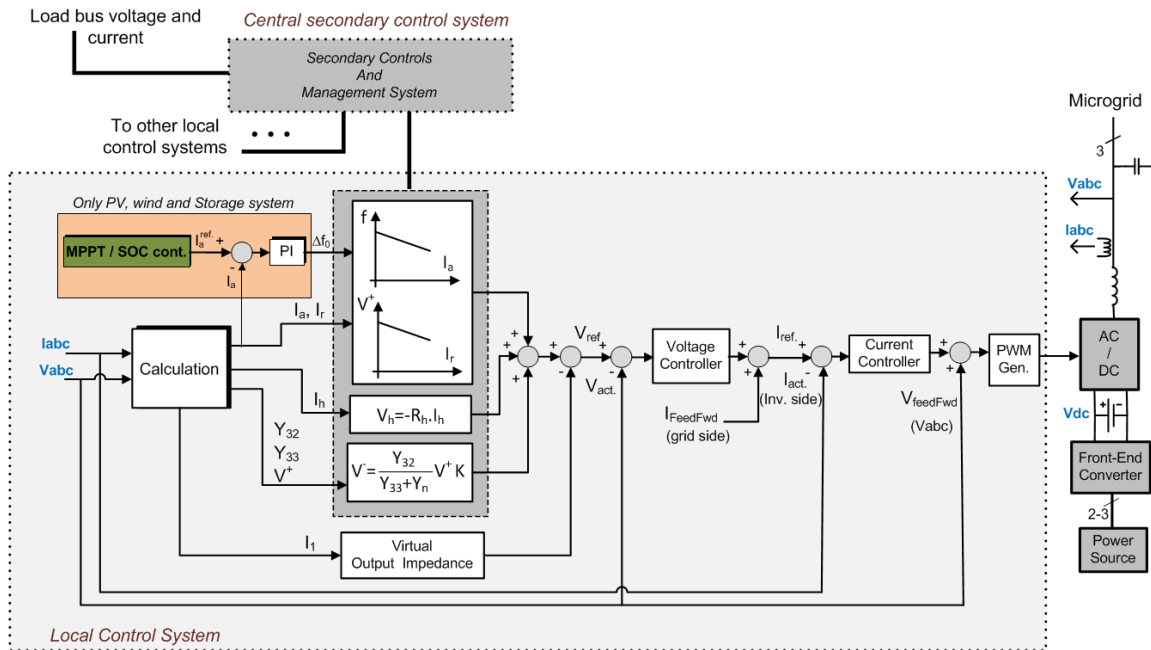
Figure 6. 6. Entire local control system - Reference sent to interface inverter
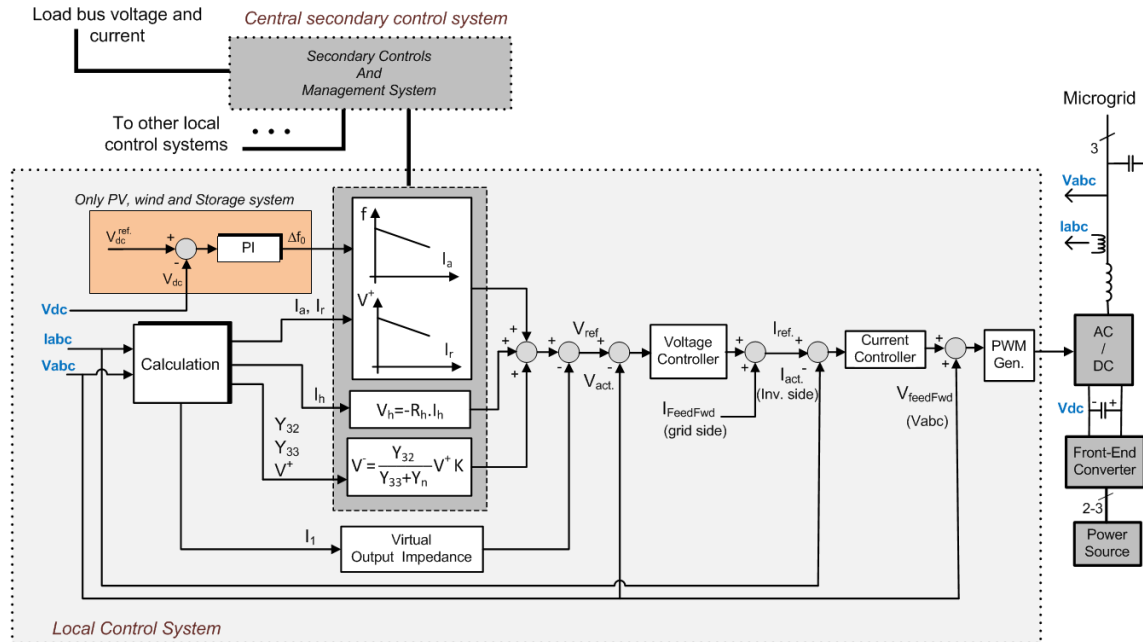
Figure 6. 7. Entire local control system - Reference sent to front-end converter

6.3 SIMULATION RESULTS

The proposed control scheme has been applied to a microgrid comprised of two converter-interfaced power sources which are connected to a load center through transmission lines. One of the sources is a Photo Voltaic energy source and the other one is a micro-turbine generator set. The load center consists of a constant balanced load and a switched load which includes balanced, unbalanced as well as harmonic load. Figure 6.8 shows the simulated microgrid. Table 1 shows the circuit parameters of the microgrid which are used in the simulation. Management System sets the sharing coefficients for each current component. *PV* unit generates active current in accordance with the *MPPT* system and shares the other components of the load with the sharing coefficients set by Management System. Secondary control sets bias of droop characteristics for active and reactive current to control frequency and voltage magnitude at the load bus. For the converters, interface converter of *PV* source is able to generate twice as much harmonic

97
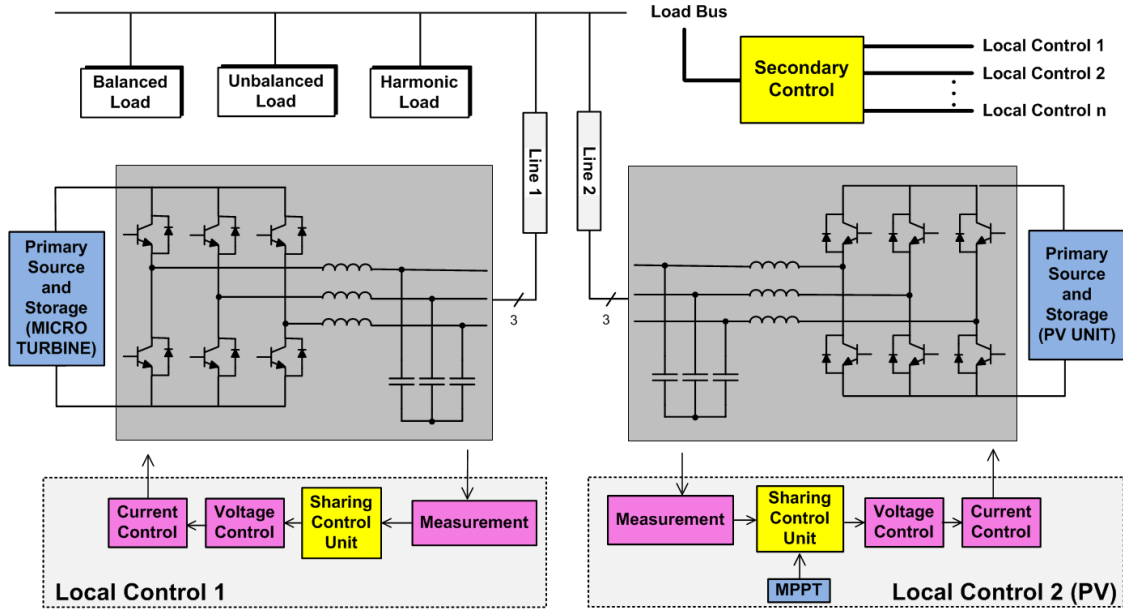
Figure 6. 8. The simulated microgrid

simulation shown in this chapter no specific optimization function is considered. It is

assumed that due to different structures as well as switching frequencies of the interface

Table 6.1. Parameters of the simulated system

DC bus voltage:	*700V*	Line impedance:	*0.754+0.377j*
AC bus rated *RMS* voltage (phase):	*120V*	Virtual impedance:	*0.754+0.377j*
AC bus rated frequency:	*60Hz*	Constant loads:	*22.5kW + 22.5kVar*
Switching frequency:	*12kHz*	Switched Load:	Unbalanced load of *12kW + 8kVar* and a thyristor rectifier with firing angle of *30* degrees
LC filter inductance:	*1mH*	Load Switching times	**Case 1:** *t=0.5 s* (switching on) and *t=1.5 s* (switching off) **Case 2:** *t=1 s* (switching on) and *t=4 s* (switching off)
LC filter capacitance:	*123uF*	Strategy of the sharing control:	Harmonics with the ratio of *1/2*, unbalance current with the ratio of *2/1* and reactive current equally. Active current of PV is controlled by MPPT which varied during the simulation, and the other source generates the rest.

as the other converter generates, but due to a smaller capacitor on the *DC* bus, it is set to generate half as much unbalance current as the other one generates to reduce ripple on the *DC* bus voltage. Reactive current is set to be shared equally between the two converters.

Case 1: In the case 1 of the simulations active power reference from *MPPT* is sent to the interface inverter and *DC* bus is assumed to be controlled by the front-end unit. Active current of *PV* source follows the *MPPT* command which varies from *t=3 S* to *t=3.5 S* and the other source is expected to supply the rest of demanded active current. The switched load is switched in at *t=0.5 S* and switched out at *t=1.5 S*. Figure 6.9 shows the active current of the two sources along with the *MPPT* reference for *PV* active current. It can be seen that *PV* follows the *MPPT* command regardless of the value of the load and the other source supplies the rest of the demanded load. When *MPPT* command changes from *75 A* to *125 A* the other source changes its output active current in the opposite way to keep the balance between load and generation. Figures 6.10, 6.11, and 6.12 show reactive, harmonic and unbalance current sharing between the two sources, both with and without the switched load. It can be seen that sharing of the other components is done with the sharing coefficients requested by the Management System which are shown in table 1. Figure 6.13 and 6.14 show magnitude and frequency of the voltage at load bus. It can be seen that by the performance of the secondary control voltage magnitude deviation from *120 V* and frequency deviation from *60 Hz* are always compensated. Secondary control which works by setting the bias of active and reactive current droop characteristics does not disturb the performance of the active current control for *PV* source.
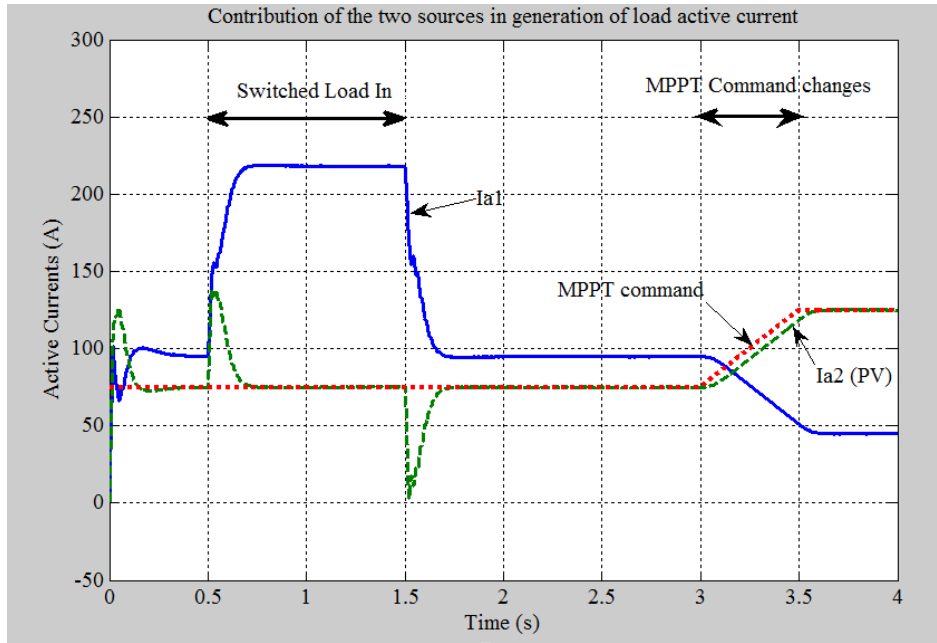
Figure 6. 9. Active currents of the two sources and *MPPT* command for the *PV* source
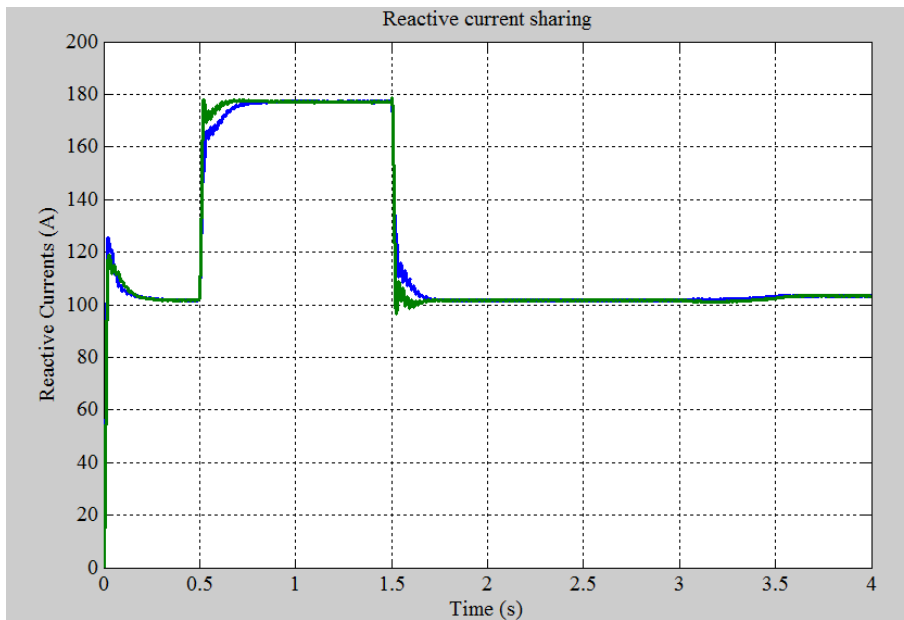
Figure 6. 10. Sharing of reactive current equally between the two sources
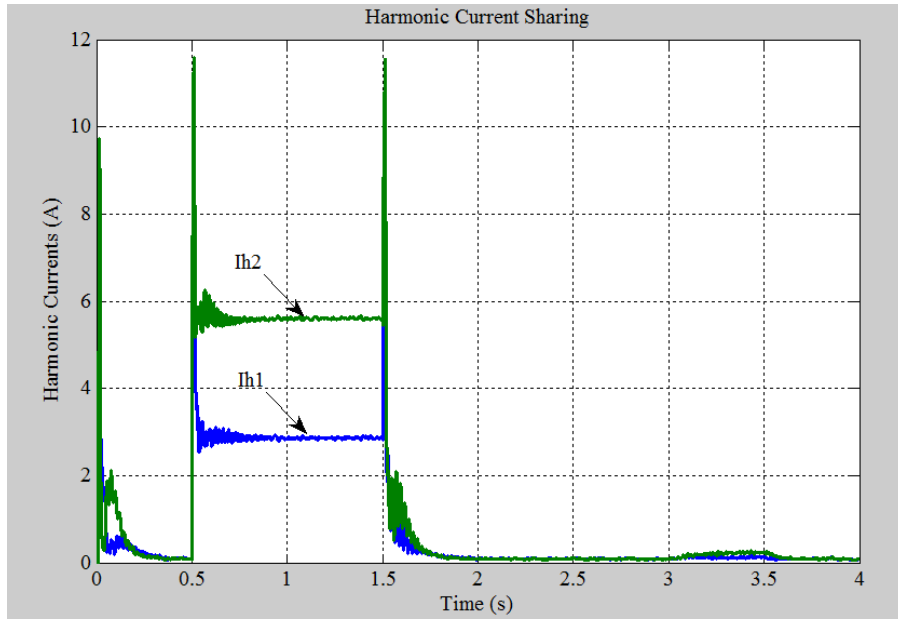
Figure 6. 11. Sharing of harmonics between the two sources; *PV* interface converter generates twice as the other interface converter
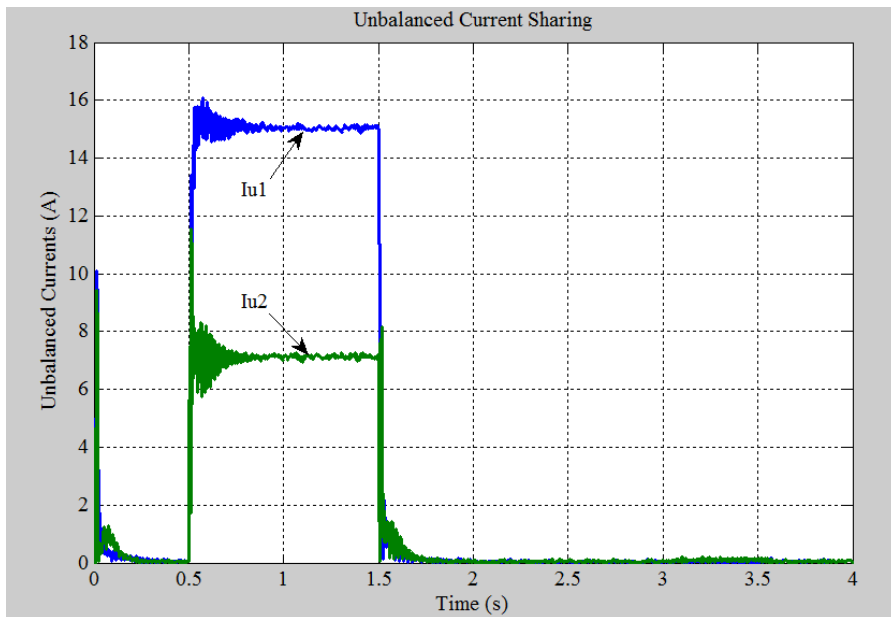
Figure 6. 12. Sharing of unbalance current between the two sources; *PV* interface converter generates half as much as the other interface converter
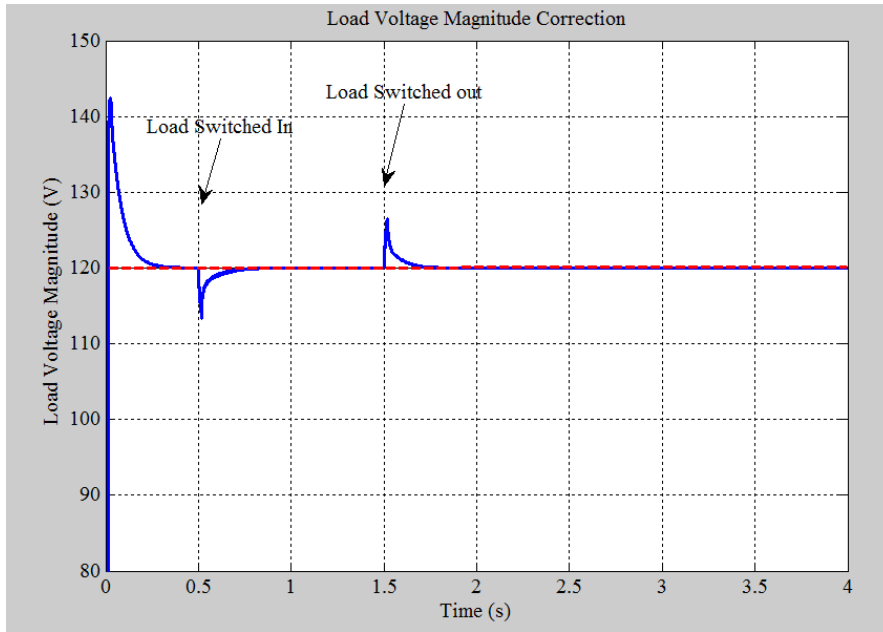
Figure 6. 13. Reinstatement of voltage magnitude at load bus by secondary control
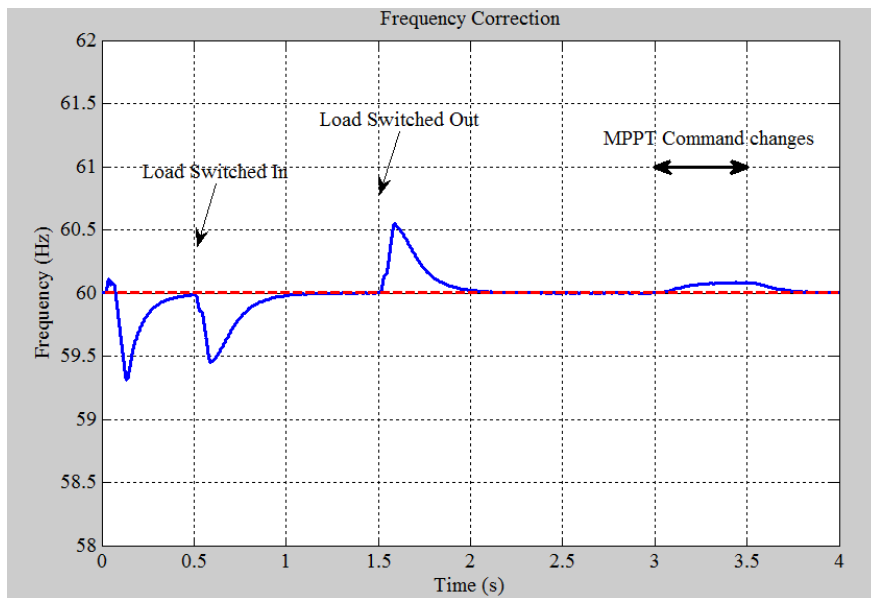
Figure 6. 14. Correction of the frequency at load bus by secondary control

Case 2: In the case 2 of the simulations, active power reference from *MPPT* is sent to the front-end *DC-DC* converter and interface inverter maintains *DC* bus voltage constant. The duration of the simulation is 10 seconds. Active power reference for *PV* source is constant until *t=7 S* when it keeps increasing linearly all the way up to *t=8.5 S*. The switched load is switched in at *t=1 S* and switched out at *t=4 S*. Output power of the inverter matches the reference from *MPPT* in steady state and the other source is expected to supply the rest of demanded active current. Interface inverter controls *DC* bus voltage which is shown in Figure 6.15. Figure 6.16 shows the output active power of the inverter which matches *MPPT* command reference regardless of losses.
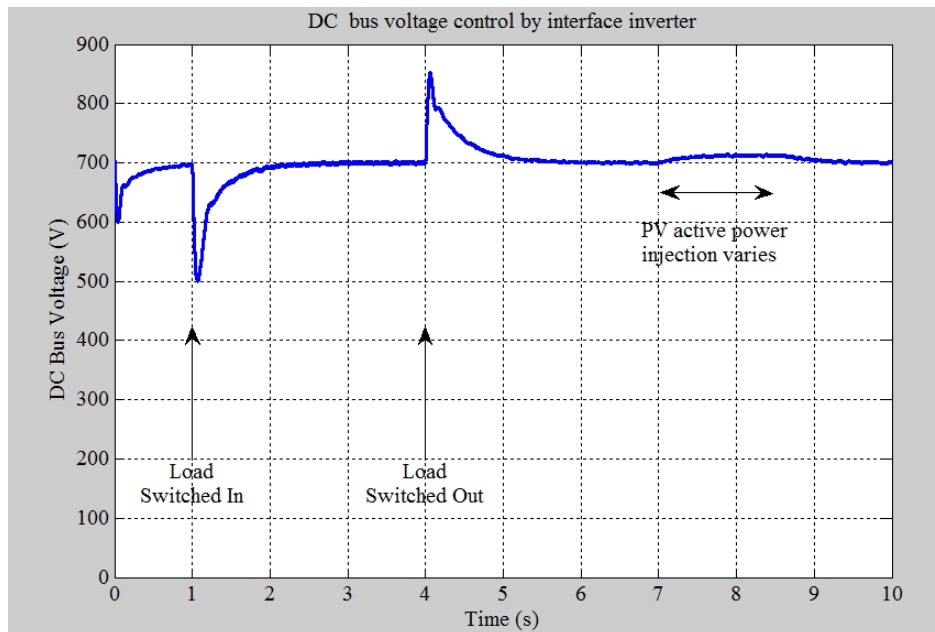
Figure 6. 15. Control of *DC* bus voltage by the inverter under load switching and variation of active power injection by front-end converter
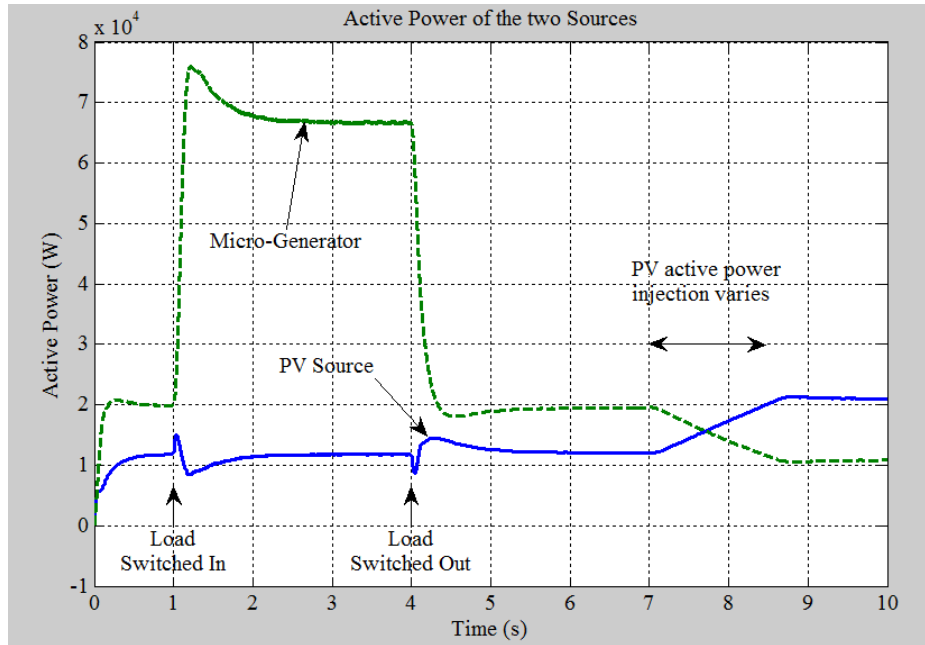
Figure 6. 16. Active power of the two sources under load switching and *MPPT* command variation

6.4 SUMMARY

Because interface converters in the cooperative control method operate in voltage-controlled mode, output current depends on the existing load, while for some types of power units such as *PV* and wind as well as battery storage units, output active current need to be set internally. If these units operate in current-controlled mode to set their active current to an internally made reference, distributed controls such as droop control method cannot be applied to these units to contribute to sharing of other current components. In this chapter, a control method was presented which enables *PV* and wind power units as well as storage systems to generate the active current which is commanded from their *MPPT/SOC* control system while contributing to generation of the other current components with respect to the sharing coefficients that are set by the Management System. The added control loop manipulates the bias of active current

104

droop characteristics to set the output active current as required. The secondary control also adjusts the bias of active and reactive current droop characteristics to control frequency and voltage magnitude at load bus, but this does not disturb the active current control as the relative change in the bias of active current droop characteristics of converters made by secondary control is zero. If active power reference is applied to the front-end converter, that converter will function like a current source to the *DC* bus. Then, interface converter would have the duty of maintaining *DC* bus voltage at the required level. Simulation results show the validity of the presented control scheme.

CHAPTER VII

MICROGRID POWER MANAGEMENT SYSTEM

Coordinated control of converters in a microgrid was presented in previous chapters and it was shown how converters in an autonomous microgrid can share components of power /current without any communication with each other. It was also shown that converters can improve the quality of load bus voltage by operating in cooperation through secondary control. Control of converter current based on *CPC* power theory enables the microgrid to independently share current components among converters such that each power source generates different ratio of each current component as shown in Figure 7.1 which might be required for optimization of various parameters in a microgrid.
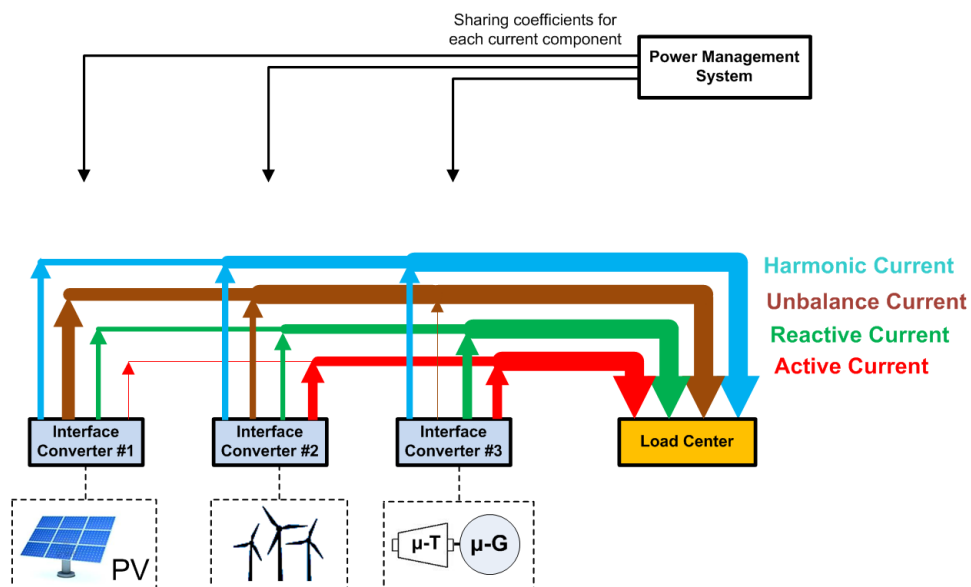
Figure 7. 1. Independent sharing of each current component

The scope of a microgrid's operational objective is not limited to simply meeting local power demands, but also considering factors such as emissions, fuel availability and cost, weather conditions, the spot-market price of electricity, etc. [58]. In another words there are local objectives such as feeding the loads as well as system-level objectives such as stability, reliability and cost [59]. System-level objective functions or optimization functions determine the coordination among converters. In order to automatically set the coordination among converters and reset the sharing factors after any change in the configuration of the microgrid or operating condition of the system, a Management System is required so the system always remains optimum with no need for human intervention. Control topology should be arranged in a way that ensures proper coordination of sources throughout the microgrid with regard to the optimization function. In some microgrid control configurations such as in [58] and [60] local controls can talk together through a platform and no system-level control is utilized. In the distributed control of an autonomous microgrid described in this dissertation, there is a system-level control as well as local controls such as in [59]. In this scheme, local control systems operate autonomously but their setting for current component sharing is reset by the system-level control following any changes in the operating condition of the microgrid. The speed of data transfer between local and system-level control doesn't need to be very fast, therefore a low-bandwidth communication link would be enough for data transfer. *PMS*[1] in system-level control should be able to [61]

- efficiently share current components among power sources,

---

[1] Power Management System

- quickly responds to disturbances and transients due to changes in the system operating mode,

- determine the final power generation set-points of the *DG*s to balance power and restore frequency of the system,

- provide means of resynchronization with the main grid.

In this chapter, different optimization functions for a Management System will be reviewed and the most popular one will be extended and a mathematical representation of that by the use of *CPC* power theory will be given along with simulation results. Such an algorithm can be developed for other optimization functions as well by making use of *CPC* theory.

7.1 OPTIMIZATION FUNCTIONS

Most of the optimization functions in previous works such as in [21, 23, 62] have focused on sharing only active and reactive powers among power supplies; however, optimization of the microgrid may require control over all major current components. In [62] harmonic and unbalanced components are supplied by some specific converters in the grid which are called compensators. These components are not shared among all power converters as might be required for some optimization purposes. Authors in [63] have recently used programmable resistive behavior to share harmonics with optimization purpose of equal power loading. *PMS* in [64] shares active and reactive power among inverter-connected sources in the microgrid using virtual frequency-voltage frame droop control.

Various objective functions can be considered in the optimization of a microgrid. These include [58, 61, 65, 59]

- Equal per-unit power loading of the units,

- Minimization of economic factors such as fuel cost, operation and maintenance cost, start-up/shut-down cost,

- Maximizing the customer's power availability and/or power quality,

- Minimization of environmental impacts from the generators,

- Minimization of total power loss,

- Maximizing the total efficiency of the microgrid; *kWh* generated energy per *kJ* fule consumed,

- Improving the dynamic response and maintaining stability margins during and after transients.

Minor objective functions may also be considered such as

- Minimization of the need for storage system by maximizing load factor (smooth out peaks and valleys of the load),

- Maximizing Var support to the greater grid when operating in grid-connected mode,

- Generation of reactive power as close as possible to the load to reduce power loss,

- Minimizing the number of converters involved.

Among these, "equal loading utilization", "power loss minimization", "fewer converters involved", and "larger converters involved" have been more commonly used [59]. There are also constraints that should be considered during the optimization, such as power availability of a renewable resource, bus voltage and frequency requirements, equality of load and supplies, and physical electrical characteristics of the microgrid.

Constraints arising from phase current limits and avoidance of over-modulation may be accounted for by more complex constraint functions.

Considering the independent controllability of harmonic and unbalance current, other minor objective functions may be considered during the optimization process. These include

- a higher share of generation of harmonic and unbalanced currents by the converters which are electrically closer to the loads to prevent deterioration of voltage quality at load bus,

- a higher share of generation of unbalanced currents by converters with larger DC bus capacitor to reduce ripple on DC bus voltage

- generation of reactive, harmonic and unbalance current by interface converters of PV and wind power sources to fully utilize them when active power generation is far below ratings,

- Improvement of voltage THD and voltage imbalance at critical load buses.

Constraints for the generation of harmonic and unbalanced currents are maximum unbalanced current of the converter, maximum harmonic current of the converter, microgrid voltage quality, allowable DC bus voltage ripple, etc. In the optimization process, other sources of current components such as compensators also need to be controlled in coordination with interface converters in order to contribute in generation of some or all of the current components [66]. Interface converters need, at the minimum, to have high enough ratings to supply the active rated power of the prime-mover, but the final ratings need to be somewhat higher to be able to supply the necessary reactive

power [67]. Considering harmonic and unbalance power necessitates even higher ratings for interface converters. Energy storage should be provided to ensure the immediate availability of energy for the load. The rating of the storage system depends on the technology of the prime mover [67].

7.2 CONSIDERED OPTIMIZATION FUNCTION

In this chapter "equal loading utilization" which is more commonly used for active and reactive power sharing is extended to all major current components. Constraints such as rating and configuration of the converters and rating of the primary sources as well as active current command from *MPPT* system of *PV* and wind turbine power sources have been considered.

Microgrids may contain fuel cells, wind turbines, *PV* units, micro-turbines and hydrogen power sources that are connected through interface converters along with compensating converters which can contribute to the generation of non-active current components.

The objective can be explained as follows:

- Power units with local reference generation for active current, such as wind power units and *PV* units follow their local active current reference to increase the efficiency of the unit.

- The additional required active current for loads will be supplied by the other units with respect to the rating of the primary power supply.

- Reactive current of the load will be supplied by interface converters as well as compensating converters, with respect to their remaining capacity.

- Harmonic and unbalanced current are shared among all converters in the microgrid according to their remaining capacity after the last step. If this lowers power quality at a load bus below a certain limit, converters which are electrically closer to that load bus will generate a larger portion of harmonic and unbalance to avoid voltage distortion and imbalance due to harmonic and unbalance current transmission. Also, it may be preferred that converters with larger energy storage on the *DC* bus, generate a larger portion of unbalance current to reduce ripple on the *DC* bus voltage.

- **Constraints**: Physical limitation of the microgrid characteristics, namely power rating of generating units and current rating of semiconductor devices, is the primary constraint. Equality of loads and supplies is always considered during the solution of the optimization function.

7.3 MATHEMATICAL REPRESENTATION

Current components are calculated for each source in the microgrid according to the optimization function.

a. Calculation of active current shares

Active currents of *PV*, wind, and storage systems, i_{PV}^a, i_{wind}^a, and i_{store}^a, are determined by their local controllers. Additional demanded active current should be supplied by other units.

$$i_1^a + i_2^a + \cdots + i_{N1}^a = i_{load}^a - (i_{PV}^a + i_{wind}^a + i_{store}^a) \tag{7-1}$$

where *N1* is the number of all generating units other than *PV*, wind and storage systems.

Considering (7-1), minimization of the following function, j^a, yields active current references for the rest of generating units. This means to minimize the difference between active current loading percentages of these units.

$$j^a = \sum_{\substack{m,n=1 \\ m \neq n}}^{N1} \left(\frac{i_m^a}{i_{m-max}} - \frac{i_n^a}{i_{n-max}} \right)^2 \qquad (7\_2)$$

b. Calculation of reactive current shares

Equality of reactive power generation and consumption bring about:

$$i_1^r + i_2^r + \cdots + i_{N_c}^r = i_{load}^r \qquad (7\text{-}3)$$

where N_c is the number of all converters connected to microgrid both interface converters and compensators.

Considering (7-3), and having known active current of power sources, minimization of the following function, j^r, yields reactive current of both interface converters and compensator units. This minimizes the difference between reactive current loadings with respect to available capacity of the units.

$$j^r = \sum_{\substack{m \, and n=1 \\ m \neq n}}^{Nc} \left(\frac{i_m^r}{\sqrt{i_{m-max}^2 - i_m^{a\,2}}} - \frac{i_n^r}{\sqrt{i_{n-max}^2 - i_n^{a\,2}}} \right)^2 \qquad (7\_4)$$

Note that active current of compensators in the grid is zero, $(i_{comp.}^a = 0)$.

c. Calculation of harmonic current shares

Equality of harmonic loads and generation bring about

$$i_1^h + i_2^h + \cdots + i_{N_c}^h = i_{load}^h \qquad (7\text{-}5)$$

113

Considering (7-5), minimization of the following function, j^h, yields harmonic currents of the converters.

$$j^h = \sum_{\substack{m\ and\ n=1 \\ m \neq n}}^{Nc} \left(\frac{i_m^h}{\sqrt{i_{m-max}^2 - i_m^{a\,2} - i_m^{r\,2}}} - \frac{i_n^h}{\sqrt{i_{n-max}^2 - i_n^{a\,2} - i_n^{r\,2}}} \right)^2 \qquad (7\_6)$$

Voltage THD^J is checked at the load bus. If THD is not acceptable, share of units that are electrically closer to the load are increased to prevent large voltage distortion due to flow of harmonics through transmission lines.

d. Calculation of unbalance current shares

$$i_1^u + i_2^u + \cdots + i_{N_c}^u = i_{load}^u \qquad (7\text{-}7)$$

Considering (7-7), minimization of the following function, j^u, yields unbalance currents of the converters.

$$j^u = \sum_{\substack{m\ and\ n=1 \\ m \neq n}}^{Nc} \left(\frac{i_m^u}{\sqrt{i_{m-max}^2 - i_m^{a\,2} - i_m^{r\,2} - i_m^{h\,2}}} - \frac{i_n^u}{\sqrt{i_{n-max}^2 - i_n^{a\,2} - i_n^{r\,2} - i_n^{h\,2}}} \right)^2 \qquad (7\_8)$$

Voltage imbalance is checked at the load bus. If it is not acceptable, share of units that are electrically closer to the load will be increased until imbalance is below the permissible limit.

During the solution of aforementioned equations, the constraint of maximum power of generator units and maximum current of semiconductors is checked at each step.

---

[1] Total Harmonic Distortion

Sharing ratios for active and reactive current determines the slopes of characteristic line of I_a–f and I_r–V droop control and sharing ratios for harmonic current is inversely proportional to virtual harmonic impedance implemented in local control system. Sharing ratios for unbalance current component is dispatched to each primary control as well as the secondary control to be considered in calculation of unbalance component of the output voltage reference for each converter.

7.4 SIMULATION

A microgrid comprised of three converter-interfaced power sources, which are connecting to a load center through lines impedances as in Figure 7.2, is used to verify the optimization method. Unit *2* is considered to be a unit with local reference generation for active power such as a *PV* power unit and units 1 and 3 generate active power according
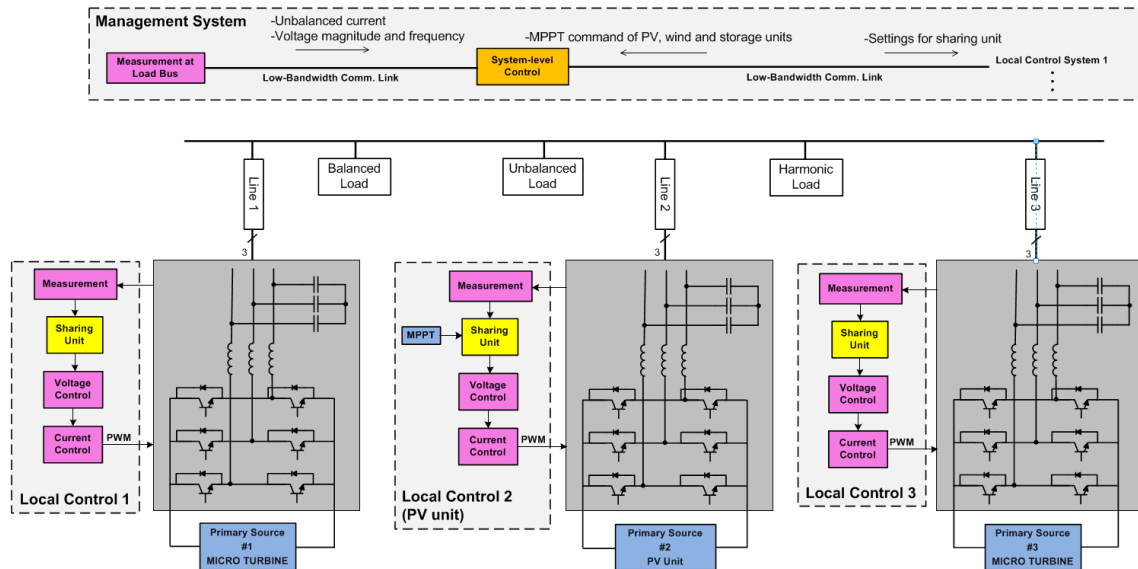
Figure 7. 2. Simplified model of a microgrid used for the simulation

Table 7.1. Parameters of the simulated system

DC bus voltage:	700V	Impedance of lines:	Line 1: 1.508+0.754j Line 2: 0.754+0.377j Line 3: 0.754+0.377j
AC bus rated RMS voltage (phase):	120V	Constant loads:	I_a=195A ; I_r=222A ; I_u=0 ; I_h=0
AC bus rated frequency:	60Hz	Switched Load:	I_a=144A ; I_r=149A ; I_u=33.5A ; I_h=9.6A
Switching frequency:	12kHz	Load Switching times:	t=0.5 s (switching on) and t=1.5 s (switching off)
LC filter inductance:	1mH	MPPT of source 2:	[t=0s-3s : I_a=65A] ; [t=3s-3.5s : I_a=ramp] ; [t=3.5s-4s : I_a=115A]
LC filter capacitance:	123uF	Current Rating of each source:	$I_{1-max} = I_{2-max} = I_{3-max} = 200A$
Virtual impedance:	0.754+0.377j	Strategy of the system level control:	Equal Loading Utilization with consideration of load voltage THD level and DC bus ripple
DC bus Capacitor:	C1=1800 μF C2=900 μF C3=1800 μF	Secondary control strategy:	Load bus voltage amplitude control. Load bus frequency control.

to the sharing coefficients received from the management system such as a micro-turbine generator set. The load center includes a constant balanced load, and a load which is unbalanced and distorted switches ON at *0.5s* and OFF at *1.5s*. *MPPT* output of source *2* changes during the simulation. Load and *MPPT* command information is shown in table 7.1. Active current of source *2* is determined by *MPPT* and the rest of active power required by the load along with reactive, unbalance and harmonic components of the load current is supplied by the all of the units according to the share factors received from system-level control. To clarify the simulation results, rating of the units are considered to be equal. Initially the *MPPT* command is set to *65 A* which results in almost equal active power for the three sources and thereby equal reactive current due to equal ratings. In high loading condition from *0.5s* to *1.5s*, active currents of source *1* and *3* change from

65 A to *137 A* to supply the load and active current of *PV* source remains unchanged in steady state due to the unchanged *MPPT* command. Reactive currents of three sources change according to (7-4). Reactive current of sources *1* and *3* which was initially *74 A* increases to *112.5 A* and that of source *2* which was also initially *74 A*, increases to *146 A*. From *3.5s* to *4s* when with light loading condition, *MPPT* command changes, the solution of optimization function keeps being updated and therefore active and reactive current of the three sources change until *MPPT* command is constant again. The new active current of source *2* is *115 A* and that of sources *1* and *3* decreases to *40 A* to balance the load and generation. During this time a shift of reactive current load from source *2* to source *1* and *3* occurs to satisfy optimization requirements. New reactive currents of the three sources are *79 A*, *64 A*, and *79 A*. Active and reactive currents of sources are shown in Figure 7-3 and 7.4. Due to larger impedance of line between source *1* and load, harmonic current of source *1* is set to be half of harmonic current of the other sources. Also due to a lower value of capacitance on the *DC* bus of the source *2*, unbalance current of source *2* is set to be half of the unbalance current of the other sources. Harmonic and Unbalance currents of sources are shown in Figure 7-5 and 7-6. System-level control also improves magnitude and frequency of load bus voltage after each load change in the system by changing the bias of droop characteristics of active and reactive current control. These results are shown in Figure 7.7 and 7.8. Simulation results show the exact sharing of active, reactive, unbalance and harmonic current components among sources as well as improvement of the load voltage.
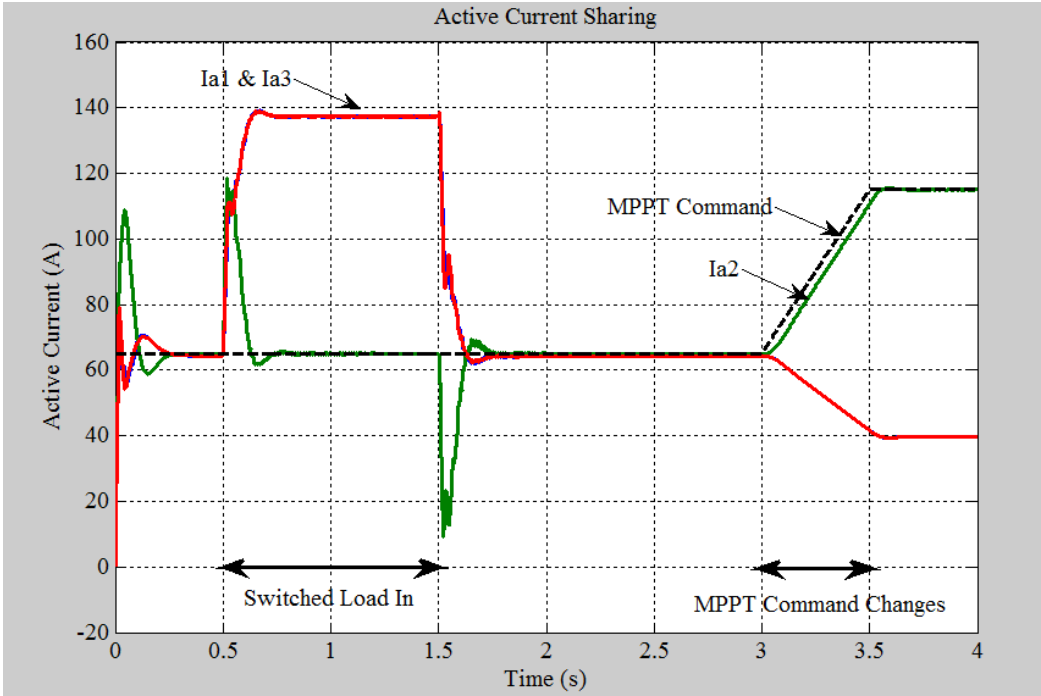
Figure 7. 3. Active current sharing among sources along with *MPPT* command for source 2
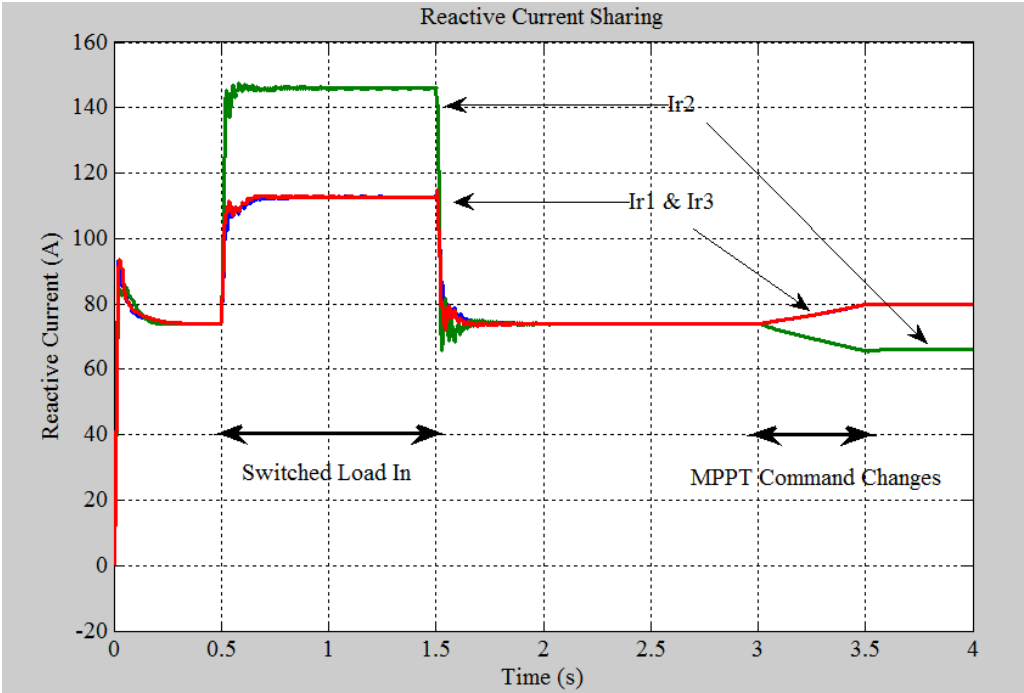
Figure 7. 4. Reactive current sharing among sources based on the solution of optimization function
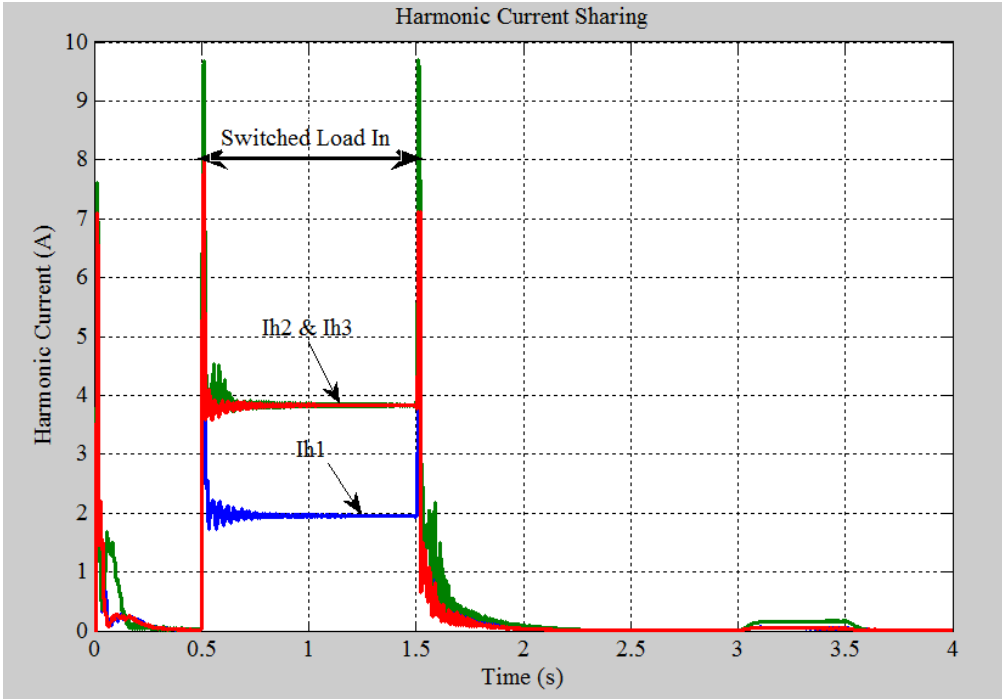
Figure 7. 5. Harmonic current sharing among sources
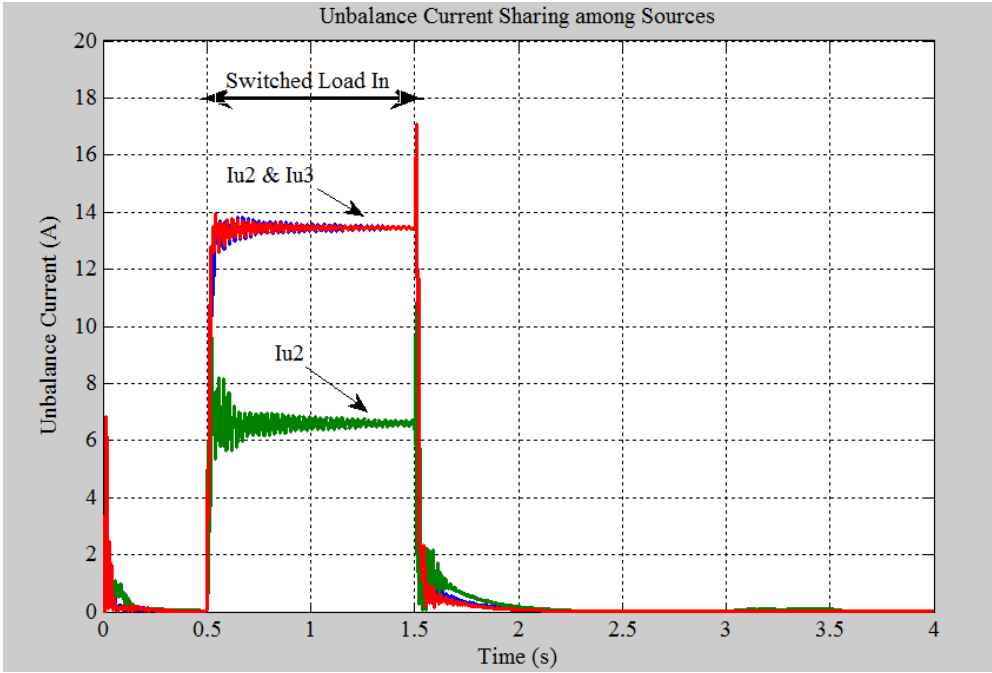
Figure 7. 6. Unbalanced load sharing among sources

119
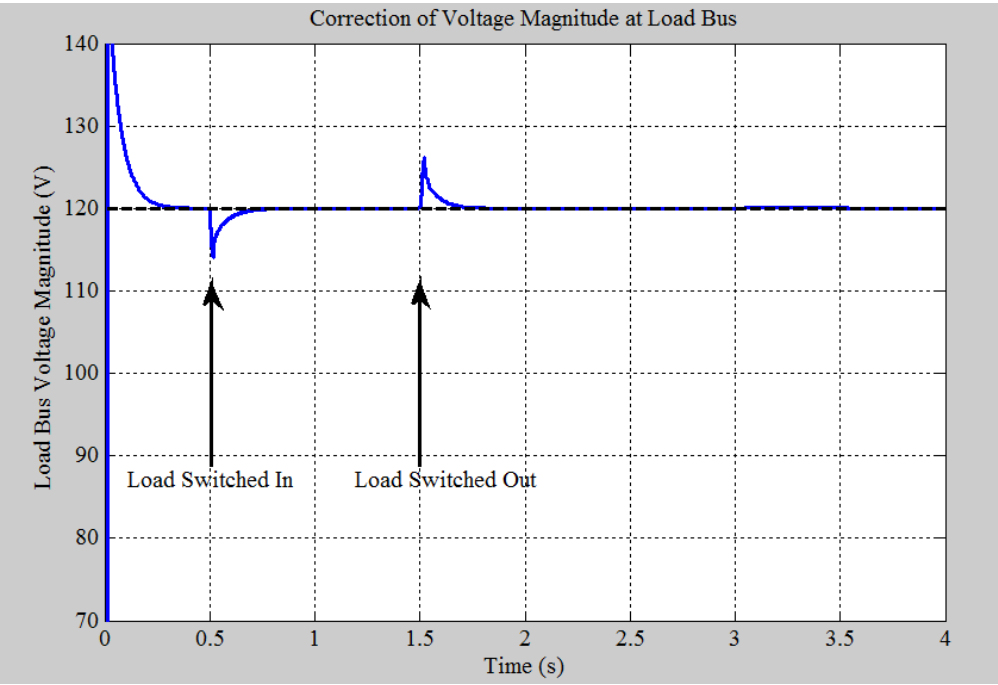
Figure 7. 7. Reinstatement of voltage magnitude at load bus
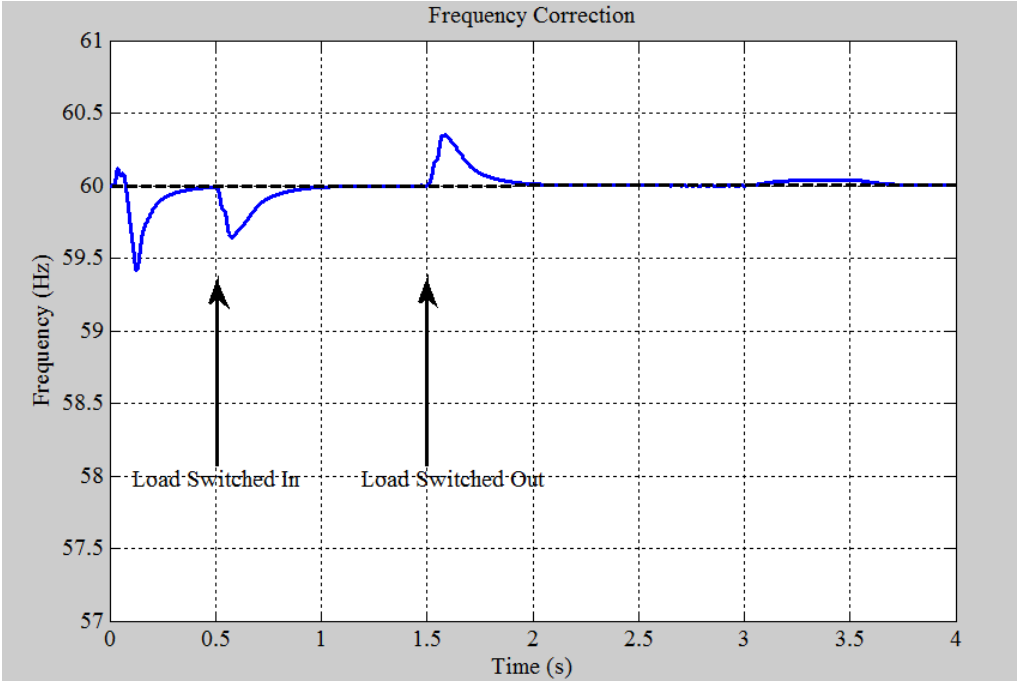
Figure 7. 8. Correction of the frequency

120

7.5 **SUMMARY**

In order for a microgrid system to stay optimized after any change in the configuration of the system, operating condition of the micogrid, or constraints for the microgrid operation, a power management system is required so that it resets the coordination settings among power units after any such change in the system. The proposed management system in this chapter, not only coordinates the generation of active and reactive power among units but also for harmonic and unbalanced currents. Therefore, units with only non-active current generation capability such as compensators and active power filters are considered too. The management system calculates the sharing coefficients according to the considered objective function. It also receives information of locally made active power reference from units such as *PV* and wind power source. A commonly used objective function was considered in this chapter and a mathematical approach based on *CPC* power theory was presented. The algorithm can be established for other objective functions as well. A sample microgrid was simulated and the results show that generation of each current component is controlled according to the results of the solution for objective function. Power quality improvement at the load bus was considered as a minor objective function and magnitude and frequency of voltage was improved at this bus.

CHAPTER VIII

CONCLUSIONS AND FUTURE WORK

8.1 CONCLUSION

In order to optimize various parameters in an autonomous microgrid or in electrical islands such as shipboard distribution systems, aircraft distribution systems, or offshore oil/gas platforms, control of power sources should be closely coordinated. This work proposed a cooperative control method for independent control of load current components to be shared among sources in a microgrid, so that converters in the microgrid can contribute to generation of each current component in any percentage. This cooperative control method is accomplished by utilizing the higher degrees of controllability of power electronic converters compared to electrical machines, along with advanced power theories and distributed control methods.

Coordinated control of all major components of the demanded current among converters allows for an extended degree of optimization of a microgrid's operation. Sharing factors for each current component are determined by a management system considering an objective function as well as constraints such as ability of the interface power converters to provide each component of current. Converters' abilities depend on the availability of primary sources, converter rating, converter structure and switching frequency. Thus, the constraints will be different for various converters and may even

122

vary over time for a particular converter.

In the distributed control method each interface converter is controlled as a voltage source where the exact amount of generation of current components by each converter depends on the existing load as well as the specified share factors. However, for some types of power sources such as Photo Voltaic, heat-led CHP[1] sources, wind power units and storage systems, the reference value for the active current component is determined according to a local control system. A control method was also presented in this dissertation which enables these units to generate active current which is commanded by MPPT/SOC control system while contributing to generation of the other current components with regard to the sharing coefficients that are set by the management system.

Microgrids in autonomous operation are prone to voltage magnitude deviation, frequency error, imbalance, and harmonic distortion. Load variation has an adverse impact on the quality of voltage. While any load step generally affects the magnitude of voltage at the load bus, nonlinear and unbalanced loads cause distortion and imbalance of the load voltage. The voltage is even deteriorated by performance of the load sharing units in local control systems due to coordinated control of power sources. A secondary control layer was designed which receives power quality indices of the load bus and applies correction signals to each local control system so that in addition to load sharing, load voltage quality is improved to standard limits.

While control of converters is distributed, a management system is required so that it resets the coordination settings among power units after any change in the

___

[1] Combined Heat and Power

configuration of the system, operating condition of the micogrid, constraints for the microgrid operation, etc. A mathematical representation of an optimization function was presented along with simulation results. "Equal Loading Utilization" is the basis for the optimization function and includes all major current components. By sharing of active load and ancillary functions such that total current of each converter is in accordance to its rating, this objective function prevents saturation of a unit while other units have available capacity for generation of current components. It also prevents unnecessary shut down of a unit which is usually costly and delays the availability of the unit for regeneration. All connected converters including units with only non-active current generation capability such as compensators and active power filters are also considered in the optimization.

Simulation results for each part of the proposed control approach verify that load components can be shared according to sharing coefficient dedicated by the management system with less than 5% error and power quality can be improved according to standard limits.

8.2 FUTURE WORK

8.2.1 Optimization of power quality throughout the microgrid

In this dissertation, loads are considered to be concentrated at a certain bus, while in a real microgrid, that might not be true. Here, quality of voltage at a certain bus was targeted for improvement by the secondary control. If loads are distributed in multiple buses, according to sensitivity of each set of bus loads, an objective function should be considered in which power quality of buses are given different weights.

8.2.2 Considering other objective functions

Equal loading utilization was specified as the objective and a mathematical expression to achieve that objective was developed based on CPC power theory. Other objective functions can be considered based on operational priorities such as power loss minimization, generation cost minimization, reliability, etc. Thus, expressions for other objective functions should be developed for the coordination framework developed in this work.

8.2.3 Comparison among central, master/slave, and distributed control method in coordinated control of power units

A distributed control method was used in this dissertation for coordination among sources which has the advantage of independence from communication links and lack of single point of failure. This control system has its own precision as well as response time. Also performance of this control scheme was not evaluated in transient states. It would be worthwhile to compare other types of control systems such as communication based centralized control and master-slave control based on such metrics as precision, transient performance, stability margins, etc. Also if the delay due to low bandwidth communication links had been considered in the simulations of this dissertation, response time would have increased.

REFERENCES

[1] Hassan Farhangi, "The Path of the Smart Grid", *IEEE Power and Energy magazine. 2010*

[2] T.C.Green, M. Prodanovic "Control of inverter-based micro-grids*," Elsevier electric power system research , pp. 1204-1213, 2007.*

[3] I. Vechiu1, A. Llaria, O. Curea and H. Camblong, "Control of Power Converters for Microgrids," *in Ecologiv Vehicles Renewable Energies, Monaco, March 26-29 2009.*

[4] Josep M. Guerrero, Juan C. Vasquez, José Matas, Luis García de Vicuña, and Miguel Castilla, "Hierarchical Control of Droop-Controlled AC and DC Microgrids—A General Approach Toward Standardization," *IEEE Transaction on Industrial Electronics, vol. 58, no. 1, pp. 158-172, January 2011.*

[5] Josep M. Guerrero, "Editorial special issue on power electronics," *IEEE Transaction on power electronics, vol. 25, no. 12, pp. 2885-2888, December 2010.*

[6] Elizabetta Tedeschi, Paolo Tenti, Paolo Mattavelli, and Daniella Trombetti, "cooperative control of electronic power processors in micro-grids," *in IEEE, 2009, pp. 1-8.*

[7] Elizabetta Tedeschi and Paolo Tenti, "cooperative design and control of distributed harmonic and reactive compensators," *in IEEE international school of nonsinusoidal currents and compensation, Lagow, Poland, 2008, pp. 1-6.*

[8] Helmo K. Morales Parede, Alessandro Costabebe,r and Paolo Tenti, "Application of conservative power theory to cooperative control of distributed compensatorsin smart grids," *in IEEE internatinal school on nonsinusoidal currents and compensation, Lagov, Poland, June 15-18 2010, pp. 190-196.*

[9] Paolo Tenti, Daniela Trombetti, Elizabetta Tedeschi, and Paolo Mattavelli, "comensation of load unbalance, ractive power and harmonic distortion by cooperative operation of distributed compensators," *European conference on power electronics and applications, pp. 1-10, 2009.*

[10] Elisabetta Tedeschi, "Cooperative Control Of Distributed Compensation Systems In Electric Networks Under Non-Sinusoidal Operations" *Universita' Degli Studi Di Padova, PhD Dissertation 2009.*

[11] Shen-Yuan Kuo; Tzung-Lin Lee; Chien-An Chen; Po-Tai Cheng; Ching-Tsai Pan; , "Distributed Active Filters for Harmonic Resonance Suppression in Industrial Facilities," *Power Conversion Conference - Nagoya, 2007. PCC '07 , vol., no., pp.391-397, 2-5 April 2007*

[12] Po-Tai Cheng; Tzung-Lin Lee; , "Distributed Active Filter Systems (DAFSs): A New Approach to Power System Harmonics," *Industry Applications, IEEE Transactions on , vol.42, no.5, pp.1301-1309, Sept.-Oct. 2006.*

[13] Tzung-Lin Lee, Po-Tai Cheng, "Design of a New Cooperative Harmonic Filtering Strategy for Distributed Generation Interface Converters in an Islanding Network," *IEEE Transaction on power electronics, vol. 22, pp. 1919-1927, September 2007.*

[14] Tzung-Lin Lee; Po-Tai Cheng; Akagi, H.; Fujita, H.; , "A Dynamic Tuning Method for Distributed Active Filter Systems," *Industry Applications, IEEE Transactions on , vol.44, no.2, pp.612-623, March-april 2008.*

[15] Josef Tlustý, Jiří Škramlík, Jan Švec, and Viktor Valouch, "Cooperative Control of Active Power Filters in Power Systems without Mutual Communication," *Mathematical Problems in Engineering, vol. 2010, pp. 1-13, December 2010.*

[16] Tzung-Lin Lee, Jian-Cheng Li, and Po-Tai Cheng, "Discrete Frequency Tuning Active Filter for Power System Harmonics," *IEEE Transaction on Power Electronics, vol. 24, no. 5, pp. 1209-1217, May 2009.*

[17] Tzung-Lin Lee and Shang-Hung Hu, "Discrete Frequency-Tuning Active Filter to Suppress Harmonic Resonances of Closed-Loop Distribution Power Systems," *IEEE Transaction on Power Electronics, vol. 26, no. 1, pp. 137-148, January 2011.*

[18] Po-Tai Cheng, Chien-An Chen, Tzung-Lin Lee, and Shen-Yuan Kuo, "A Cooperative Imbalance Compensation Method for Distributed-Generation Interface Converters," *IEEE Transaction on Industry Application, vol. 45, no. 2, pp. 805-815, March/April 2009.*

[19] Min Dai, "Control Of Power Converters For Distributed Generation Applications" *Ohio State University, PhD Dissertation 2005.*

[20] V´asquez Quintero, Juan Carlos, "Decentralized Control Techniques Applied to Electric Power Distributed Generation in Microgrids," *universitat politècnica de catalunya, Barcelona, PhD Dissertation 2009.*

[21] De Brabandere , Bruno Bolsens, Jeroen Van den Keybus, Achim Woyte, Johan Driesen, and Ronnie Belmans Karel, "*A Voltage and Frequency Droop Control Method for Parallel Inverters," IEEE Transaction on Power Electronics, vol. 22, no. 4, pp. 1107-1115, July 2007.*

[22] Josep M. Guerrero , José Matas, Luis García de Vicuña, Miguel Castilla, and Jaume Miret, "Decentralized Control for Parallel Operation of Distributed Generation Inverters Using Resistive Output Impedance," *IEEE Transaction on Industrial Electronics, vol. 54, no. 2, pp. 994-1004, April 2007.*

[23] Yun Wei Li; Ching-Nan Kao; , "An Accurate Power Control Strategy for Power-Electronics-Interfaced Distributed Generation Units Operating in a Low-Voltage Multibus Microgrid," *Power Electronics, IEEE Transactions on , vol.24, no.12, pp.2977-2988, Dec. 2009.*

[24] Wei Yao; Min Chen; Matas, J.; Guerrero, J.M.; Zhao-Ming Qian; , "Design and Analysis of the Droop Control Method for Parallel Inverters Considering the Impact of the Complex Impedance on the Power Sharing," *Industrial Electronics, IEEE Transactions on , vol.58, no.2, pp.576-588, Feb. 2011.*

[25] Marwali, M.N.; Jin-Woo Jung; Keyhani, A.; , "Control of distributed generation systems - Part II: Load sharing control," *Power Electronics, IEEE Transactions on , vol.19, no.6, pp. 1551- 1561, Nov. 2004*

[26] Loix, T.; De Brabandere, K.; Driesen, J.; Belmans, R.; , "A Three-Phase Voltage and Frequency Droop Control Scheme for Parallel Inverters," *Industrial Electronics Society, 2007. IECON 2007. 33rd Annual Conference of the IEEE , vol., no., pp.1662-1667, 5-8 Nov. 2007*

[27] Guerrero, J.M.; Hang, L.; Uceda, J.; , "Control of Distributed Uninterruptible Power Supply Systems," *Industrial Electronics, IEEE Transactions on , vol.55, no.8, pp.2845-2859, Aug. 2008*

[28] Vasquez, J.C.; Guerrero, J.M.; Luna, A.; Rodriguez, P.; Teodorescu, R.; , "Adaptive Droop Control Applied to Voltage-Source Inverters Operating in Grid-Connected and Islanded Modes," *Industrial Electronics, IEEE Transactions on , vol.56, no.10, pp.4088-4096, Oct. 2009*

[29] Jaehong Kim; Guerrero, J.M.; Rodriguez, P.; Teodorescu, R.; Kwanghee Nam; , "Mode Adaptive Droop Control With Virtual Output Impedances for an Inverter-Based Flexible AC Microgrid," *Power Electronics, IEEE Transactions on , vol.26, no.3, pp.689-701, March 2011*

[30] E. Barklund, Nagaraju Pogaku, Milan Prodanovic´, C. Hernandez-Aramburo and Tim C. Green, "Energy Management in Autonomous Microgrid Using Stability-

Constrained Droop Control of Inverters," *IEEE Transaction on Power Electronics, vol. 23, no. 5, pp. 2346-2352, September 2008.*

[31] Hauck Matthias, Späth Helmut, "Control of a Three Phase Inverter Feeding an Unbalanced Load and Operating in Parallel with Other Power Sources" *in Proc. EPE-PEMC'02 Conf., 2002, pp. 1-10.*

[32] Vasquez, J.C.; Guerrero, J.M.; Savaghebi, M.; Teodorescu, R.; , "Modeling, analysis, and design of stationary reference frame droop controlled parallel three-phase voltage source inverters," *Power Electronics and ECCE Asia (ICPE & ECCE), 2011 IEEE 8th International Conference on , vol., no., pp.272-279, May 30 2011-June 3 2011*

[33] Zmood, D.N.; Holmes, D.G.; , "Stationary frame current regulation of PWM inverters with zero steady-state error," *Power Electronics, IEEE Transactions on , vol.18, no.3, pp. 814- 822, May 2003.*

[34] Zmood, D.N.; Holmes, D.G.; Bode, G.H.; , "Frequency-domain analysis of three-phase linear current regulators ," *Industry Applications, IEEE Transactions on , vol.37, no.2, pp.601-610, Mar/Apr 2001.*

[35] Guerrero, J.M.; Matas, J.; de Vicuna, L.G.; Castilla, M.; Miret, J.; , "Wireless-Control Strategy for Parallel Operation of Distributed-Generation Inverters," *Industrial Electronics, IEEE Transactions on , vol.53, no.5, pp.1461-1470, Oct. 2006*

[36] Massimo Bongiorno, Jan Svensson, and Ambra Sannino "Dynamic Performance of Current Controllers for Grid-connected Voltage Source Converters under Unbalanced Voltage Conditions"

[37] Jeong-Ik Jang; Dong-Choon Lee; , "High Performance Control of Three-Phase PWM Converters under Nonideal Source Voltage," *Industrial Technology, 2006. ICIT 2006. IEEE International Conference on , vol., no., pp.2791-2796, 15-17 Dec. 2006*

[38] Mattavelli, P.; , "Synchronous-frame harmonic control for high-performance AC power supplies," *Industry Applications, IEEE Transactions on , vol.37, no.3, pp.864-872, May/Jun 2001.*

[39] Yunwei Li; Vilathgamuwa, D.M.; Poh Chiang Loh; , "Microgrid power quality enhancement using a three-phase four-wire grid-interfacing compensator," *Industry Applications, IEEE Transactions on , vol.41, no.6, pp. 1707- 1719, Nov.-Dec. 2005*

129

[40] Hailian Xie Angquist, L. Nee, H.-P., "Novel flux modulated positive and negative sequence deadbeat current control of voltage source converters" *IEEE Power Engineering Society General Meeting, 2006.*

[41] Azevedo, G.; Rodriguez, P.; Rocabert, J.; Cavalcanti, M.; Neves, F.; , "Voltage quality improvement of microgrids under islanding mode," *Energy Conversion Congress and Exposition (ECCE), 2010 IEEE , vol., no., pp.3169-3173, 12-16 Sept. 2010*

[42] Borup, U.; Enjeti, P.N.; Blaabjerg, F.; , "A new space-vector-based control method for UPS systems powering nonlinear and unbalanced loads," *Industry Applications, IEEE Transactions on , vol.37, no.6, pp.1864-1870, Nov/Dec 2001.*

[43] Savaghebi, M.; Vasquez, J.C.; Jalilian, A.; Guerrero, J.M.; Tzung-Lin Lee; , "Selective harmonic virtual impedance for voltage source inverters with LCL filter in microgrids," *Energy Conversion Congress and Exposition (ECCE), 2012 IEEE , vol., no., pp.1960-1965, 15-20 Sept. 2012.*

[44] Borup, U.; Blaabjerg, F.; Enjeti, P.N.; , "Sharing of nonlinear load in parallel-connected three-phase converters," *Industry Applications, IEEE Transactions on , vol.37, no.6, pp.1817-1823, Nov/Dec 2001.*

[45] De, D.; Ramanarayanan, V.; , "Decentralized Parallel Operation of Inverters Sharing Unbalanced and Nonlinear Loads," *Power Electronics, IEEE Transactions on , vol.25, no.12, pp.3015-3025, Dec. 2010.*

[46] Hirofumi Akagi, Edson Hirokazu Watanabe, Mauricio Aredes, "Instantaneous power theory and applications to power conditioning" *ISBN: 9780470107614, Hoboken, NJ : John Wiley, 2007.*

[47] Czarnecki L.S., "Instantaneous reactive power p-q theory and power properties of three-phase systems," *Power Delivery, IEEE Transactions on , vol.21, no.1, pp. 362- 367, Jan. 2006*

[48] Czarnecki L.S., "On some misinterpretations of the instantaneous reactive power p-q theory," *IEEE Trans. Power Electron., vol. 19, no. 3, pp. 828–836, May 2004.*

[49] Czarnecki L.S., "Orthogonal decomposition of the currents in a 3-phase nonlinear asymmetrical circuit with a nonsinusoidal voltage source," *Instrumentation and Measurement, IEEE Transactions on , vol.37, no.1, pp.30-34, Mar 1988*

[50] Czarnecki L.S., "Powers of Asymmetrically Supplied Loads in Terms of the CPC Power Theory" *Electrical Power Quality and Utilisation Journal, Vol.XIII, nº 1, 2007, pp. 97-104.*

[51] Ginn, H.L.; , "Control method for grid-connected converters in systems with non-ideal supply voltage," *Applied Measurements for Power Systems (AMPS), 2011 IEEE International Workshop on , vol., no., pp.96-101, 28-30 Sept. 2011.*

[52] Ginn, H.L., "CPC based converter control for systems with non-ideal supply voltage," *Nonsinusoidal Currents and Compensation (ISNCC), 2010 International School on, vol., no., pp.117-122, 15-18 June 2010.*

[53] Ginn, H.L.; Guangda Chen; , "Control method for voltage source converters in systems with high frequency variability," *Power Electronics and Drive Systems, 2009. PEDS 2009 International Conference on , vol., no., pp.1008-1013, 2-5 Nov. 2009.*

[54] Rosendo Macias, J.A.; Gomez Exposito, A.; , "Efficient moving-window DFT algorithms," *Circuits and Systems II: Analog and Digital Signal Processing, IEEE Transactions on , vol.45, no.2, pp.256-260, Feb 1998*

[55] Hatem A. Darwish; Magdy Fikri; , "Practical Considerations for Recursive DFT Implementation in Numerical Relays," *Power Delivery, IEEE Transactions on , vol.22, no.1, pp.42-49, Jan. 2007*

[56] Simone Buso, Paolo Mattavelli: *Digital Control in Power Electronics.* Morgan and Claypool Publishers, 2006

[57] W. Kramer, S. Chakraborty, B. Kroposki, and H. Thomas, "Advanced Power Electronic Interfaces for Distributed Energy Systems, Part 1: Systems and Topologies" *Technical Report, NREL/TP-581-42672, March 2008*

[58] C.M. Colson, M.H. Nehrir, and R.W. Gunderson, "Multi-agent Microgrid Power Management" *18th IFAC World Congress, Milano (Italy) August 28 - September 2, 2011*

[59] Eiko Kruger, Junqi Liu, Ferdinanda Ponci, Antonello Monti, "Optimization of task sharing towards multi-agent control of PEBB based power systems," *ISGT, pp.1-7, 2012 IEEE PES Innovative Smart Grid Technologies, 2012*

[60] J. Oyarzabal, J. Jimeno, J. Ruela, A. Engler, and C. Hardt, "Agent based microgrid management system, "*in Proc. Int. Conf. Future Power Syst., pp. 1–6, Nov. 2005*

[61] Katiraei, F.; Iravani, M.R., "Power Management Strategies for a Microgrid With Multiple Distributed Generation Units" *Power Systems, IEEE Transactions on , vol.21, no.4, pp.1821-1831, Nov. 2006*

[62] Farhad Shahnia, Ritwik Majumder, Arindam Ghosh, Gerard Ledwich, Firuz Zare, "Operation and control of a hybrid microgrid containing unbalanced and nonlinear loads" *Electric power systems research, Elsevier, 2010*

[63] Vandoorn, T.; Meersman, B.; De Kooning, J.; Vandevelde, L.; , "Controllable Harmonic Current Sharing in Islanded Microgrids: DG Units With Programmable Resistive Behavior Toward Harmonics," *Power Delivery, IEEE Transactions on , vol.27, no.2, pp.831-841, April 2012*

[64] Yan Li; Yun Wei Li , "Power Management of Inverter Interfaced Autonomous Microgrid Based on Virtual Frequency-Voltage Frame," *Smart Grid, IEEE Transactions on , vol.2, no.1, pp.30-40, March 2011*

[65] Bolognani, S.; Zampieri, S., "Distributed control for optimal reactive power compensation in smart microgrids," *50th IEEE Conference on Decision and Control and European Control Conference (CDC-ECC), pp.6630-6635, 12-15 Dec. 2011*

[66] Tenti, P.; Trombetti, D.; Tedeschi, E.; Mattavelli, P., "Compensation of load unbalance, reactive power and harmonic distortion by cooperative operation of distributed compensators," *13th European Conference on Power Electronics and Applications, EPE '09.,pp.1-10, 8-10 Sept. 2009*

[67] Lasseter R.H., Piagi P. "Control and design of microgrid components," *Power Systems Engineering Research Center, Publication 06-03, January 2006*